Integrated Assessment of Atmospheric Environmental Management in China

Von der Fakultät Energie-, Verfahrens- und Biotechnik der Universität Stuttgart
zur Erlangung der Würde einer

Doktor-Ingenieurin (Dr.-Ing.)

genehmigte Abhandlung

Vorgelegt von

Ganlin Huang

geboren in Hunan, China

Hauptberichter:	Prof. Dr.-Ing. Rainer Friedrich
Mitberichter:	Prof. Dr. Andreas Kronenburg
Tag der Einreichung:	11. Dezember 2017
Tag der mündlichen Prüfung:	02. Mai 2018

Institut für Energiewirtschaft und Rationelle Energieanwendung

Universität Stuttgart

2018

Acknowledgements

First of all, I would like to thank my first supervisor, Prof. Rainer Friedrich. Without his help and guidance, this dissertation would never have been possible. He always supported me promptly with just the right insight, explanation, direction, and great encouragement throughout the course of the dissertation.

I would also like to thank Prof. Andreas Kronenburg for being my second examiner and for his clear and helpful comments.

Special thanks to my colleagues in IER, Joachim Ross, Christian Schieberle, Naixin Li, etc. The fruitful and open-hearted discussions with them provided a pleasing academic atmosphere and helped me finding directions and solutions in case of difficulties.

I am really thankful for the support and professional advice regarding a wide range of aspects involved in data collection and methodological improvement from Frank Dentener, Matti Jantunen, Matthieu Pommier, Michael Gauss, and Zbigniew Klimont.

All the time on the list, I would like to thank my parents and husband, who always hold my back and provide support in every possible way. Last but not least, I am happy to thank my beloved baby to be born, who accompanied and encouraged me in the last months of this work.

Table of Contents

List of Figures

List of Tables

List of Acronyms and Abbreviations

AIC	Akaike Information Criterion
ALRI	Acute Lower Respiratory Infection
API	Air Pollution Index
AQG	Air Quality Guideline
AQI	Air Quality Index
BA	Bias Adjustment
BAU	Business As Usual
BC	Black Carbon
BL	Baseline Scenario
BTH	Beijing-Tianjin-Hebei region
CCS	Carbon Capture and Storage
CI	Confidence Interval
CIESIN	Center for International Earth Science Information Network
CLMT	Climate Change Mitigation Scenario
CO_2	Carbon Dioxide
$CO_{2\text{-eq}}$	CO_2 Equivalent
COMB	Combined Reduction Scenario
COPD	Chronic Obstructive Pulmonary Disease
CRFs	Concentration-Response Functions
CTMs	Chemical Transport Models
ECMWF	European Centre for Medium-Range Weather Forecasts
EEA	European Environment Agency
EMEP	European Monitoring and Evaluation Programme
FAC2	Fraction of Predictions within a Factor of Two
FGD	Flue Gas Desulfurization
FUND	The Climate Framework for Uncertainty, Negotiation and Distribution
FYP	Five-Year Plan
GAINS	Greenhous Gas – Air Pollution Interactions and Synergies
GBD	Global Burden of Disease
GDP	Gross Domestic Product
GHG	Greenhouse Gas
GPW	Gridded Population of The World
GTOPO30	Global 30 Arc-Second Elevation Data Set

GW	Gigawatt
GWP	Global Warming Potentials
HEI	Health Effects Institute
HRAPIE	Health Risks of Air Pollution In Europe
IEA	International Energy Agency
IHD	Ischemic Heart Disease
IMF	International Monetary Fund
IPCC	Intergovernmental Panel on Climate Change
LC	Lung Cancer
LLE	Loss of Life Expectancy
MAC	Marginal Abatement Costs
MARS	Meteorological Archival and Retrieval System
MB	Mean Bias
MDC	Marginal Damage Costs
MEP	Ministry of Environmental Protection of China
MGE	Mean Gross Error
MHPRC	Ministry of Health of The People's Republic of China
MSC-W	Meteorological Synthesizing Centre-West
Mt	Million Tonnes
Mtce	Million Tonnes of Coal Equivalent
MTFR	Maximum Technically Feasible Reduction Scenario
NBSC	National Bureau of Statistics of China
NDRC	National Development and Reform Commission of China
NH_3	Ammonia
NMB	Normalized Mean Bias
NMGE	Normalized Mean Gross Error
NO_2	Nitrogen Dioxide
NO_x	Nitrogen Oxides
O_3	Ozone
OECD	Organization For Economic Co-Operation and Development
PM	Particulate Matter
PM_{10}	Particulate Matter with less than 2.5 micrometres in diameter
$PM_{2.5}$	Particulate Matter with less than 10 micrometres in diameter
ppm	Parts Per Million
PPP	Purchasing Power Parity

PRD	Pearl River Delta
PWC	Population-Weighted Concentration
r	Correlation Coefficient
RMSE	Root Mean Square Error
RR	Relative Risk
SCPRC	State Council of The People’s Republic of China
SCR	Selective Catalytic Reduction
SNCR	Selective Non-Catalytic Reduction
SO_2	Sulfur Dioxide
stroke	Cerebrovascular Disease
TM5	Tracer Model 5
TSP	Total Suspended Particles
UN	United Nations
USEPA	United States Environmental Protection Agency
VOCs	Volatile Organic Compounds
VOLY	Value of a Life Year lost
WHO	World Health Organization
WPP	World Population Prospects
WTP	Willingness-To-Pay
YOLL	Years of Life Lost
YRD	Yangtze River Delta

Abstract

China is facing severe challenges of air pollution and greenhouse gas (GHG) emissions with rapid economic development, industrialization and urbanization. Continued reductions in air pollutants and GHG emissions are critical, as they pose serious threats to human health and the environment. Air pollution and climate change are largely affected by similar sources and may interact with each other through atmospheric chemical reactions.

This study developed a methodology to analyse the integrated impacts of atmospheric environmental policies on human health and climate change in China. Emission estimation, air quality modelling, health impact assessment, and economic evaluation are synthesized following the full-chain impact pathway from sources of emissions via environmental quality changes to physical and economic impacts. A quantitative assessment of the economic health and climatic benefits from emission reduction of air pollutants and GHG under different present and future scenarios in China is presented. Sensitivity and uncertainty analyses are conducted to provide information on the robustness of the results.

The modelling results show that the years of life lost (YOLL) attributable to $PM_{2.5}$ exposure are 8.2 and 13.4 million in 2010 and 2030 considering current legislation in China. The corresponding damage costs amount to about 3.9 and 5.2% of China's gross domestic product (GDP) in 2010 and 2030, respectively. Aggressive control policies will lead to significant benefits in the aspects of health and climate change mitigation. The integrated benefits of the three investigated policy scenarios are estimated to be 239.9 (95% CI: 41.5, 1387.8), 353.1 (32.9, 3789.4), and 619.5 (87.2, 4403.5) billion EUR_{2010} in 2030, respectively. Clear provincial disparities on emissions, concentration levels, and attainable benefits from policy measures exist in China. Higher per capita benefits from policy measures are estimated for provinces with high population density and energy intensity.

The integrated assessment methodology developed in this study enables simultaneous consideration of air pollution induced health effects and GHG related climatic effects in the process of environmental policy development in China. The reduction potential and integrated benefits from policy measures estimated in this study provide valuable policy insights for China and other developing countries.

Kurzfassung

China sieht sich mit enormen Herausforderungen in den Bereichen der Luftverschmutzung und der Treibhausgas-Emissionen (THG) im Zusammenhang mit rasanter ökonomischer Entwicklung, Industrialisierung und Urbanisierung konfrontiert. Eine fortschreitende Reduktion von Luftschadstoffen und THG-Emissionen ist entscheidend, da diese eine ernsthafte Bedrohung sowohl für die menschliche Gesundheit als auch für die Umwelt darstellen. Die Luftverschmutzung und der Klimawandel sind eng miteinander verbunden, da sie größtenteils von denselben Schadstoff-Quellen beeinflusst werden und sich in der Atmosphäre über chemische Reaktionen gegenseitig beeinflussen können.

In dieser Studie wurde eine Methode zur Beurteilung der ganzheitlichen Auswirkungen der atmosphärischen Umweltgesetzgebung auf die menschliche Gesundheit und den Klimawandel in China entwickelt. Ein Modell der Emissionsabschätzung, Luftqualitätsmodelle, Modelle der Wirkungen auf die menschliche Gesundheit und ein ökonomische Bewertungsmodell wurden durch die ganzheitliche Betrachtung des Übertragungsweges von den Quellen der Emissionen über die Änderung der Qualität der Umwelt zu den physischen und ökonomischen Auswirkungen verbunden. Eine quantitative Auswertung der ökonomischen, gesundheitlichen und klimatischen Vorteile durch die Reduktion von Luftschadstoffen und THG für verschiedene Szenarien in der Gegenwart und Zukunft in China wird vorgestellt. Um Informationen bezüglich der Robustheit der Ergebnisse zu erhalten, wurden Sensitivitäts- und Unsicherheitsanalysen erstellt.

Die modellierten Ergebnisse zeigen, dass die der Langzeitexposition mit $PM_{2.5}$ zuzuschreibenden verlorenen Lebensjahre (Years of life lost YOLL) unter Berücksichtigung der momentanen Gesetzgebung in China 8,2 und 13,4 Millionen in den Jahren 2010 und 2030 betragen. Die zugehörigen Schadenskosten betragen in etwa 3,9% und 5,2% von Chinas Bruttoinlandsprodukts (BIP) in den Jahren 2010 und 2030. Strenge Kontrollgesetzgebungen können zu signifikanten Verbesserungen der beschriebenen Folgen in den Bereichen der Gesundheit und des Klimawandels führen. Die ganzheitlichen Gewinne der drei untersuchten politischen Szenarien betragen 239,9 (95 % CI: 41,5; 1387,8), 353,1 (32,9; 3789,4) und 619,5 (87,2; 4403,5) Mrd. EUR_{2010} im Jahr 2030. Es existieren klare Unterschiede bei den Emissionen, der Höhe der Konzentrationen und den erreichbaren Verbesserungen durch politische Maßnahmen zwischen den verschiedenen Provinzen Chinas. Die pro-Kopf-Verbesserungen durch politische Maßnahmen

werden für Provinzen mit hoher Populationsdichte und Energieintensität höher eingeschätzt.

Die in dieser Studie entwickelte Methode zur ganzheitlichen Bewertung ermöglicht die gleichzeitige Betrachtung von durch Luftverschmutzung verursachten gesundheitlichen Auswirkungen und mit THG zusammenhängenden klimatischen Auswirkungen bei der umweltpolitischen Entscheidungsfindung in China. Die in dieser Studie abgeschätzten Reduktionspotenziale und ganzheitlichen Verbesserungen durch politische Maßnahmen ermöglichen wertvolle Erkenntnisse im Bereich der Gesetzgebung für China und andere Schwellenländer.

1 Introduction

1.1 Background and context

Air quality in China has attracted worldwide attention, especially after the severe haze pollution events in 2013. Rapid economic development, industrialization, and urbanization in developing countries have led to increased air pollution and greenhouse gas (GHG) emissions. In recent decades, China has achieved an unprecedented economic growth with an annual growth rate of gross domestic product (GDP) recorded at over 8%. At the same time, the total energy consumption in China has increased by a factor of five from 1980s to 2010s (NBSC, 2016). China has become the largest contributor to the emissions of multiple air pollutants, e.g. sulfur dioxide (SO_2), nitrogen oxides (NO_x), particulate matter (PM), volatile organic compounds (VOCs), ammonia (NH_3), and GHG in the world (Gregg et al., 2008; Klimont et al., 2009; Xing et al., 2011; Zhao et al., 2013a).

There has been an increasing concern that China's strong economic ascendance, which undoubtedly improves peoples' living quality and technology development, has come at a substantial cost to the environment and public health. Air pollution is now a major challenge for China. In 2013 the notorious heavy smog events during the months of January, October, and November blanketed over 70 major cities in North China, covering 15% of national territory (Guan et al., 2014). As a major component of smog, fine particulate matter with less than 2.5 micrometres in diameter ($PM_{2.5}$) is most of the time the primary pollutant among non-attainment pollutants.

In heavily polluted cities like Beijing, the record of $PM_{2.5}$ concentration reached over 800 μg/m^3, far beyond the highest limit (500 μg/m^3) indicated in the Technical Regulation on Ambient Air Quality Index (MEP, 2012b). Among the 74 Chinese cities which reported monitored air quality data in 2013, over 93% of which have annual average $PM_{2.5}$ concentrations above the national standard (35 μg/m^3), with the highest at 155 μg/m^3 in Xingtai, Hebei. Many cities are facing regular episodes of serious haze events, being stamped as "uninhabitable for human beings" (Li et al., 2015). There is evidence that anthropogenic emissions of air pollutants in China have influences on the local, regional, and even global atmospheric environment (Dickerson et al., 2007; Liang et al., 2004; Rohde and Muller, 2015).

Negative health effects of air pollution have been widely proven from the aspects of toxicology, clinic and epidemiology (Chen et al., 2013; Cohen et al., 2006; Zhang et al., 2012). Ambient PM pollution is found to be the fourth leading risk factor for health in China in 2010 (Yang et al., 2013a). Air pollution impairs the functions of respiratory and cardiovascular systems, which can increase the risks of acute health symptoms (e.g. cough, asthma, bronchitis) and chronic diseases (e.g. chronic obstructive pulmonary disease, heart disease, lung cancer) (Chen et al., 2004; Lim et al., 2012; Pan et al., 2007; Pope et al., 2002; Zhou et al., 2016).

Air pollution was found to have contributed to 0.3 to 2 million annual premature deaths in China (Ma et al., 2016; Matus et al., 2012; Yang et al., 2013a). Several studies (Chen et al., 2013; Kan et al., 2004; Wang et al., 2013a) attempted to quantify the loss of life expectancy (LLE) related to air pollution in China and reported up to 5 years loss. Zhang et al. (2008) estimated that the total economic cost caused by PM pollution was approximately 29 billion U.S. dollar in 2004. Hou et al. (2012) suggested that the health related economic losses caused by PM exposure account for 2.1% of China's GDP for the year 2009.

In addition to the aforementioned air pollutants, extensive emissions of GHG are released during the process of energy consumption. China's energy consumption is overwhelmingly dominated by fossil fuels with coal contributing to over 70% of primary energy consumption (NBSC, 2016). The carbon dioxide (CO_2) emissions in China reached 7.7 billion tons in 2009 (Du et al., 2015). The proportion of Chinese CO_2 emissions increased from 13% of global emissions in 2000 to 23% in 2010 (He et al., 2010).

It is evident that human activities, especially the rising GHG emissions, are changing the climate across the planet (IPCC, 2014). Characterized by global warming, climate change can lead to changes in the likelihood of the occurrence and the strength of extreme weather and climate events or both, e.g. glacial melting, changes in natural ecosystems (Hoegh-Guldberg and Bruno, 2010; Mendelsohn et al., 2012; Rosenzweig et al., 2008). In addition, climate variability is estimated to have negative impacts on human health (Patz et al., 2005).

As a focus for global GHG abatement, China has been a target of carbon tariff policies implemented by developed countries with strict climate change policies. It is estimated that China would suffer a GDP loss of 4% as a result of carbon tariffs imposed in Organization for Economic Cooperation and Development (OECD) countries penalizing carbon-intensive exporters (Böhringer et al., 2011). It can be concluded that China is facing severe challenges of both air pollution control and GHG mitigation.

Air pollution and climate change influence each other through complex atmospheric interactions. Increasing emissions of air pollutants and GHG can each change the energy balance between the atmosphere and the earth's surface which influences the temperature and the chemical composition of the atmosphere (Cifuentes et al., 2001). Classic air pollutants and GHG are largely derived from the same sources, such as fossil fuel combustion and agriculture (Bollen et al., 2009; Swart et al., 2004). Air pollution control measures can help to reduce GHG emissions, and climate change mitigation actions can bring positive impacts on air quality improvement (Chae and Park, 2011; Gielen and Chen, 2001).

Ancillary benefits of GHG reduction policies, such as reduction of air pollutants and air pollution control costs, may offset all or part of the policy implementation costs and provide supportive information for the government to formulate aggressive policies. Understanding the impact of air pollution reduction on climate change helps to achieve a win-win situation and maximize the benefits. Hence, investigating the integrated impacts of air pollution and climate change management strategies is essential for optimal policy-making.

1.2 State and trends of atmospheric environmental management in China

The Chinese government released the Ambient Air Quality Standards (GB3095-1982) in 1982 for the first time. The target air pollutants were total suspended particles (TSP), SO_2, and NO_x. Along with economic development, increasing energy demand supplied by a coal-dominated energy structure brought a series of environmental pressures. In 1996 respirable particulate matter with less than 10 micrometres in diameter (PM_{10}) was added to the Ambient Air Quality Standards' target air pollutant list. 46 environmental protection key cities were required to release weekly air quality records since 1997.

PM_{10} and nitrogen dioxide (NO_2) replaced TSP and NO_x as indicative air pollutants since 2000, and 46 cities started to report daily air quality. In the 21st century, air pollution problem in China became increasingly more complicated as a result of the sky-rocketing economic growth of China, characterised by large amount of coal consumption and a dramatic increase in the number of urban motor vehicles. The main sources of air pollutants shifted from primarily coal burning to a combination of coal burning and vehicle usage (Wang and Hao, 2012).

From 2000 to 2005 emissions of SO_2 in China increased over 27%, even though the Chinese government set a target for a 10% reduction (MEP, 2006). The implemented emission reduction measures failed to offset the impact of the massive increase in fossil-fuel consumption. During the 11th Five-Year Plan (FYP) period (2006-2010), stricter regulations were enforced for SO_2 reduction, e.g. all new and most existing thermal power plants were required to install flue gas desulfurization (FGD) systems, and small units with low energy efficiency were gradually shut down. The control measures significantly reduced SO_2 emissions by 14% from 2005 to 2010 (MEP, 2011).

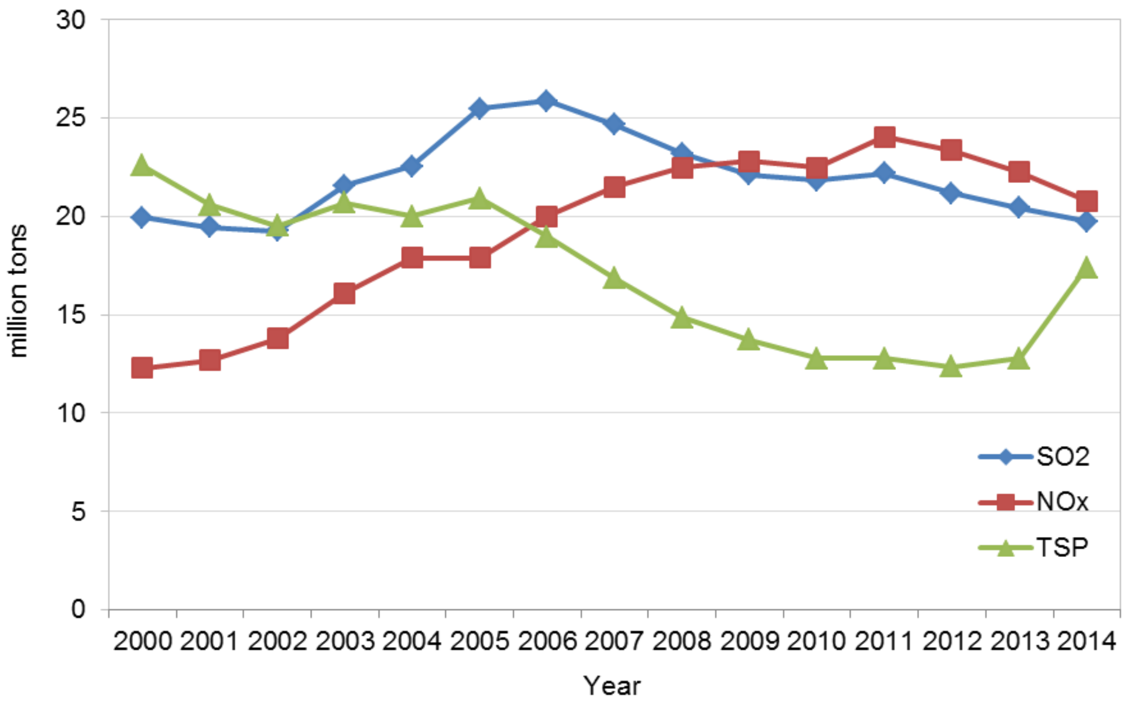

Figure 1.1. Emissions of SO_2, NO_x and TSP in China 2000-2014.
Source: based on NBSC (2015).

However, the less regulated NO_x and VOCs have continued to increase. Figure 1.1 shows the emissions trends of SO_2, NO_x, and TSP reported by Ministry of Environmental Protection of China (MEP). Many studies reported even higher NO_x emissions (Liu et al., 2017; Zhang et al., 2007). As a result of large NO_x and

VOC emissions, photochemical smog and high ozone (O_3) concentration were observed across China. TSP emissions in China decreased continuously during the 11th FYP; however this trend slowed down during the 12th FYP (2011-2015). Due to the growing concerns on PM pollution and technology development, the scope of environmental statistics was expanded to include more emission sources, as reflected by the increase of reported TSP emissions from 2013 to 2014.

Rapid urbanization in China has formed several metropolitan regions, mega-cities, and medium and small-sized cities connected by highways. The scope of air pollution evolved from local primary pollution to regional secondary pollution (Huang et al., 2014). The principle pollutants in most pollution days of key cities are $PM_{2.5}$ and PM_{10} (Yang et al., 2011). Simulation results indicate that large areas of China are covered with high $PM_{2.5}$ concentrations (Wang et al., 2013c; Xing et al., 2015). The number of haze days increased significantly in most parts of central-eastern China during the last decades (Song et al., 2014).

With the increasing public concern about the health impacts of $PM_{2.5}$ pollution, the Ambient Air Quality Standards (GB 3095-2012) issued in February 2012 added limits on $PM_{2.5}$ and O_3 concentration. Table 1.1 presents the current ambient air quality standards in China compared with the interim targets and air quality guidelines (AQG) set by World Health Organization (WHO). It can be seen that the setting of Chinese standards has gradually become in line with the world standards. The annual mean $PM_{2.5}$ limits of Class I (15 μg/m^3) and Class II (35 μg/m^3) standards in China correspond to the WHO's interim target 3 (IT-3) and interim target 1 (IT-1), respectively.

From January 2013, 113 cities in China have been required to monitor and publish $PM_{2.5}$ concentration. As a response to the severe haze pollution in China, the Chinese government issued the Air Pollution Prevention and Control Action Plan in September 2013. The Action Plan set a target of reducing urban PM_{10} concentration by 10% from 2012 to 2017, and more ambitious $PM_{2.5}$ reduction targets for key regions (SCPRC, 2013). This was the first time that quantitative concentration control goals with specific time limits were set by the Chinese government (Jin et al., 2016).

Table 1.1. Comparison of ambient air quality standards of China and WHO.

Pollutant	Averaging period	China[a] (μg/m^3)		WHO[b] (μg/m^3)			
		Class I	Class II	IT-1	IT-2	IT-3	AQG
$PM_{2.5}$	Annual mean	15	35	35	25	15	10
	24-hour mean	35	75	75	50	37.5	25
PM_{10}	Annual mean	40	70	70	50	30	20
	24-hour mean	50	150	150	100	75	50
O_3	8-hour mean	100	160	160	-	-	100
	Hourly mean	160	200	-	-	-	-
NO_2	Annual mean	40	40	-	-	-	40
	Hourly mean	200	200	-	-	-	200
SO_2	Annual mean	20	60	-	-	-	-
	24-hour mean	50	150	125	50		20
	Hourly mean	150	500	-	-	-	-

Source: [a]MEP (2012a); [b]WHO (2005). Note: IT (Interim Target); AQG (Air Quality Guideline).

Besides classic air pollutants, GHG emissions have also increased sharply with the growth of energy consumption. China surpassed the United States as the country emitting the most CO_2 in 2007 (IEA, 2016). With an increasing attention paid to climate change, the Chinese government made a commitment to achieve a 40-45% reduction in carbon intensity (carbon emissions per unit of GDP) by 2020, as compared to the 2005 levels, in the climate conference in Copenhagen in 2009.

Energy caps have only recently been more widely discussed as a mechanism for limiting energy use (Luo et al., 2016). The government has been setting up plans to reduce energy intensity (energy consumption per unit of GDP) in the overall context of national sustainable development strategy. Policies relating to energy sectors, such as replacing coal with natural gas and renewable energy, and improving energy efficiency through promoting advanced technologies, are implemented with the aim of mitigation and adaptation to climate change.

In China, the central government has been releasing a series of economic and social development initiatives in the form of FYP, which outlines the directions, targets and methods of future developments. The national environmental planning within the FYP framework dominates the environmental governance in China. Energy saving and emission reduction have been mentioned in China's annual reports since the 6th FYP (1981-1986). The national total emission control policies were initiated in the 9th FYP (1996-2000), and further specified in the 10th FYP (2001-2005). However, only until the 11th FYP (2006-2010), a binding energy intensity target was introduced, stringent measures were implemented and the control targets were achieved.

In the 12th FYP, a binding carbon intensity target was included for the first time. Table 1.2 summarizes the main national energy and mandatory emission reduction targets in the 12th (2011-2015) and the most recent 13th (2016-2020) FYP. Based on the Copenhagen commitment, 17% and 18% reduction targets of carbon intensity during the corresponding FYP period were set consecutively in the 12th and 13th FYP. Although the energy intensity of China was reduced by 18.2% from 2010 to 2015, which exceeded the target of the 12th FYP (16%), the Chinese government set a more conservative reduction target regarding energy intensity in the 13th FYP (15%).

After the 12th FYP, the share of non-fossil fuel to overall energy consumption was increased to 12% by 2015, and was expected to reach at least 15% by 2020. It can be seen from Table 1.2 that the actual reduction rates of SO_2, NO_x and NH_3 emissions all exceeded the targets during the 12th FYP. With the reduction target for NH_3 remaining at 10%, the targets for SO_2 and NO_x reduction were almost doubled in the 13th FYP compared to those in the 12th FYP. It is worth noting that owing to the decreasing baseline levels (2010 level for 12th FYP and 2015 level for 13th FYP), the absolute reduction amount would be lower given the same reduction percentage.

Table 1.2. Main energy and emission reduction targets in the 12th and 13th Five-Year Plan of China.

Variable	12th FYP targets	12th FYP achievements	13th FYP targets
	(Compared to 2010)		(Compared to 2015)
Energy intensity	-16%	-18.2%	-15%
Carbon intensity	-17%	-20%	-18%
Non-fossil fuel percentage	11.4%	12%	15%
Sulfur dioxide	-8%	-18%	-15%
Nitrogen oxides	-8%	-18.6%	-15%
Ammonia nitrogen	-10%	-13%	-10%

Source: SCPRC (2011b, 2016).

Additionally, the 13th FYP for the first time included reduction of VOCs (10% reduction nationwide by 2020 compared to 2015) as an expected target. VOCs are a critical component and precursor of both $PM_{2.5}$ and O_3, which are emitted from not only fossil fuel consumption, but also solvent use and industrial processes. The addition of VOC control target indicates that the focus of pollution control in China will expand from energy sector to multiple sources.

Previous experience in atmospheric environmental management provides directions for the design and assessment of environmental policies. Post-pollution treatment is a common problem of environmental protection in developing countries. China's air pollution control in the last decades has emphasized the end-of-pipe control. However, experience from developed countries has proven the cost efficiency of energy conservation and energy structure improvements. Such measures can result not only in less air pollutants in the short-term, but also yield considerable co-benefits of GHG reduction in the long-term.

Regional air pollution in metropolitan clusters, such as the Beijing-Tianjin-Hebei (BTH) region, Pearl River Delta (PRD) and Yangtze River Delta (YRD), has been one of the most challenging issues in pollution control of China. It is estimated that regional transport contributes around 50% of the PM concentrations in urban and rural areas in China (Chen et al., 2017; Sun et al., 2017). Policy development and evaluation should support joint prevention and control of regional air pollution.

It has only been recently that concretized concentration control targets were specified in some environmental plans. Total emission control has been a prominent feature of China's air pollution management for a long period of time. This is to some extent owing to the fact that emission control is easier to implement and holds higher degree of certainty as compared to air quality control. However, the 11th FYP experience has proven that achieving certain emission reduction target of a single pollutant does not necessarily bring air quality improvement (Jin et al., 2016).

Previous policies were mostly problem-oriented, i.e. they address one issue at a time with little consideration on the interacting impacts of reducing one pollutant on the other pollutants. It is evident that reducing a single type of pollutant can hardly be effective or efficient to improve air quality and achieve sustainable development (Reis et al., 2005). Synchronous reduction of classic air pollutants and GHG is critical for addressing health and environmental problems in China. Climate friendly air pollution control strategies call for the development of comprehensive environmental policies which integrates various atmospheric environmental problems.

It should be emphasized that the objectives of policy measures are to improve air quality, protect public health, and minimize welfare loss (Sabel et al., 2016). To ensure the achievement of these objectives, policy-making must be supported by an integrated assessment of the impacts of potential control options on concentration, public health and climate change.

1.3 Concepts of integrated assessment and research review

Atmospheric environmental management and its evaluation are multidisciplinary in nature, and demand a variety of expertise and methodology. To support decision-making, an integrated assessment should be made to coordinate all or at least the most important information, i.e. damages, benefits, and costs. Thus integrated assessment is defined as a multidisciplinary process of synthesizing knowledge across scientific disciplines with the purpose of providing all relevant information to decision makers (Friedrich, 2016).

An integrated assessment should comprehensively explore possible future trajectories of human and natural system, develop insights into key questions of policy formation, prioritize research needs in order to enhance the ability to identify robust policy options (Bruce et al., 1996). From an air pollution control standpoint, if the primary aim is to reduce health impacts caused by $PM_{2.5}$ in an efficient way, the following information should be integrated:

1) the effects of considered measures on energy consumption and structure; 2) the impacts of control measures on primary and precursors of secondary PM emissions from all sources, i.e. natural and anthropogenic; 3) the co-benefits or trade-off of the measures on the reduction of emissions of other species such as GHG; 4) the effects of control measures on $PM_{2.5}$ concentration and the associated health impacts; and 5) the integrated impacts of the measures in a common unit, preferable conceivable monetary unit (e.g. euro), which makes the various impacts comparable and supports a cost-benefit analysis.

A growing number of studies have attempted to provide scientific advice on the integrated health and GHG reduction benefits of atmospheric environmental strategies in different geographic domain. On a global scale, many studies focused on the co-benefits of global climate change policies (Rafaj et al., 2013; Rao et al., 2016; West et al., 2013). In regional and country level, studies were mostly conducted for developed countries, especially Europe and the United States (Dudek et al., 2003; Friedrich et al., 2011; Matus et al., 2008; Preiss et al., 2013; Tollefsen et al., 2009).

In the case of China, few studies have been conducted on national level. He et al. (2010) showed that significant co-benefits can be achieved by implementing two sets of energy policies in China. Dong et al. (2015) analysed the emission reduction potentials of carbon mitigation policy and air pollutant abatement technologies on the provincial level in China. Most studies have focused on energy intense provinces (Aunan et al., 2004, 2006; Vennemo et al., 2009), metropolitan areas, and big cities (Chen et al., 2007; Liu et al., 2013). From a sectoral point of view, specific interests have been placed on the energy (Wang and Smith, 1999; Zhao et al., 2016), industry (Hasanbeigi et al., 2013; Yang et al., 2013b), and transport sector (Geng et al., 2013; Mao et al., 2012).

Existing integrated assessment studies of atmospheric environmental management in China are quite limited in terms of geographic and sectoral coverage and methodological development as compared with those of developed countries. A large proportion of previous studies only considered emission reduction benefits without addressing the impacts of policy measures on environmental quality and human health (Xu and Masui, 2009; Zhang and Wang, 2011).

Analyses have highlighted the potential GHG reduction effects of short-term pollution control measures (Gielen and Chen, 2001; Nielsen and Ho, 2013). There is a lack of attention to the long-term benefits of climate change mitigation policies. Furthermore, very few studies addressed the underlying uncertainties of the assessment (Rabl et al., 2014), which are however essential information for rational decision-making.

Hence, there is a pressing need for an integrated assessment framework that covers the full impact pathway of atmospheric environmental management, which synthesizes advanced models and appropriate parameters from various contributing disciplines, and allows for estimation and monetization of integrated impacts resulting from national, regional, and local policy measures in China, along with careful consideration of uncertainty.

1.4 Scope and objectives

Based on the context discussed above, this study aims to 1) establish an integrated assessment modeling framework to analyse the impacts of atmospheric environmental policies on human health and climate change in China; 2) improve the methodology for conducting integrated assessment of atmospheric environmental policies in China and other developing countries; 3) address the magnitude, in physical and economic terms, of the national and regional benefits of air pollution control and climate change mitigation measures; 4) enable the consideration of integrated impacts in the process of environmental policy development; 5) provide insights for the formulation and implementation of China’s atmospheric environmental policies.

For the application of integrated assessment, five scenarios, i.e. a baseline scenario for the year 2010, a business as usual (BAU) scenario, and three policy scenarios for the year 2030 are developed. Emissions of air pollutants and GHG from all relevant sources are estimated for 32 regions in China (not including Taiwan) under all the scenarios. Mitigation potentials of air pollution control and climate change mitigation measures are identified.

Atmospheric models are applied to simulate ambient concentration levels of $PM_{2.5}$, which is selected as the indicative pollutant to estimate air pollution induced health effects. To adjust the bias of concentration modelling, simulated results are compared with monitoring data. Health impacts of $PM_{2.5}$ pollution under different scenarios, in terms of years of life lost (YOLL), are analysed through synthesizing concentration data, population and health data, and concentration-response functions (CRFs). The achievable health benefits from policy measures are compared on provincial level.

The impacts of policy measures on human health and climate change are aggregated by transferring physical impacts to monetary values. The integrated benefits of policy scenarios are investigated on national and provincial level. Finally, sensitivity and uncertainty analyses are conducted to help to draw reliable conclusions from policy assessment.

1.5 Thesis organization

This thesis is composed of 5 chapters with Chapter 1 setting the background and context, stating the state and trends of atmospheric environmental management in China, describing the concepts of integrated assessment and limits of previous studies, and defining the scope and objectives of this work. The rest of the thesis is structured as follows. Firstly the overall methodology of this study is illustrated in Chapter 2. The general framework of integrated assessment is introduced followed by detailed description of the models, methods, and data sources used in the analysis.

The main results and findings from the scenario study, regarding emissions estimation, air quality simulation, air pollution induced health effects, and monetized and aggregated health and GHG reduction benefits from policy measures, are presented in Chapter 3. Based on an overall discussion of the results, implications for China's air pollution control and climate change mitigation policies are addressed. In Chapter 4, sensitivity analyses of the assessment results in regards to certain parameters and an overall uncertainty analysis are discussed.

Lastly, conclusions of the overall thesis along with recommendations for future research are summarized in Chapter 5.

2 Overall methodology

This study aims to develop a methodology to conduct an integrated assessment of environmental policies in China. Integrated assessment is a multidisciplinary process of synthesizing knowledge across scientific disciplines with the purpose of providing all relevant information for environmental policy-making (Friedrich, 2016). This chapter describes firstly the framework of the methodology, and then specifies the data and methods used in each module.

2.1 Framework of integrated assessment

The framework of integrated assessment of environmental policies is presented in Figure 2.1. The principal approach for estimating and monetizing policy impacts is named the impact pathway approach (Bickel and Friedrich, 2005). It is a bottom-up-approach, which can be used to estimate and monetize socio-environmental damages to support the internalization of external costs.

Previous studies are mostly limited to the GHG reduction co-benefits of air pollution control policies or the air quality co-benefits of carbon policies in China (Dong et al., 2015; He et al., 2010; Peng et al., 2017). The integrated assessment framework of this study, however, supports simultaneous assessment of the effects of air quality management and climate change mitigation policies in terms of changes in emissions, concentration and exposure levels, and physical and economic impacts. The main steps of the methodology are as follows:

- Scoping: the exact question to be answered is decided. The elements that should be included in the assessment are defined, which involves specifying as precisely as possible all the main factors of the issue, and the connections between each other.

- Scenario development: a baseline scenario for a recent past year, a BAU scenario, and policy scenarios for a future year are defined and generated. Emissions of air pollutants as well as GHG are analysed for all the scenarios based on activity data and emission factors.

- Concentration modelling: the emission data of the developed scenarios and meteorological data are used as inputs for atmospheric models which simulate the transport and chemical transformation of air pollutants in the troposphere, and output concentration maps of the targeted air pollutant for the study area.

- Health impact assessment: based on the modelled concentration and population data (e.g. gridded population, health data), impacts on human health caused by air pollution are estimated using CRFs derived from epidemiological studies, which relate a change in the concentration of a pollutant with a change in the incidence of a health endpoint.

- Economic evaluation: in order to aggregate endpoints and present an intuitive comparison of different scenarios, monetary valuation of air pollution and GHG emission induced impacts on human health and climate change effects is conducted. Health benefits resulting from reduction of air pollutants emissions and GHG reduction benefits are transformed into a monetary unit using results from contingent valuation studies and the costs of climate change analysis. The effectiveness of the designed policy scenarios is then compared and analysed.

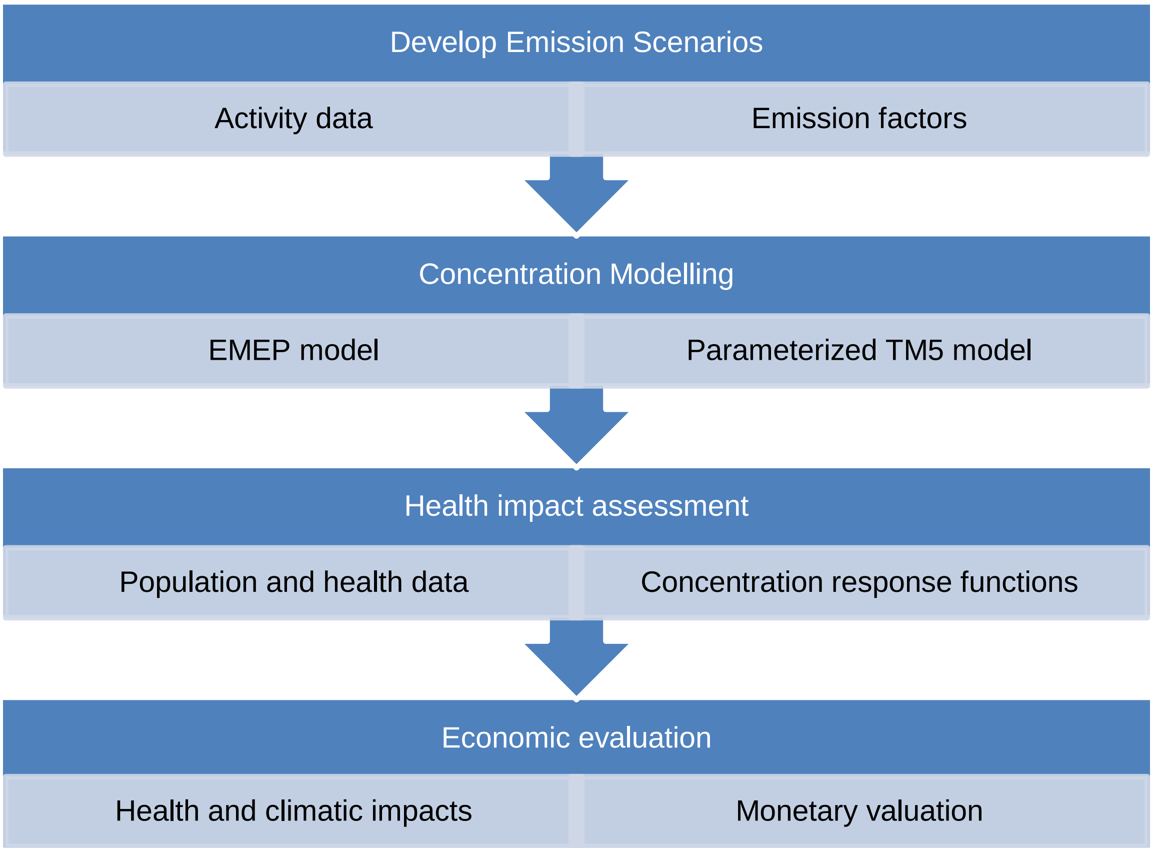

Figure 2.1. The framework of integrated assessment.

2.2 Data and methods

2.2.1 Selection of air pollution indicator

Air pollution is the result of diverse pollutants. Normally air pollution control strategies aim to reduce multiple air pollutants. Many air pollutants are emitted from similar sources (e.g. coal combustion), and therefore their concentrations are significantly correlated (collinearity). Due to the presence of such collinearity, current epidemiological studies do not have the capacity to attribute the health effects caused by air pollution to a particular pollutant. Simply adding up the health effects calculated from different air pollutants can cause “double counting”, which will result in overestimation (Héroux et al., 2015; Künzli et al., 2000).

Many toxicological studies and epidemiologic analyses have confirmed that the toxicity hazard of PM is the most serious among air pollutants (Brunekreef, 1997; Hart et al., 2011; Puett et al., 2009). PM is a complex mixture of solid particles and liquid droplets such as black carbon (BC), sulphates, trace metals, and organics (USEPA, 2016). Typically classified by size according to its nominal median aerodynamic diameter (measured in micrometres), PM has contributions from both primary sources (i.e. emitted directly into the atmosphere) and secondary processes (i.e. formed in the atmosphere from precursor emissions). It is currently the principle air pollutant affecting China’s urban air quality (Yang et al., 2011).

$PM_{2.5}$, also known as fine inhalable particles, has a larger specific surface area than coarser particles, and is more likely to become the carrier and reaction body of other contaminants. It is able to get deep into lung and even enter the bloodstream through respiratory system, and cause acute and chronic respiratory and cardiovascular diseases. There are extensive epidemiological studies that relate $PM_{2.5}$ to negative health impacts (Brunekreef, 2007; Lepeule et al., 2012; Pope and Dockery, 2006; Puett et al., 2008; Zeger et al., 2008).

Epidemiologic cohort studies of long-term exposure, which form the basis of CRFs used for health impact assessment, found $PM_{2.5}$ to be the most robust indicator of adverse (mortality) impacts (Chen et al., 2008; Pope et al., 2002), and demonstrated that analysing PM induced health effects achieve optimum results (Ma et al., 2016). Hence, $PM_{2.5}$ is selected as the indicative pollutant to estimate the health effects of air pollution in China in this study. Although CRFs of other air pollutants (e.g. NO_2, O_3) exist, they are not included in this study considering higher uncertainty and poorer data availability (Heinrich et al., 2013).

2.2.2 Design of emission scenarios

2.2.2.1 General approach of emission estimation

Estimates of emissions of air pollutants and GHG are the fundamental input for chemical transport models (CTMs) and impact assessment on human health and climate change. In this study the Greenhouse gas – Air pollution Interactions and Synergies (GAINS) model is used to produce emissions scenarios. GAINS estimates emissions of pollutant based on activity data (consumption of fuel, industrial processes and production), uncontrolled emission factors, removal efficiency of emission control measures, and the penetration rate of such measures as illustrated by Equation 2.1.

$$Em_{i,j}(t) = \sum_{k,m} act_{j,k}(t) * ef_{i,j,k,m} * X_{i,j,k,m} \qquad \text{Equation 2.1}$$

Where,

$Em_{i,j}(t)$ = emission of pollutant i in region j in year t.

$act_{j,k}(t)$ = activity level of type k in region j in year t.

$ef_{i,j,k,m}$ = emission factor of pollutant i for activity k in region j after application of control measure m.

$X_{i,j,k,m}$ = penetration rate of the abatement measure m for pollutant i for activity k in region j.

The geographical domain of the emission estimation model covers 32 regions in China which include 31 provinces and province-level autonomous regions and municipalities in mainland China, and a combined region of Hong Kong and Macau. Taiwan was not included. Emissions of SO_2, NO_x, PM in several size classes, VOCs, NH_3, CO_2 and other GHG are estimated at provincial level, which can then be aggregated to get the national total. For calculating total GHG emissions, the global warming potentials (GWP) defined in the Kyoto protocol are used (Amann et al., 2011).

The emission sources are categorized to ten major sectors: (1) power and heating plants; (2) fuel conversion; (3) residential combustion; (4) industrial combustion; (5) industrial processes; (6) road vehicles; (7) Non-road machinery; (8) agriculture; (9) waste; (10) non-energy use of fuels.

2.2.2.2 Scenario design

Five scenarios are analysed in this study: a baseline scenario for a past year (2010), a BAU scenario, and three policy scenarios for a future year (2030) as listed in Table 2.1. Emissions of SO_2, NO_x, PM, VOCs, NH_3, and GHG are estimated for all the scenarios based on assumptions of socio-economic drivers and effects of various measures. Activity data, emission factors, application rate of control measures of different scenarios are collected (BL, BAU, and CLMT) and modified (MTFR and COMB) using the GAINS model based on multiple studies (Klimont et al., 2013, 2016; Wang et al., 2014; Zhao et al., 2013b).

Table 2.1. List of emission scenarios.

Scenario name	Abbr.	Year	Description
Baseline	BL	2010	Current situation
Business as usual	BAU	2030	Future estimation under current legislation
Maximum technically feasible reduction	MTFR	2030	Adoption of best available end-of-pipe control technologies
Climate change mitigation	CLMT	2030	2 degree climate change mitigation pathway
Combined reduction	COMB	2030	Combination of MTFR and CLMT

The baseline scenario for 2010 (BL) serves as an estimation of current situation, which is the basis for future projection and supports model validation. 2030 is selected as a representative future year, considering that it is not too close that there would not be enough time for policy implementation, or too far away that the uncertainty of future projection would be too high. The BAU scenario is the estimation under current legislation, which assumes efficient enforcement of committed legislation as of the end of 2010 (e.g. China's Twelfth FYP), but no future policies.

The GDP of China is projected to increase from 3,472 billion EUR_{2010} (euros in 2010 price) in 2010 to 11,400 billion EUR_{2010} in 2030 (Klimont et al., 2016), and the population is assumed to grow from 1.34 billion in 2010 to 1.42 billion in 2030. The Chinese government has set a target to reduce CO_2 emissions per unit GDP by 40-45% by 2020 compared with 2005 levels (SCPRC, 2009). Based on the plans for renewable energy of the National Development and Reform Commission of China (Wang and Hao, 2012), the installed capacities of hydropower, nuclear power, wind power, solar power, and biomass power are projected to be 350, 70, 60, 9, and 30 gigawatt (GW) in 2030, respectively.

The proportion of electricity production from coal-fired power plants is expected to be 73% in 2030 in the BAU scenario, and the total heat supply of 345 Mtce (million tonnes of coal equivalent). Energy saving and emission reduction plans, regulations, and standards (NDRC, 2004, 2005, 2007a, 2007b, SCPRC, 2010, 2011a, 2011c, 2012) released by the Chinese government are assumed to be realized on time. Two types of control measures are considered for the policy scenarios including end-of-pipe control measures such as installations of FGD systems, selective catalytic reduction (SCR) modules and static precipitators, and climate change mitigation measures, e.g. promotion of renewable energy, energy efficiency improvements, and installation of carbon capture and storage (CCS) systems.

The maximum technically feasible reduction (MTFR) scenario assumes implementation of best available end-of-pipe control technologies ignoring political or economic constraints for the year 2030. The activity levels of the MTFR scenario are assumed to be the same as in the BAU scenario. Full penetration of best available abatement measures, which are applied in developed countries, is projected for various sectors in China by 2030. It can be considered as a best estimation of end-of-pipe control measures.

The climate change mitigation (CLMT) scenario describes a situation that emissions of GHG are reduced to an amount that limits average temperature increase to 2°C compared to preindustrial times. The activity levels of the CLMT scenario rely on the International Energy Agency (IEA) 2 degree pathway (IEA, 2012). The emission factors and the penetration rate of the abatement measure are assumed to be the same as in the BAU scenario.

This scenario simulates the impacts of solely climate change mitigation measures. The main measures considered in the CLMT scenario are deploying CCS in power generation and industrial sectors, promoting clean energy (e.g. wind, nuclear, solar, biofuels and hydropower), developing and implementing smart grids and efficient heating and cooling, and vehicle fuel economy improvements.

The combined reduction (COMB) scenario is a combination of the MTFR and CLMT scenarios. It adopts the activity levels in the CLMT scenario and the emission factors as well as application rates of end-of-pipe control measures in the MTFR scenario. It is the best estimation of fully implementation of both end-of-pipe and climate change mitigation measures.

2.2.3 Atmospheric modelling and exposure assessment

Results of two atmospheric models are integrated in the study to link changes in emissions to changes in concentrations of air pollutant ($PM_{2.5}$): the Meteorological Synthesizing Centre-West (MSC-W) of the European Monitoring and Evaluation Programme (EMEP) and the parameterized Tracer model 5 (TM5). A population exposure level assessment is then conducted based on ambient air pollution level and gridded population data.

2.2.3.1 Concentration modelling for BL and BAU scenarios

For concentration levels of $PM_{2.5}$ in the BL scenario of 2010 and the BAU scenario of 2030, simulation results of the regional EMEP MSC-W model are obtained from the Norwegian Meteorological Institute. EMEP is a 3D Eulerian model, typically used to tackle problems within the fields of particles, acid deposition, and tropospheric O_3 (Simpson et al., 2012), which takes emissions and meteorology data as input and simulates ambient concentrations of air pollutants. The model domain covers 5-55°N and 62-135.2°E with a resolution of 0.1 by 0.1 degree.

Although CTMs have proven to be capable of producing atmospheric pollution phenomena, there are many sources of uncertainty in their use for operational applications (Kukkonen et al., 2012), e.g. uncertainties in meteorological data and formation processes. PM deficit, a systematic underestimation of total PM, has been reported in a number of chemical transport modelling studies (Bessagnet et al., 2016; Fu et al., 2012; Monteiro et al., 2013; Vautard et al., 2007).

Though the underestimation of $PM_{2.5}$ concentration by large-scale atmospheric models is generally observed (Prank et al., 2016; Xing et al., 2015), no previous work has conducted systematic bias adjustment especially for China. In this study, the developed methodology is extended with a bias adjustment approach aiming to reduce the bias between observed and simulated annual average $PM_{2.5}$ concentration in China.

Figure 2.2. Locations of selected cities for bias adjustment of concentration modelling.

The modelled results of $PM_{2.5}$ concentration in China for 2010 are compared with monitoring data to evaluate and adjust modelling bias. $PM_{2.5}$ measurement data in 2010 for China is quite limited. National monitoring stations began to monitor and publish $PM_{2.5}$ concentration only after 2013. Even though other data sources exist (e.g. measurements from scientific studies (Wang et al., 2013b; Yu et al., 2013; Zhang et al., 2013b; Zhao et al., 2013c) and the U.S. embassy in China), they have a limited geographic coverage (normally only for one or several cities) and are not consistent in monitoring and reporting methods.

Considering the spatial scale of the study and data availability and reliability, the air pollution index (API) data based on PM_{10} measurements of 86 major cities in China for the year 2010 reported by the data center of the MEP are used for the validation. Figure 2.2 displays the locations of the 86 cities, which spread almost across the whole China.

The API of a certain pollutant is calculated by:

$$I_C = I_{low} + \frac{I_{high} - I_{low}}{C_{high} - C_{low}}(C - C_{low}) \qquad \text{Equation 2.2}$$

Where,

I_C = API of observed concentration level C.

I_{high}, I_{low} = API breakpoints corresponding to concentration breakpoints of C_{high}, C_{low} closest to the observed concentration C.

Table 2.2. The air pollution index (API) and corresponding PM_{10} concentrations.

API	50	100	200	300	400	500
PM_{10} concentration (μg/m^3)	50	150	350	420	500	600

The breakpoints of API and PM_{10} concentration set by MEP are shown in Table 2.2. $PM_{2.5}$ concentration is calculated based on API derived PM_{10} concentration and estimated ratio of $PM_{2.5}$ / PM_{10}. Taking the results of previous studies in China (Cao et al., 2011; Liu et al., 2008; Wang et al., 2002), the conversion factor of $PM_{2.5}$ / PM_{10} is set as 0.65 in this study. Annual average $PM_{2.5}$ concentrations derived from monitoring records are obtained for 86 cities in China, and are used as representatives of $PM_{2.5}$ observations for bias adjustment.

To increase model skills, different bias-adjustment techniques have been developed to remove systematic errors (Djalalova et al., 2010; Kang et al., 2010; McKeen et al., 2005; Silibello et al., 2015). In this study, the effects of three bias adjustment approaches are examined: (1) an additive correction of the mean bias (Equation 2.3), (2) a multiplicative ratio correction (Equation 2.4), (3) a linear regression correction taking the monitored data as a dependent variable, while modelled data and other supplementary data (meteorology, population density) as independent variables (Equation 2.5).

$$C_i^{adj} = C_i^{model} + \frac{1}{n}\sum_n (C_i^{model} - C_i^{obs}) \qquad \text{Equation 2.3}$$

$$C_i^{adj} = C_i^{model} * \frac{\sum_n C_i^{obs}}{\sum_n C_i^{model}} \qquad \text{Equation 2.4}$$

Where,

C_i^{adj}, C_i^{model}, C_i^{obs}= bias adjusted, original modelled, observed concentrations in city i of n cities.

$$O(i) = c + a_1 \cdot X_1(i) + a_2 \cdot X_2(i) + \cdots + a_n \cdot X_n(i) \qquad \text{Equation 2.5}$$

Where,

$O(i)$ = estimated value of $PM_{2.5}$ concentration for city i.

$X_1(i), X_2(i), \ldots, X_n(i)$ = *n* number of individual supplementary variables for city i.

$c, a_1, a_2, \ldots, a_n$ = n+1 parameters of the regression model.

Apart from the modelled value of $PM_{2.5}$, the linear regression model considers also supplementary data including altitude, population density, temperature, wind speed and relative humidity, following the methodology developed in Horálek et al. (2013). The altitude data field (in meters) of the Global 30 Arc-Second Elevation Data Set (GTOPO30) that covers the same domain as of the concentration modelling is extracted through a spatial data access tool (ORNL DAAC, 2017).

The population density (in inhs.km^{-1}) is based on the Gridded Population of the World (GPW) data set (CIESIN, 2005) and the United Nations' (UN) World Population Prospects (WPP) (UN, 2015). Meteorological parameters such as temperature at 2 meters (in K), wind speed at 10 meters (in m.s^{-1}), relative humidity at 2 meters (in %) are collected from the Meteorological Archival and Retrieval System (MARS) of the European Centre for Medium-range Weather Forecasts (ECMWF).

Linear regression models considering different combination of independent variables are developed and compared. The linear regression is applied for the logarithmically transformed data of population density, monitored and modelled $PM_{2.5}$ values, as suggested by Horálek et al. (2013). The Akaike information criterion (AIC) is used for model variables selection. The results of the bias adjustment are shown in section 3.2.2.

2.2.3.2 Concentration modelling for policy scenarios

Owing to the calculation intensity and long running time of CTMs, usually only a limited number of scenarios can be calculated. To enable concentration modelling of massive policy scenarios, a parameterized version of the TM5 model, which is computationally much less intensive than the EMEP model, is used. The model is composed of linearized source-receptor matrices describing the spatial response of $PM_{2.5}$ concentration to changes in precursor emissions in a given source region.

The source-receptor matrices are derived through a sample of the TM5 model runs with systematic perturbations of emissions from each source regions (Amann et al., 2008). The resulting changes of $PM_{2.5}$ concentrations over the model domain have been related to the assumed perturbation in emissions. The parameterized TM5 model covers the domain of 10-60°N and 60-144°E with a resolution of 1 by 1 degree. For each of the 28 source regions, changes of annual emissions of primary $PM_{2.5}$ (primary organic matter, BC) and the precursors (SO_2, NO_x, NMVOCs) are required as input to estimate the corresponding $PM_{2.5}$ concentration changes.

NH_3, which is also a precursor of secondary $PM_{2.5}$, is not included in this version of the model. NH_3 emissions mainly come from livestock and fertilizer applications, which are not the focus of current air pollutant control strategies in China (Xing et al., 2011). The differences of NH_3 emissions among BAU and policy scenarios are relatively small. Therefore, it has little impacts to the modelling results.

2.2.3.3 Population data and exposure assessment

The exposed population includes all residents in mainland China. Gridded population data is obtained by spatially distributing the total population data of China for the year 2010 and 2030 from the WPP medium fertility estimates (UN, 2015) according to the spatial pattern of the GPW data set (CIESIN, 2005). It is forecasted that the population in China will increase from 1.34 billion in 2010 to 1.42 billion in 2030 (UN, 2015). The resulting population distribution is shown in Figure 2.3. It is assumed that population in each grid grows at the same rate with the national population growth rate from 2010 to 2030; the population age structure in each grid is identical with the national age structure.

In order to show the residents' exposure level to $PM_{2.5}$, population-weighted concentration (PWC) of $PM_{2.5}$ is calculated using the following formula:

$$PWC = \frac{\sum(Pi * Ci)}{\sum Pi} \qquad \text{Equation 2.6}$$

Where,

PWC = population-weighted $PM_{2.5}$ concentration,

Pi = population in grid i,

Ci = $PM_{2.5}$ concentration in grid i.

Exposure depends not only on the ambient concentration of pollutants at any given time and location, but also on the exposure patterns, intake fractions, risk factors and sensitivity of the exposed population (Brauer et al., 2012). PWC represents a rough but commonly used estimate of the potential for human exposure, and gives intuitive and easy-to-compare quantification about air quality improvements in different scenarios.

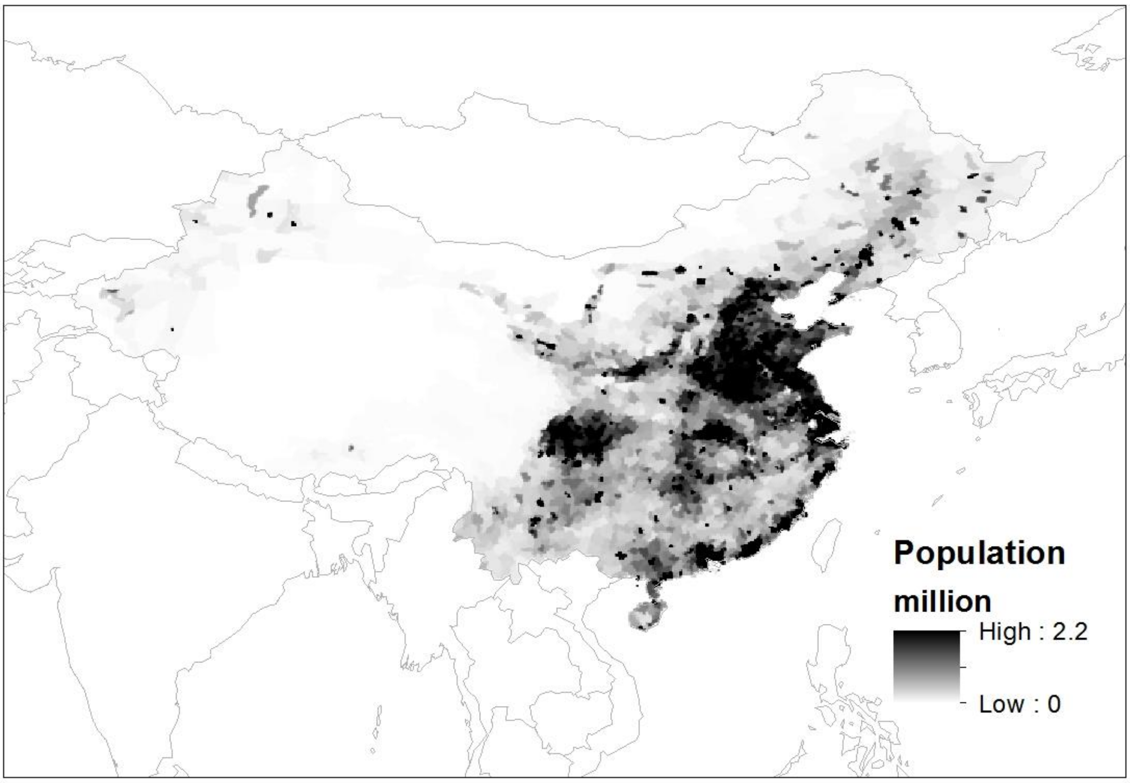

Figure 2.3. Distribution of the Chinese population in 2010.
Source: based on CIESIN et al. (2005) and UN (2015).

2.2.4 Assessment of health effects caused by air pollution

Air pollution reduction resulting from implementing control measures are estimated through establishing a relationship between emissions and exposure of people to concentration of pollutant as illustrated in previous sections. The next step of an integrated assessment, i.e. estimating the relevant impacts on human health caused by air pollution, is discussed in this chapter.

2.2.4.1 Selection of health endpoints

As discussed before, $PM_{2.5}$ is selected as the surrogate air pollutant for health impact assessment in this study. All residents in China (excluding Taiwan province) are included as the exposed population. Exposure to ambient air pollution is associated with a broad spectrum of acute and chronic health problems or health endpoints ranging from coughing to death (HEI, 2001; Næss et al., 2007). Many studies have quantified the damage costs of air pollution and found that premature mortality makes by far the largest contribution (Bickel and Friedrich, 2005; Künzli et al., 2000; Voorhees et al., 2014; Wang et al., 2013a).

Epidemiological studies suggest that chronic health effects caused by long-term exposure to air pollution may be 5-10 times larger than acute effects caused by short-term exposure in terms of overall public health effects (Kunzli et al., 2001; Pope, 2000). Moreover, YOLL can only be derived from changes of chronic mortality. Hence, considering the availability and reliability of baseline health data and the corresponding CRFs for China, and the significance of the health endpoints, chronic mortality is chosen as the representative health endpoint in this study, which includes all-cause mortality and mortality caused by ischemic heart disease (IHD), cerebrovascular disease (stroke), chronic obstructive pulmonary disease (COPD), lung cancer (LC), and acute lower respiratory infection (ALRI).

Table 2.3. Baseline incidence rates by age group for 2010 (cases per person per year).

Age group	All-cause mortality	IHD mortality	Stroke mortality	COPD mortality	LC mortality	ALRI mortality
0	4.35E-03	0.00E+00	2.34E-05	5.89E-06	0.00E+00	3.47E-04
1-4	1.13E-03	0.00E+00	3.40E-06	8.99E-07	0.00E+00	1.08E-04
5-9	2.17E-04	0.00E+00	2.40E-06	4.00E-07	0.00E+00	4.85E-06
10-14	1.51E-04	0.00E+00	1.80E-06	7.51E-07	0.00E+00	1.45E-06
15-19	3.39E-04	7.05E-06	8.00E-06	1.55E-06	2.05E-06	5.10E-06
20-24	4.56E-04	1.41E-05	1.29E-05	2.55E-06	2.70E-06	4.80E-06
25-29	5.25E-04	2.41E-05	2.21E-05	1.65E-06	8.40E-06	4.10E-06
30-34	7.03E-04	3.64E-05	4.15E-05	7.50E-06	1.86E-05	5.25E-06
35-39	1.07E-03	6.69E-05	8.52E-05	1.08E-05	3.62E-05	8.25E-06

Age group	All-cause mortality	IHD mortality	Stroke mortality	COPD mortality	LC mortality	ALRI mortality
40-44	1.73E-03	1.36E-04	2.01E-04	2.65E-05	8.77E-05	1.03E-05
45-49	2.81E-03	2.49E-04	3.96E-04	5.22E-05	1.82E-04	2.14E-05
50-54	4.02E-03	3.65E-04	6.77E-04	1.19E-04	3.38E-04	2.15E-05
55-59	6.23E-03	5.92E-04	1.16E-03	2.31E-04	6.06E-04	4.18E-05
60-64	1.04E-02	1.08E-03	2.15E-03	5.86E-04	1.05E-03	7.58E-05
65-69	1.64E-02	1.82E-03	3.76E-03	1.22E-03	1.59E-03	1.62E-04
70-74	3.01E-02	3.74E-03	7.39E-03	3.26E-03	2.42E-03	4.11E-04
75-79	5.14E-02	6.93E-03	1.34E-02	6.33E-03	3.51E-03	9.25E-04
80-84	9.35E-02	1.42E-02	2.48E-02	1.36E-02	4.04E-03	2.49E-03
85+	2.38E-01	4.01E-02	5.67E-02	3.78E-02	5.72E-03	9.36E-03
All ages	6.21E-03	7.78E-04	1.35E-03	5.94E-04	3.96E-04	1.23E-04

Source: derived from China Public Health Statistical Yearbook 2011 (MHPRC, 2011). Note: IHD (ischemic heart disease); stroke (cerebrovascular disease); COPD (chronic obstructive pulmonary disease); LC (lung cancer); ALRI (acute lower respiratory infection).

The baseline data of mortality is derived from China Public Health Statistical Yearbook 2011 (MHPRC, 2011). The incidence rates of considered health endpoints by age group for the year 2010 are presented in Table 2.3. Though the incidence rate may differ over different regions of China, this study assumes the same incidence nationwide, lacking reliable region specific health data. As no official future projections of incidence are available, and with the purpose to identify only the impact of air pollution reduction, it is assumed that the baseline incidence in 2030 is the same as in 2010.

2.2.4.2 Quantification of air pollution induced health effects

Epidemiologic studies (e.g. cohort study, time-series study) examine the relationship between health effects and people's exposure to air pollution, and report CRFs, which are crucial for health impact assessment (WHO, 2013). Time-series studies capture acute health risks attributable to short-term exposure to air pollution.

Cohort studies provide information about the association of ambient air pollution with risk of chronic diseases, long-term mortality or morbidity, and LLE (Kunzli et al., 2001). The HRAPIE (Health Risks of Air Pollution In Europe) report provides comprehensive recommendations for CRFs to be used in quantifying the health impacts of PM (WHO, 2013). Following the HRAPIE recommendations, CRFs indicating changes of mortality induced by long-term exposure to $PM_{2.5}$ are considered in this study.

Many studies report such CRFs with linear or log-linear form (Cao et al., 2011; Hoek et al., 2013; Kan et al., 2004; Pope et al., 2002). Recent studies (Apte et al., 2015; Burnett et al., 2014; Xie et al., 2016) argue that the relationship between ambient $PM_{2.5}$ concentration and mortality is nonlinear, especially at high concentration levels. In order to capture the effects of different CRFs, this study expands the methodology to employ both linear and nonlinear CRFs as illustrated by Equation 2.7. A sensitivity analysis is carried out using different CRFs expressed as the relative risk (RR) of mortality.

$$for\ C \leq C0,$$

$$RR(C) = 1$$

$$for\ C > C0,$$

$$RR(C) = \begin{cases} 1 + \beta\,(C - C0), & Linear\ function \\ exp[\beta\,(C - C0)], & Log - linear\ function \\ 1 + \alpha\left\{1 - exp\left[-\gamma\,(C - C0)^{\delta}\right]\right\}, & nonlinear\ function \end{cases}$$

Equation 2.7

Where,

RR(C) = relative risk of the endpoint at concentration C, *C0* = baseline concentration considered,

β, α, γ, δ = coefficients of the concentration-response relationships.

The lowest level of exposure to $PM_{2.5}$ that does not cause negative health effects has not been clearly identified. However, zero exposure is impossible to achieve (Brauer et al., 2012), and apparently is not a practical goal for air pollution control. Therefore, this study adopts the WHO guideline (WHO, 2005) for annual mean $PM_{2.5}$ (10 μg/m^3) as the baseline concentration (C0).

The coefficients of the concentration-response relationships are estimated by epidemiologic studies. For linear and log-linear functions, two values of the coefficient β for all-cause mortality are considered in this study: 0.004 (95%CI: 0.001, 0.008) from Pope et al. (2002), which is one of the lowest value among existing U.S. cohort studies of $PM_{2.5}$ exposure (WHO, 2013); 0.0009 (95%CI: -0.0003, 0.0018) from a Chinese cohort study of Cao et al. (2011). For the nonlinear function, the coefficients from Burnett et al. (2014) for mortality caused by IHD, stroke, COPD, LC, and ALRI are used.

Adopting the baseline incidence rate, exposed population, and CRF expressed as RR, the increase of mortality due to $PM_{2.5}$ exposure is estimated by:

$$E = P * B * \frac{RR(C) - 1}{RR(C)} \qquad \text{Equation 2.8}$$

Where,

E = health endpoint attributable to $PM_{2.5}$ exposure,

P = exposed population,

B = baseline incidence rate for health endpoint,

RR(C) = relative risk for the endpoint at concentration C.

Most previous studies quantify the health impacts caused by air pollution as premature deaths (He et al., 2010; Li et al., 2016; Xie et al., 2016). However, premature deaths do not reveal information on the loss of life years per death. An increase in mortality induced by air pollution should not be constructed as “excess deaths”, as one can and must die only once. $PM_{2.5}$ exposure substantially reduces people’s life expectancy, which can be quantified as LLE and YOLL (Leksell and Rabl, 2001). Through incorporating the life table methods of Miller and Hurley (2003), the differences of life expectancy under the baseline and impacted hazard rates of the whole population are estimated based on age-specific population and mortality data.

YOLL, with the definition of years of potential life lost due to premature deaths, provide a summarized measure of the health impacts caused by air pollution (Kunzli et al., 2001). The number of YOLL attributable to $PM_{2.5}$ exposure is calculated by summing the product of corresponding LLE when death occurs at age in age group i and the number of deaths observed in age group i (Equation 2.9). The YOLL attributable to $PM_{2.5}$ exposure in 2010 and 2030, as well as the reduced YOLL from changes in $PM_{2.5}$ exposure in the policy scenarios are estimated and compared.

$$YOLL = \sum_{i} LLE_i * D_i \qquad \text{Equation 2.9}$$

Where,

$YOLL$ = years of life lost,

LLE_i = loss of life expectancy when death occurs at age i,

D_i = number of observed deaths per year in the population at age i.

2.2.5 Monetary valuation of integrated impacts

Environmental policies aiming to improve air quality usually affect emissions of both air pollutants and GHG. In order to evaluate the effects of policy measures and compare different scenarios, the impacts on human health and climate change need to be transformed to a common unit to allow aggregation. Monetary valuations of the impacts on human health and climate change under different scenarios are conducted as described below.

2.2.5.1 Monetary valuation of years of life lost

In order to monetize YOLL, the value of a life year lost (VOLY) due to air pollution needs to be determined. It should be noted that VOLY is not a measure of the intrinsic value of life, but expresses the society’s collective willingness-to-pay

(WTP) to avoid a small probability of losing a life year (Desaigues et al., 2004). Unlike tradable goods, life years do not have a market price. Various approaches expressing health effects in monetary value have been developed, among which contingent valuation approach is the most widely used one (World Bank, 2007).

By carrying out surveys or observing people's behaviour, the WTP of the affected population to avoid a certain level of risk or damage is evaluated. Few studies have been conducted about air pollution induced VOLY in China (Hammitt and Zhou, 2006; Wang and Mullahy, 2006). This study adopts the VOLY from European studies (Desaigues et al., 2011; Friedrich et al., 2011), and transfers it to the value for China using the income elasticity method.

The income elasticity method allows transferring of VOLY between high and low income populations as illustrated by the following formula:

$$VOLY_B = VOLY_A * (\frac{I_B}{I_A})^{el} \qquad \text{Equation 2.10}$$

Where,

VOLY = the value of a life year lost due to air pollution in a population,

I = income per capita in a population,

el = the income elasticity of VOLY.

The value of 60,000 (lower: 37,500; upper: 215,000) EUR_{2010} for a VOLY in European countries suggested in European studies (Desaigues et al., 2011; Friedrich et al., 2011) is considered in this study. The purchasing power parity (PPP) adjusted income per capita for China and European Union (28 countries) for the year 2010 are obtained from OECD statistics (OECD, 2016). The income elasticity of the VOLY is considered to be 1 as suggested by Hammitt and Robinson (2011). Applying Equation 2.10, the VOLY for China in 2010 is 16,600 (lower: 10,400; upper: 59,500) EUR_{2010}.

In order to estimate the Chinese VOLY for 2030, an uplift factor reflecting the higher WTP for avoiding health risk related to income growth needs to be taken into account. Based on the projection of World Economic Outlook 2016 (IMF, 2016), the annual growth rate of income per capita in China is predicted to be 5% from 2010 to 2030. Considering the same elasticity value (1) as used before, the

VOLY of China for the year 2030 is 44,000 (lower: 27,500; upper: 157,800) EUR_{2010}. The damage costs due to an increased exposure to $PM_{2.5}$ are then quantified by multiplying the corresponding VOLY with the YOLL in the different scenarios.

2.2.5.2 Monetary valuation of climate change effects

A main feature of the integrated assessment methodology developed in this study is that it aims to analyse simultaneously the health impacts caused by air pollutants emissions and the impacts on climate change caused by GHG emissions. For calculating external costs of GHG, one principle methodology is the damage costs approach, which simulates the physical impacts of climate change and estimates the related monetary costs. There is a wide variety of different climatic impacts, e.g. increased water stress, change in energy consumption for heating and cooling, sea level rise, impacts on ecosystems and health. The damage costs are estimated by considering for example the value of coastal properties, loss of crops, and increased mortality caused by heat stress.

Many studies (Anthoff et al., 2009; Hope, 2008; Pearce, 2003; Tol, 2005; Wang et al., 2009) have been conducted to quantify the damage costs of climatic effects, and give suggestions on marginal damage costs (MDC) per tonne of equivalent CO_2 ($CO_{2\text{-eq}}$) emissions. Estimates of MDC differ significantly as they are affected by not only the considered climate and socio-economic relations, but also the time horizon of the marginal emissions and assumptions on the discount rate and equity weighting.

The discount rate is commonly a combination of the pure time preference rate, risk aversion, and the consumption growth rate. It reflects the preference across generations. The equity weighting is adopted to deal with the concern of widely disparate incomes within a generation. Reflecting the theory of declining marginal utility of consumption, i.e. the same absolute loss of consumption causes a higher welfare loss for a poor person than a rich person, the equity weighting gives damages in low income regions more weight than those in high income regions.

In the damage cost approach, a full evaluation of the external costs of climatic effects needs to be considered. However, it is difficult even for the most advanced models to cover all climate change damage costs, especially catastrophic climate change impacts, as there is little information about the intrinsic relationship. Side effects such as possible social damage (e.g. regional conflicts) are even more difficult to assess (Maibach et al., 2008).

An alternative approach tries to calculate external costs of GHG on the basis of abatement costs, which avoids the uncertainties of climatic effects predictions. The performance and cost of abatement options are estimated. For a chosen reduction target, the marginal abatement costs (MAC) can be viewed as a WTP value to avoid damage (Stern, 2006). However, in reality one does not know where the social optimum is, while information on damage costs is needed by policy makers to formulate environmental policies.

Climate changes costs have a high level of complexity as they spread across time and space. Estimates of economic costs of climate change show a wide range of results (Friedrich, 2016). In this study, both the damages and the abatement costs approaches are investigated to provide a comprehensive estimation of the external costs of GHG emissions.

Based on the results of the widely used the Climate Framework for Uncertainty, Negotiation and Distribution (FUND) model, Wille (2013) suggests a MDC value of 15 EUR_{2010}/t $CO_{2\text{-eq}}$ for 2030, which considers a pure time preference rate of 1%, and the global average equity weighting with the aim of limiting average temperature increase to 2°C by maintaining the concentration of GHG in the atmosphere to around 450 parts per million (ppm) of $CO_{2\text{-eq}}$.

The global average equity weighted value can be transferred to consider the equity weight for China by applying the following equation:

$$EW_C = \left(\frac{I_{avg}}{I_C}\right)^{el} \qquad \text{Equation 2.11}$$

Where,

EW_C= equity weight for China,

I_{avg}= world average income per capita,

I_C= Chinese income per capita,

el = elasticity of the marginal utility of income.

The PPP-adjusted income per capita is used as a measure of the wealth of a country. According to the long-term projections made by OECD (2012), the PPP-adjusted income per capita of China will be almost equal (1.01 times) to that of world average in 2030. Therefore, the MDC with Chinese equity weighting is estimated to be 15 EUR_{2010}/t $CO_{2\text{-eq}}$ for the year 2030.

Based on the meta-analysis of Kuik et al. (2009), the MAC in the EU considering the 2°C aim and a discount rate of 5% per year amounts 54 to 167 EUR_{2010}/t $CO_{2\text{-eq}}$ for 2030 (Friedrich, 2016). According to the agreements made in the United Nations Climate Change Conferences, the carbon reduction commitments of developing countries are lower than those of developed countries, and the time frame for peaking GHG emissions will be longer in developing countries.

Calvin et al. (2009) finds that delayed participation in the accession on limiting climate change shifts the cost burden from late action regions (e.g. China) to early action regions (e.g. European Union). Results from Okagawa et al. (2012) show that the MAC would be significantly reduced if CCS and nuclear energy are deployed as mitigation options, which is the case for China. Therefore, the lower bound of the estimates based on Kuik et al. (2009) is considered as the MAC for China (54 EUR_{2010}/t $CO_{2\text{-eq}}$ for 2030).

If the emission limits imposed by environmental strategies were optimal, the MAC would be equal to the MDC as abatement costs express the implicit valuation of damages by the society (Ottinger, 1991). To obtain a politically feasible estimation of the external cost factor for climate change, the MDC is considered as the lower bound of the estimate, and the MAC is regarded as the higher bound. This study adopts the climate change costs of 15 to 54 EUR_{2010}/t $CO_{2\text{-eq}}$ in China for the year 2030.

The benefits of GHG reductions in policy scenarios are then calculated by multiplying the reduced GHG emissions by the per unit climate change cost. Adding up the monetary benefits of the policy scenarios related to reduced emissions of air pollutants and GHG, the integrated impacts of the policy scenarios are estimated and analysed.

As is especially the case for monetary valuation, integrated assessment modelling is associated with considerable levels of uncertainties. Few studies have attempted to quantify the uncertainties of environmental damages especially for China. In this study, a systematic assessment of the uncertainties of each modelling stage is conducted to provide information on the robustness of the results and conclusions as will be shown in section 4.2.

3 Benefits to human health and climate change of reduced air pollution

Applying the integrated assessment methodology described in the previous chapter, the benefits of reduced air pollution are estimated. This chapter firstly presents the potential of air pollutants and GHG emissions reduction, the resulting change of ambient air quality, and then the analyses of the health impacts of the chosen scenarios, followed by an economic valuation of the integrated impacts on human health and climate change.

3.1 Emissions reduction of air pollutants and GHG

3.1.1 Trends of emissions

Table 3.1 shows the emissions of air pollutants and GHG for 2010 and 2030 in different scenarios. The emissions reduction potentials of future scenarios in 2030 compared with BL in 2010 are presented in Figure 3.1. Current legislation as reflected by BAU, particularly China's Twelfth FYP, will reduce the emissions of SO_2, NO_x, and PM in 2030 by 20-40% compared with those in 2010. While VOC emissions will decrease by 4%, and NH_3 emissions will increase by 22% from BL in 2010 to BAU in 2030.

Emissions of SO_2 and NO_x in MTFR will be 49% and 60% lower than those in BAU, respectively; and SO_2 and NO_x emissions in CLMT will be 22% and 8% lower than those in BAU, respectively. PM emissions in MTFR will be more than 70% lower than those in BAU. Since CLMT focuses on climate mitigation, its impacts on PM emission reduction are not so significant ($PM_{2.5}$: 7%, BC: 22%, PM_{10}: 8%). VOC emissions will be reduced by 65% from those in BAU if measures in MTFR are implemented. NH_3 emissions in policy scenarios are almost the same as those in BAU as few measures are considered for the agriculture sector which is the main contributor for NH_3 emissions. In COMB, all the considered air pollutants except NH_3 will be reduced by over 60% compared with BAU.

If no additional control policies are implemented, CO_2 emissions will increase from 8.7 billion tonnes (Gt) in 2010 to 13.7 Gt in 2030, with an average annual growth rate of 2.28%. As a higher growth rate of the national GDP is predicted, CO_2 emission per GDP in the BAU scenario in 2030 is 52% lower than the level in 2010. A similar trend is found for GHG emissions. Emissions of CO_2 estimated in the MTFR scenario are almost the same as those in BAU by 2030 as no additional CO_2 emission reduction measures are considered in MTFR.

GHG emissions in CLMT are estimated to be 41% lower than those in BAU, which indicates that deploying CCS in power generation and industrial sectors will reduce GHG emissions effectively. Combining end-of-pipe air pollutants control and climate change mitigation measures can further improve the reduction rate of GHG emissions to 46% comparing COMB with BAU.

Table 3.1. Emissions of air pollutants and GHGs.

Pollutant	Unit	BL	BAU	MTFR	CLMT	COMB
		2010	2030	2030	2030	2030
SO_2	kt SO_2/year	28142.74	19805.23	10040.25	15528.41	7579.63
NO_x	kt NO_x/year	22124.97	17918.05	7221.96	16425.30	5526.30
$PM_{2.5}$	kt PM/year	15887.93	9849.63	2162.08	9154.17	1893.84
BC	kt PM/year	1850.95	1080.91	95.66	839.36	76.92
PM_{10}	kt PM/year	21696.41	14764.94	4093.79	13542.04	3712.79
VOCs	kt VOC/year	21970.20	21034.03	7389.32	21121.88	6781.70
NH_3	kt NH_3/year	14235.12	17405.00	17364.45	17235.04	17166.90
CO_2	Mt CO_2/year	8713.00	13671.88	13678.22	7165.43	7042.76
All GHGs	Mt $CO_{2\text{-}eq}$/year	10727.50	16764.36	15909.88	9877.21	8997.14

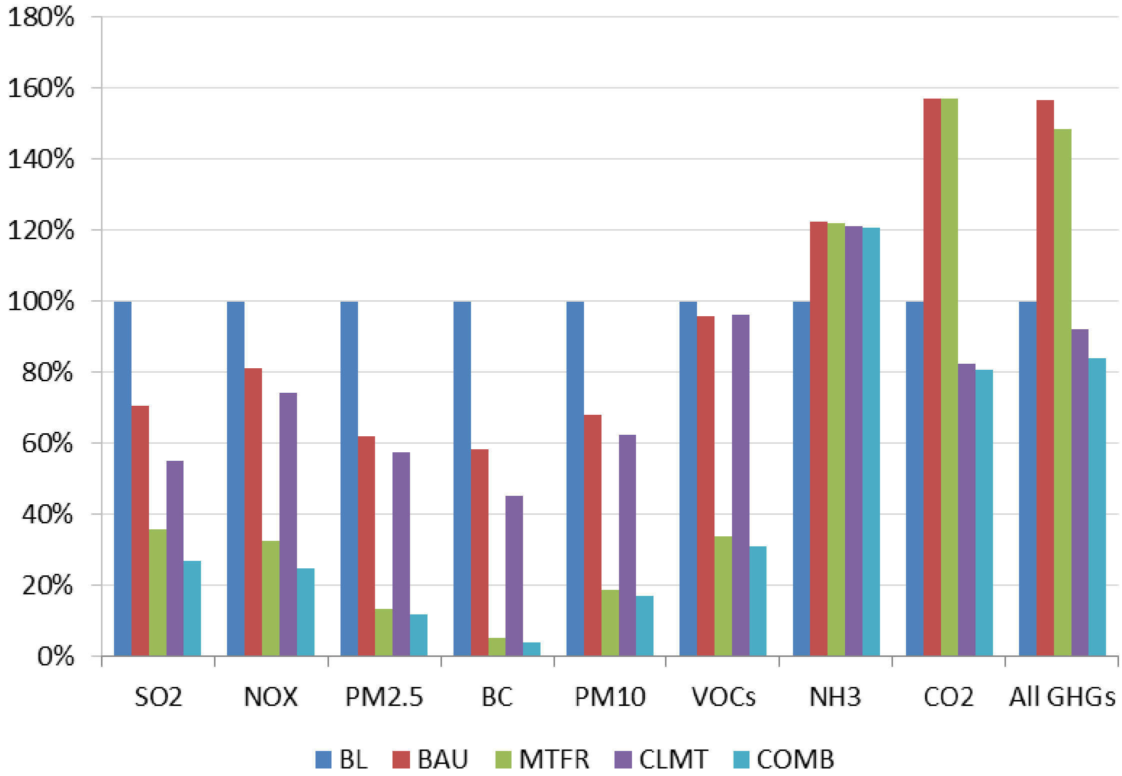

Figure 3.1. Reduction potentials of future scenarios in 2030 compared with the baseline scenario (BL) in 2010.

3.1.2 Mitigation potentials of control measures

After describing the overall trends of air pollutants and GHG emissions in different scenarios, this section discusses the emission reduction potentials by sector in MTFR and CLMT compared with those in BAU in order to identify the most effective air pollution control and climate change mitigation measures.

3.1.2.1 Emission reduction by sector of MTFR

As can be seen from Figure 3.1 and Table 3.1, MTFR reduces SO_2, NO_x, PM and VOCs effectively. Figure 3.2 presents the emission reduction of these air pollutants between MTFR and BAU by sector. For the year 2030, SO_2 emissions will be reduced from 19.8 million tonnes (Mt) in BAU to 10 Mt in MTFR. Deploying maximum technically feasible SO_2 reduction technologies (e.g. high efficiency FGD) for industrial combustion contributes to 45% of the reduction, followed by those for industrial processes (25%) and power and heating plants (17%).

NO_x emissions can be reduced by 60% (10.7 Mt) under MTFR, mainly by implementing the state-of-the-art emission standards for vehicles in transport sector and increasing installation of flue gas denitrification, including SCR and selective non-catalytic reduction (SNCR), in the industrial combustion sector.

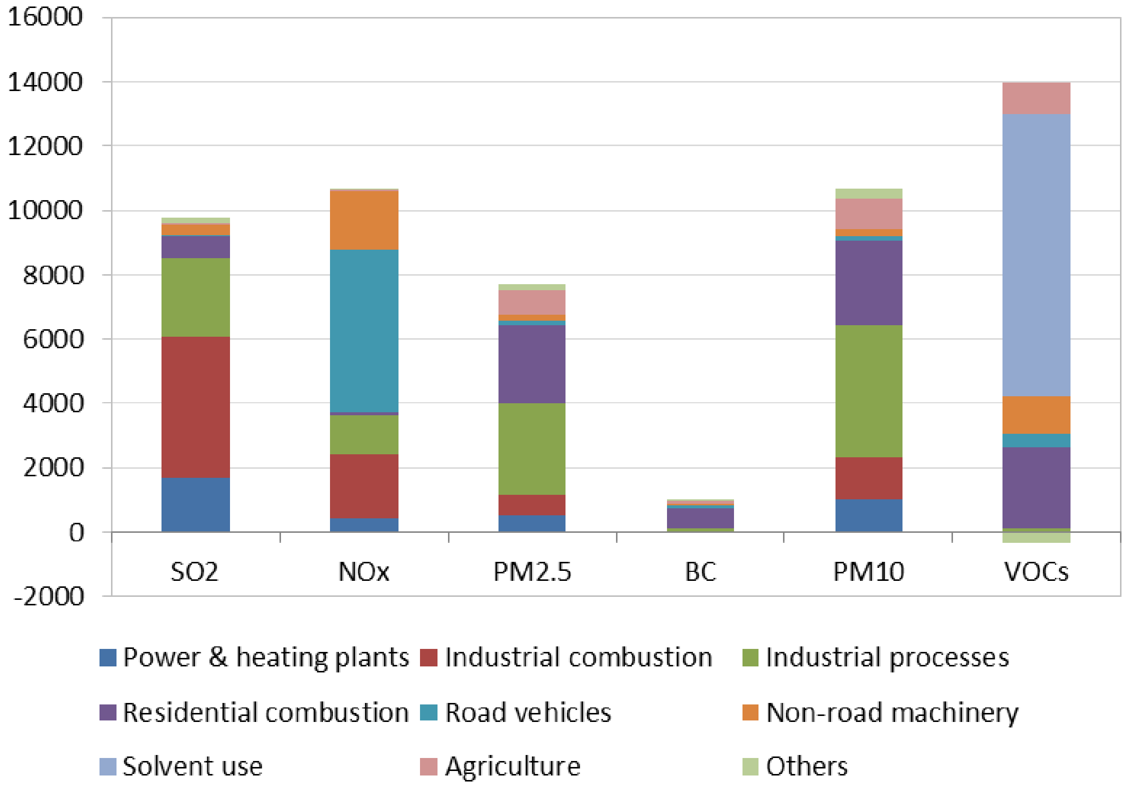

Figure 3.2. Reduced emissions of air pollutants (kt/year) from BAU to MTFR by sector in 2030.
(Emissions of SO_2, NO_x, $PM_{2.5}$, BC, PM_{10}, and VOCs in the BAU scenario in 2030 are 19.8, 17.9, 9.8, 1.1, 14.8, and 21.0 Mt/year, respectively.)

Residential combustion and industrial processes are the main contributing sectors for PM reduction under MTFR. Continued application of high efficiency filters and electrostatic precipitators in these sectors can reduce $PM_{2.5}$ emissions by over 4 Mt in 2030. Emissions of VOCs can be reduced from 21 Mt in BAU to 7.4 Mt in MTFR in 2030. As is shown in Figure 3.2, the reductions come mainly from solvent use (8.8 Mt) and residential combustion (2.5 Mt) through applying different end-of-pipe control technologies based on various spraying technologies and chemical properties of the solvent used.

3.1.2.2 Emission reduction by sector of CLMT

With the purpose of reducing GHG, some measures in CLMT (e.g. improvement of energy efficiencies and promotion of renewable energy) could also reduce the emissions of SO_2, NO_x and PM as can be seen from Figure 3.1. Figure 3.3 presents the comparison of energy use by fuel type in the BAU and CLMT scenarios in 2030. The total energy consumption in CLMT is projected to be 132.6 exajoule (EJ) in 2030, which is 25% lower than that in BAU. Although coal dominates the energy mix in both scenarios, the proportion of coal in total energy use decreases from 59% in BAU to 38% in CLMT. In other words, coal consumption in CLMT is 52% lower than that in BAU in 2030.

Less consumption of liquid fuels, especially less gasoline consumption from road vehicles, is also considered in CLMT compared with BAU. Owing to the promotion of electric vehicles, electricity consumption of road vehicles in CLMT is more than 5 times of that in BAU in 2030. The consumption of gaseous fuels in CLMT is 47% higher than that in BAU as a result of substituting coal with natural gas in power plants.

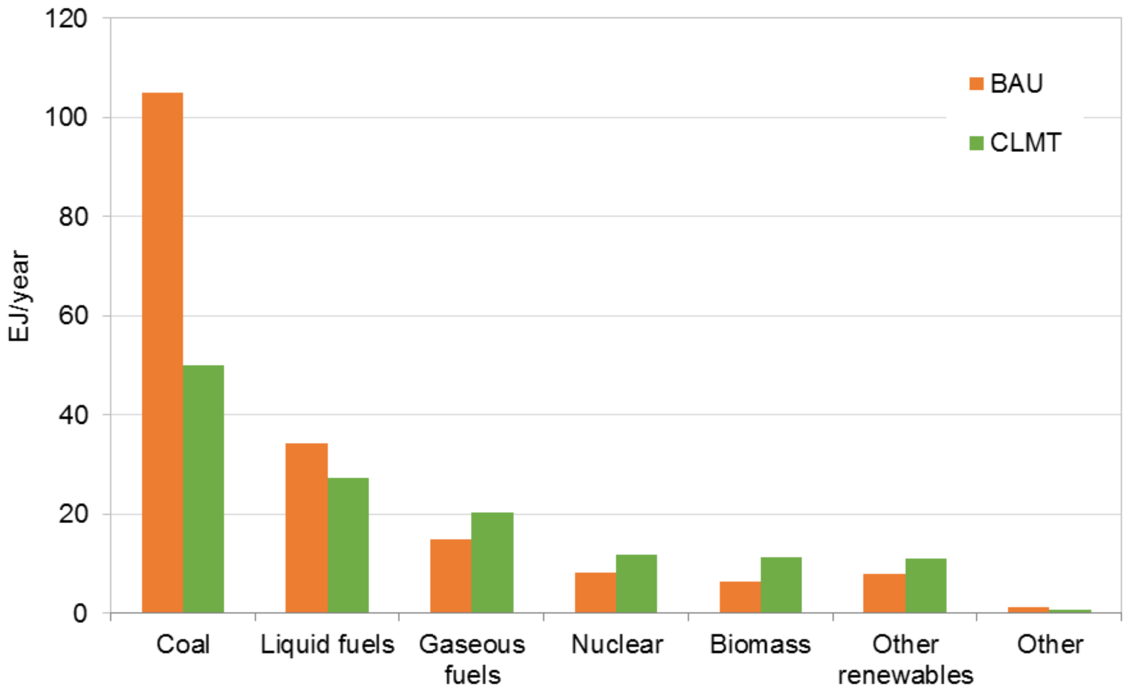

Figure 3.3. Energy use by fuel type in BAU and CLMT in 2030.

It can be seen from Figure 3.3 that higher renewable energy consumption is projected in CLMT compared to BAU. Biomass consumption in CLMT is 76%

higher than that in BAU in 2030. Higher biomass consumption in industrial combustion and power plants in CLMT increases the proportion of biomass in total energy consumption from 3.6% in BAU to 8.5% in CLMT. Nuclear and other renewables are also projected to increase over 40% in CLMT compared with those in BAU.

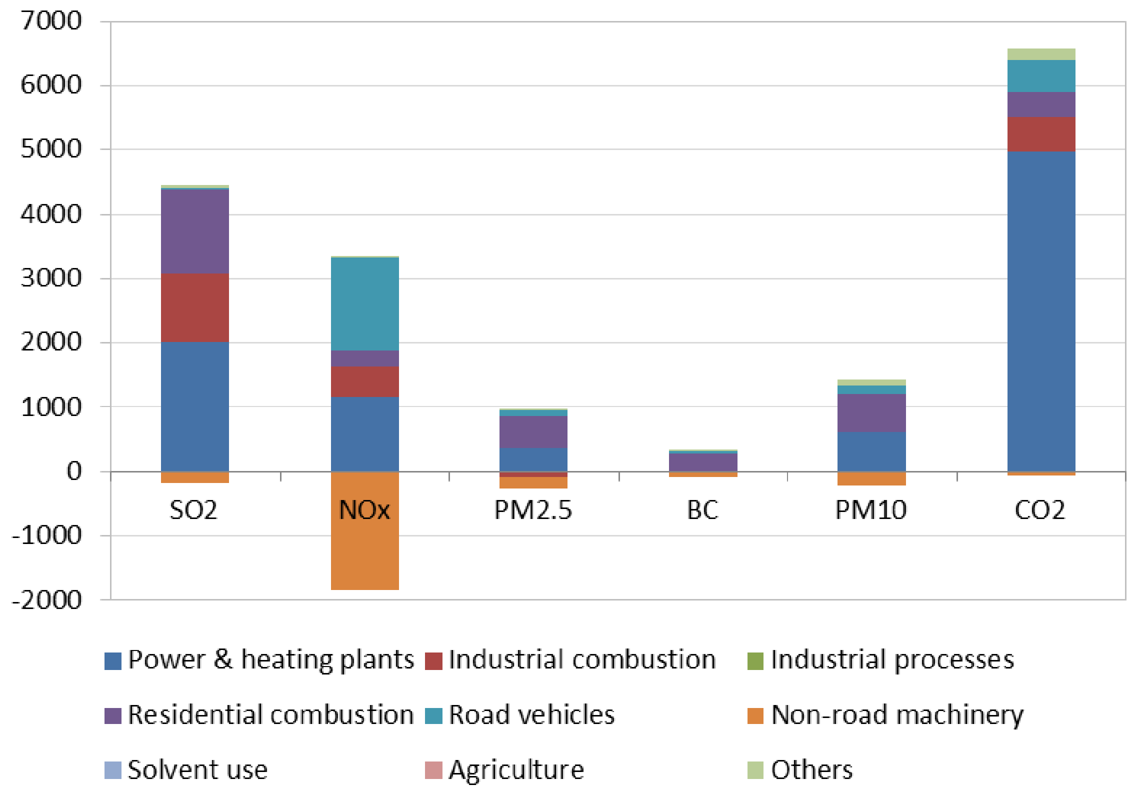

Figure 3.4. Reduced emissions of air pollutants (kt/year) and CO_2 (Mt/year) from BAU to CLMT by sector in 2030.
(Emissions of SO_2, NO_x, $PM_{2.5}$, BC, PM_{10}, and CO_2 in the BAU scenario in 2030 are 19.8, 17.9, 9.8, 1.1, 14.8, and 13671.9 Mt/year, respectively.)

The emissions of SO_2, NO_x, PM and CO_2 in CLMT are compared with those in BAU by sector (see Figure 3.4). CO_2 emissions are reduced by 6.5 Gt (48%) in CLMT, over 76% of which are attributable to measures for power and heating plants, e.g. installation of CCS, substitution of coal with gaseous fuels and renewable energy. All the modern power plants and power and heating plants with integrated gasification combined cycle are equipped with CCS in CLMT. Capacities of nuclear, wind and solar power and district heat plants in CLMT are 1.5, 2.0 and 5.3 times higher than those in BAU, respectively. Fuel substitution also contributes to emission reduction of SO_2 (2.0 Mt), NO_x (1.2 Mt) and PM (361 kt $PM_{2.5}$).

CO_2 emissions from industrial combustion are reduced by 539 Mt, mainly resulting from replacing coal and gasoline with biomass. Promotion of biomass fuels also helps to reduce SO_2 and NO_x emissions, however increases PM emissions. The energy efficiency of residential cooking and heating stoves is expected to be improved in CLMT, which contributes to both CO_2 and air pollutants reduction. For transport sector, promotion of electric cars and reduced use of heavy and light duty vehicles powered by diesel or gasoline can reduce NO_x (1.4 Mt) and CO_2 emissions (486.8 Mt) effectively. However, owing mainly to the higher consumption of diesel fuel for inland waterways, emissions of SO_2, NO_x and $PM_{2.5}$ are increased by 174, 1840 and 176 kt, respectively.

3.2 Improvement of air quality

For the BL and BAU scenarios, existing simulation results of the EMEP model are provided by the Norwegian Meteorological Institute; the changes of $PM_{2.5}$ concentration between BAU and policy scenarios are estimated with the parameterized TM5 model. The estimated $PM_{2.5}$ concentration and PWC levels, as well as bias adjustment of concentration modelling, are presented in this chapter.

3.2.1 $PM_{2.5}$ concentration and exposure

Figure 3.5 shows the annual average $PM_{2.5}$ concentration of China in BL 2010 and BAU 2030. These are simulated by the Norwegian Meteorological Institute using the EMEP model with a resolution of 0.1 by 0.1 degree. Bias adjustment based on comparison of modelled and measured $PM_{2.5}$ concentration of China in 2010 will be discussed in the next section. The reductions of $PM_{2.5}$ concentration caused by MTFR, CLMT, and COMB by 2030 are illustrated in Figure 3.6 with a spatial resolution of 1 by 1 degree. The spatial statistical distributions of $PM_{2.5}$ concentration in different scenarios are analysed and compared (see Table 3.2).

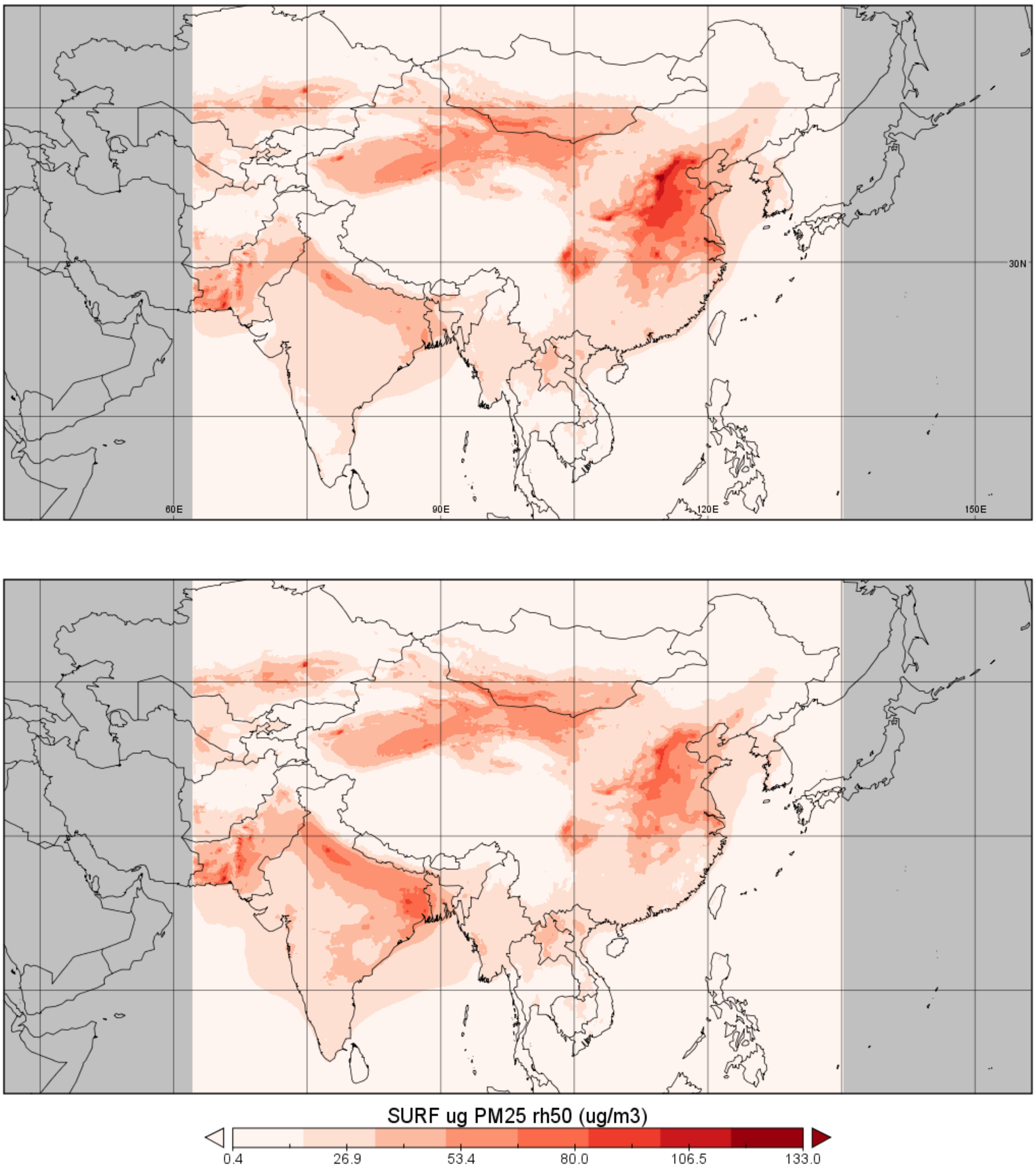

Figure 3.5. Annual average $PM_{2.5}$ concentration in China in BL 2010 (upper) and BAU 2030 (lower).
Source: Aggregated from daily $PM_{2.5}$ concentration maps provided by the Norwegian Meteorological Institute.

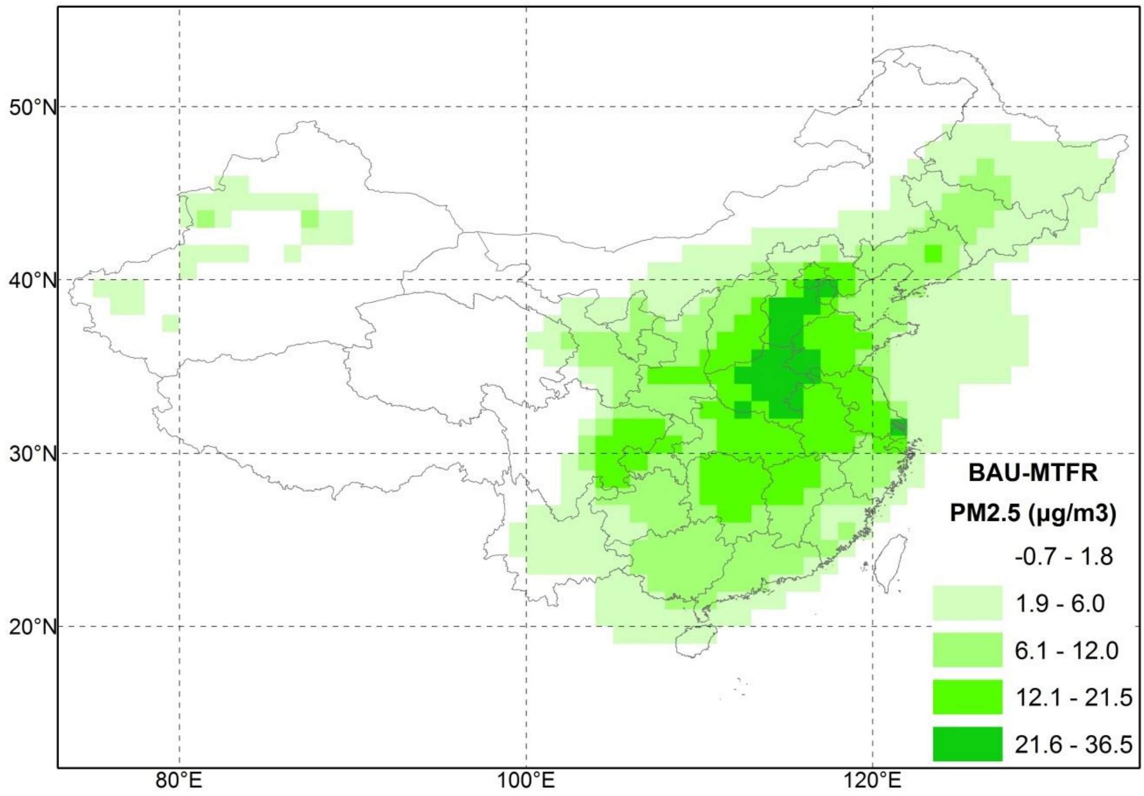
50°N
40°N
30°N
20°N
80°E
100°E
120°E
BAU-MTFR
PM2.5 (µg/m3)
-0.7 - 1.8
1.9 - 6.0
6.1 - 12.0
12.1 - 21.5
21.6 - 36.5

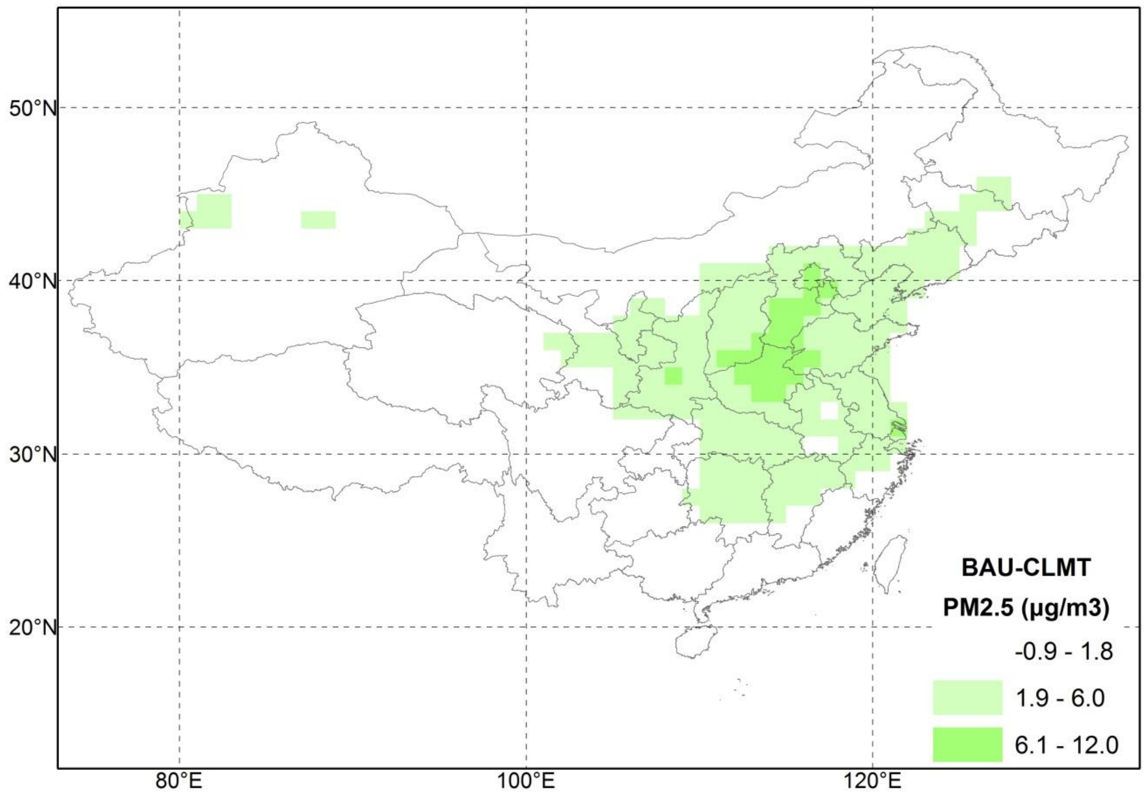
50°N
40°N
30°N
20°N
80°E
100°E
120°E
BAU-CLMT
PM2.5 (µg/m3)
-0.9 - 1.8
1.9 - 6.0
6.1 - 12.0

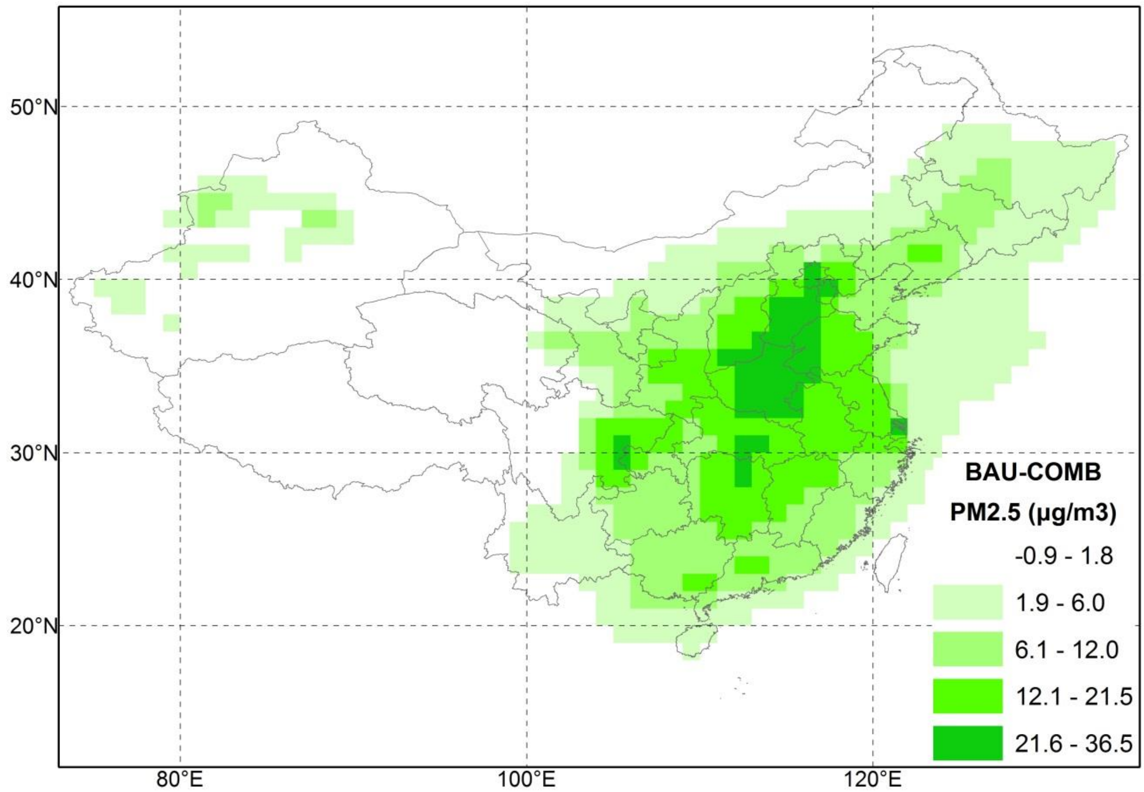

Figure 3.6. $PM_{2.5}$ concentration reduction from BAU to MTFR (upper), CLMT (middle), and COMB (lower) in 2030.

Table 3.2. Spatial statistical distribution of $PM_{2.5}$ concentration (unit: μg/m^3) in different scenarios.

Scenario	Grid number	Mean	Std.	Min	P(25)	Median	P(75)	Max
BL	97216	26.65	22.02	1.03	7.06	23.49	40.03	132.64
BAU	97216	23.36	18.65	1.05	6.56	20.28	35.51	99.89
MTFR	1101	18.11	15.19	1.01	5.39	13.84	26.99	63.93
CLMT	1101	21.46	17.10	1.09	5.93	18.60	32.67	69.62
COMB	1101	17.58	15.02	0.46	5.29	12.99	26.47	63.88

It can be seen that $PM_{2.5}$ pollution spreads almost over the whole China. $PM_{2.5}$ concentrations in over 70% of the 97216 EMEP grids covered by China are higher than the WHO guideline for $PM_{2.5}$ (10 μg/m^3) in 2010. The average $PM_{2.5}$ concentration is 26.7 μg/m^3. The highest $PM_{2.5}$ concentration is 132.6 μg/m^3. Grids with high $PM_{2.5}$ pollution levels concentrate in the Northeast of China, where also big cities with high population density are located. Combining concentration map with gridded population, PWCs of different scenarios are calculated, which can better illustrate the improvement of people's exposure to $PM_{2.5}$ in China.

Table 3.3 presents the percentages of population exposed to different levels of $PM_{2.5}$ concentration as well as the PWC in different scenarios. In 2010, over 98% of population in China are exposed to $PM_{2.5}$ concentration higher than 10 μg/m^3. 63% of population exposed to $PM_{2.5}$ concentration higher than 35 μg/m^3, i.e. worse than national secondary $PM_{2.5}$ standard. 77% of population are exposed to $PM_{2.5}$ concentration 20-80 μg/m^3. The PWC in 2010 is estimated to be 49.7 μg/m^3.

In BAU 2030, the mean $PM_{2.5}$ concentration over all the grids covered by China is 23.4 μg/m^3, 12% lower than that in BL 2010. 52% of population are exposed to $PM_{2.5}$ concentration worse than national secondary standard 35 μg/m^3. Percentages of population exposed to $PM_{2.5}$ concentration higher than 75 μg/m^3 decreased from 18% in BL 2010 to 4% in BAU 2030. The PWC in BAU is 39.6 μg/m^3, 20% lower than that in BL 2010.

The policy measures considered in the MTFR, CLMT, and COMB scenarios can further improve the $PM_{2.5}$ PWC in China to 24.38, 34.93, and 22.94 μg/m^3, respectively, which correspond to 38, 12, and 42% improvement compared with those in BAU. The average $PM_{2.5}$ concentrations of the 1101 TM5 grids covered by China in MTFR, CLMT, and COMB are 18.1, 21.5, and 17.6 μg/m^3, respectively. Most of $PM_{2.5}$ concentration reductions will occur in the larger cities of eastern China, because the majority of air pollutants emissions come from power plants and industry, which are always located near the larger cities.

The maximum $PM_{2.5}$ concentration in all the grids covered by China will become lower than 70 μg/m^3 in all the three policy scenarios. Areas in China with $PM_{2.5}$ concentration over 10 (35) μg/m^3 will decrease from 67 (24) % in BAU to 62 (16), 66 (22), and 60 (15) % in MTFR, CLMT, and COMB, respectively. Percentages of population exposed to $PM_{2.5}$ concentration higher than 35 μg/m^3 will be reduced to 23, 46, and 17% in MTFR, CLMT, and COMB, respectively.

Table 3.3. Percentages of population (%) exposed to different levels of $PM_{2.5}$ concentration and population-weighted concentration (PWC) (μg/m^3) in different scenarios in China.

$PM_{2.5}$ concentration (μg/m^3)	BL	BAU	MTFR	CLMT	COMB
	%				
<10	1.85	2.53	6.37	2.86	10.20
10-20	7.00	13.21	37.52	18.54	36.44
20-30	19.19	23.20	20.86	22.98	21.53
30-40	15.78	14.66	25.74	15.90	25.50
40-50	10.32	14.39	9.42	18.47	6.24
50-60	9.04	15.27	0.08	14.38	0.08
60-70	14.43	10.38	0.01	6.87	0.01
70-80	8.04	4.87	0.00	0.00	0.00
80-90	7.22	1.07	0.00	0.00	0.00
90-100	4.47	0.42	0.00	0.00	0.00
100-110	1.75	0.00	0.00	0.00	0.00
110-120	0.48	0.00	0.00	0.00	0.00
120-130	0.31	0.00	0.00	0.00	0.00
130-140	0.10	0.00	0.00	0.00	0.00

$PM_{2.5}$ concentration (μg/m^3)	BL	BAU	MTFR	CLMT	COMB
			%		
Total	100	100	100	100	100
PWC (μg/m^3)	49.70	39.60	24.38	34.93	22.94

It can be concluded that the control measures considered in the policy scenarios, especially those in MTFR, can effectively reduce $PM_{2.5}$ concentration and population exposure in China by 2030. The $PM_{2.5}$ concentrations modelled by CTMs are used as input data for health impact assessment. In order to validate the atmospheric model, the modelled and measured concentrations for 2010 are compared. Bias adjustment for modelled results is presented in the next section.

3.2.2 Bias adjustment

Figure 3.7 presents the scatter plot of observations and original modelled results of annual average PM2.5 concentration in 86 cities over China in 2010. It can be found that most of the data points are adjacently distributed on both sides of the y = x line with relatively more data points on the right side. This suggests that the EMEP model generally captures the right order of magnitude of the annual average $PM_{2.5}$ concentrations for each city, but most of them have a negative bias.

The underestimation may be related to underestimation of particulate emissions and the fact that CTMs often omit some components of atmospheric aerosols and therefore fail to reproduce the total PM budget (Kukkonen et al., 2012; Vautard et al., 2007). To provide a comprehensive evaluation of the reproduction of measured concentration levels by the modelled results, seven commonly used metrics whose mathematical expressions are reported by model performance evaluation studies (Denby, 2010; Legates and McCabe, 1999; Pirovano et al., 2012) are selected and estimated: fraction of predictions within a factor of two (FAC2), Mean Bias (MB), Mean Gross Error (MGE), Normalized Mean Bias (NMB), Normalized Mean Gross Error (NMGE), Root Mean Square Error (RMSE), and correlation coefficient (r).

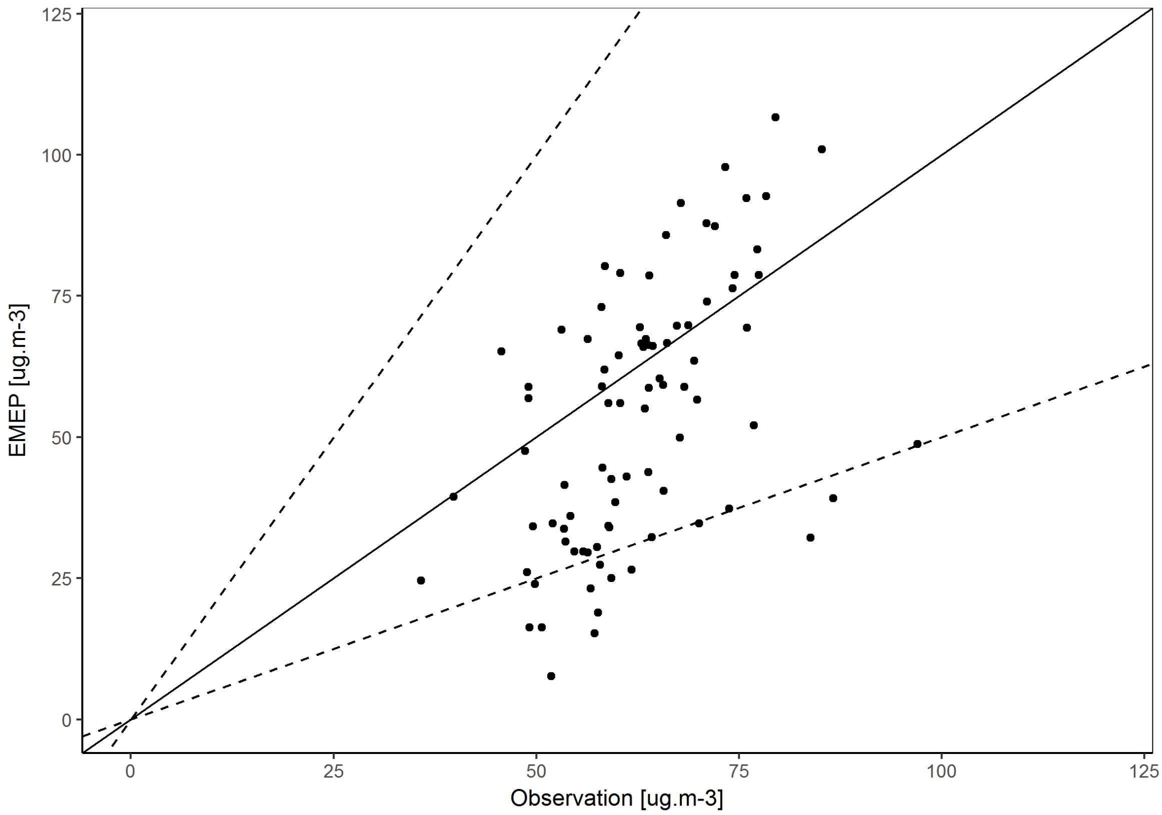

Figure 3.7. Scatter plot of observations and original modelled results of annual average $PM_{2.5}$ concentration in 86 cities over China in 2010.

Table 3.4. Parameters of the selected linear regression model.

Linear regression model	Coefficients
c(constant)	1.49
a1 (log. EMEP result)	0.17
a2 (relative humidity at 2 meters)	-0.15
a3 (altitude)	0.000030
a4 (log. Population density)	0.036

As illustrated in section 2.2.3.1, the effects of three bias adjustment approaches are examined: an additive correction of the mean bias (BA1), a multiplicative ratio correction (BA2), and a linear regression correction (BA3). Applying Equation 2.3, Equation 2.4, and Equation 2.5, the additive and multiplicative correction factors are calculated to be 8.20 and 1.15; the parameters of the linear regression correction model are shown in Table 3.4.

Apart from the modelled value of $PM_{2.5}$ concentration, three additional variables are included in the linear regression model: relative humidity at 2 meters, altitude, and population density. The performance of the bias adjustment methods expressed by the aforementioned metrics is summarized and compared with those without bias adjustment and the ideal values in Table 3.5.

Table 3.5. Performance of bias adjustment methods.

Methods	n	FAC2	MB	MGE	NMB	NMGE	RMSE	r
Original	86	0.85	-8.20	17.90	-0.13	0.29	22.37	0.49
BA1	86	0.92	0.00	17.40	0.00	0.28	20.81	0.49
BA2	86	0.88	0.00	20.32	0.00	0.32	24.09	0.49
BA3	86	1.00	-0.53	6.24	-0.01	0.10	8.10	0.64
Ideal value		1	0	0	0	0	0	1

FAC2 analyses whether the simulated values fall within a plus and minus factor of two of the measured data, which is considered as the most robust metric since it is not overly influenced by high and low outliers(Chang and Hanna, 2004). BA1, BA2, and BA3 can improve FAC2 from originally 0.85 to 0.92, 0.88, and 1.00, respectively, which are all satisfying. MB presents the average difference between simulated and observed values. BA1 and BA2 force the MB at each site to be zero, but they have no influences on r, which reflects the linear relationship between two variables.

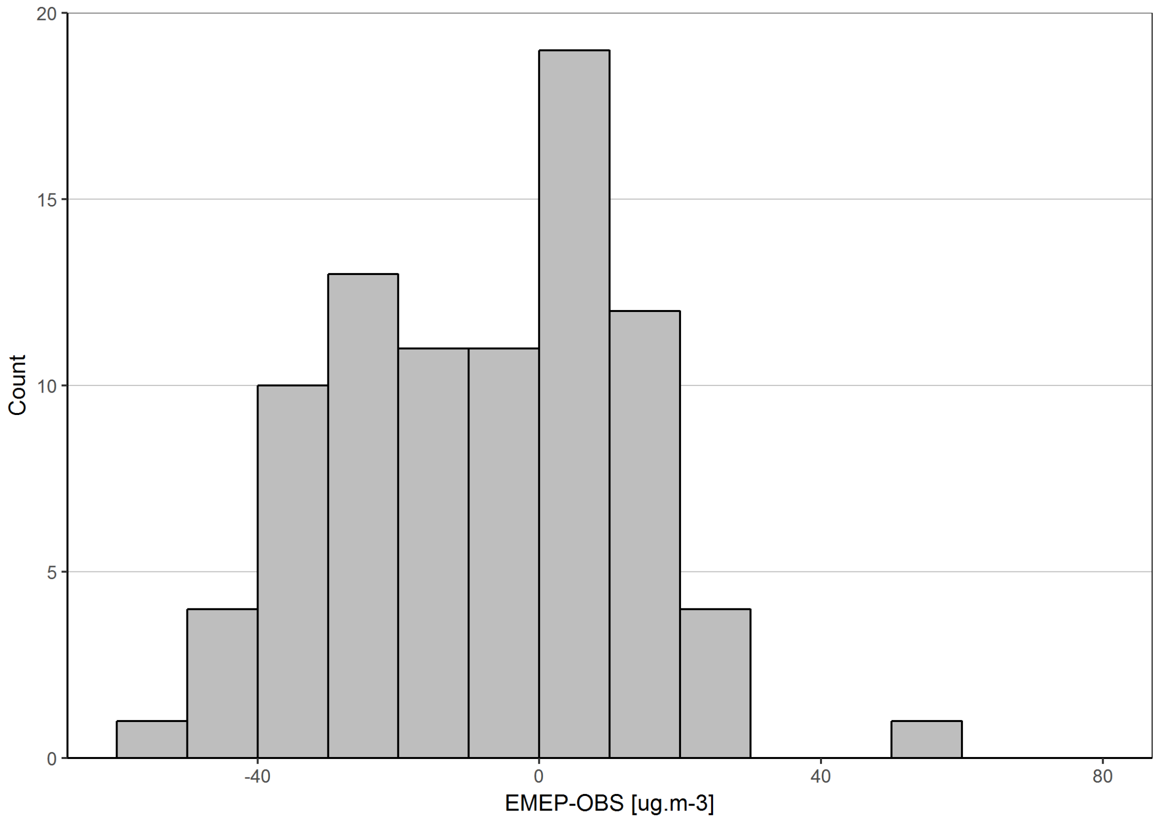
20
15
10
5
0
Count
-40
0
40
80
EMEP-OBS [ug.m-3]

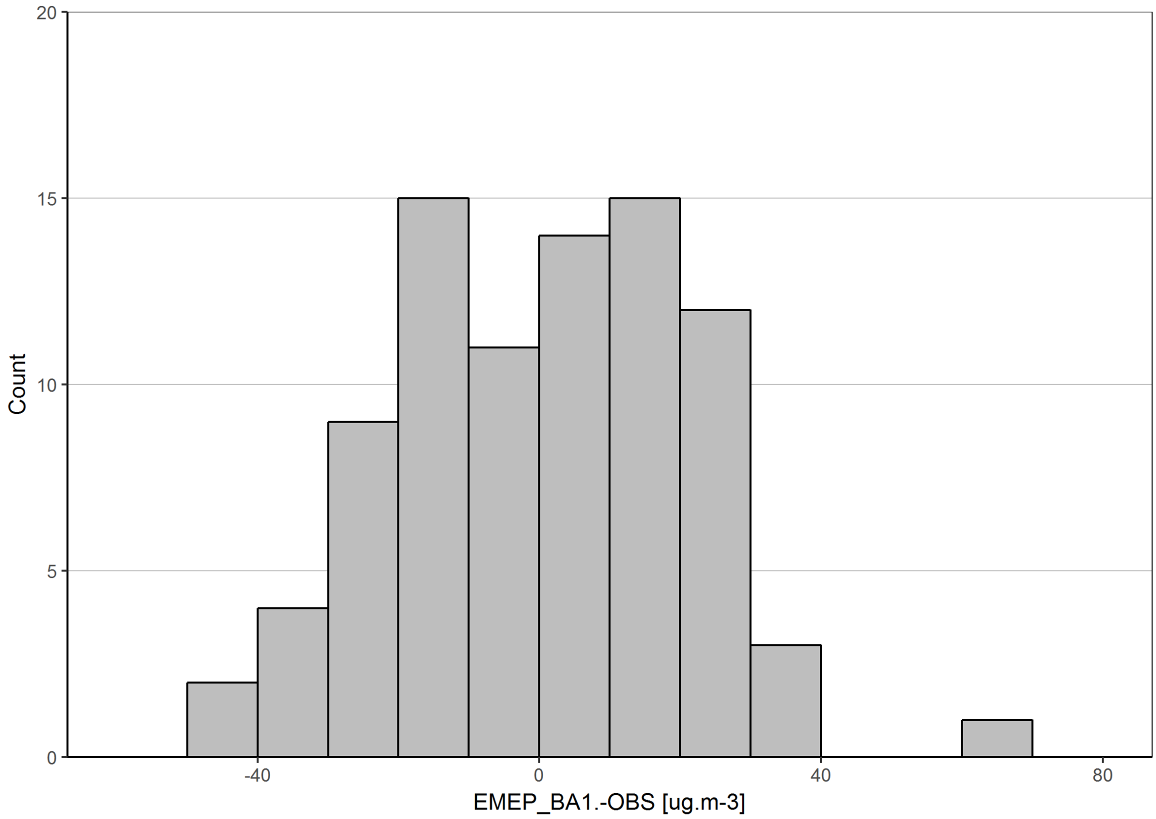
20
15
10
5
0
Count
-40
0
40
80
EMEP_BA1.-OBS [ug.m-3]

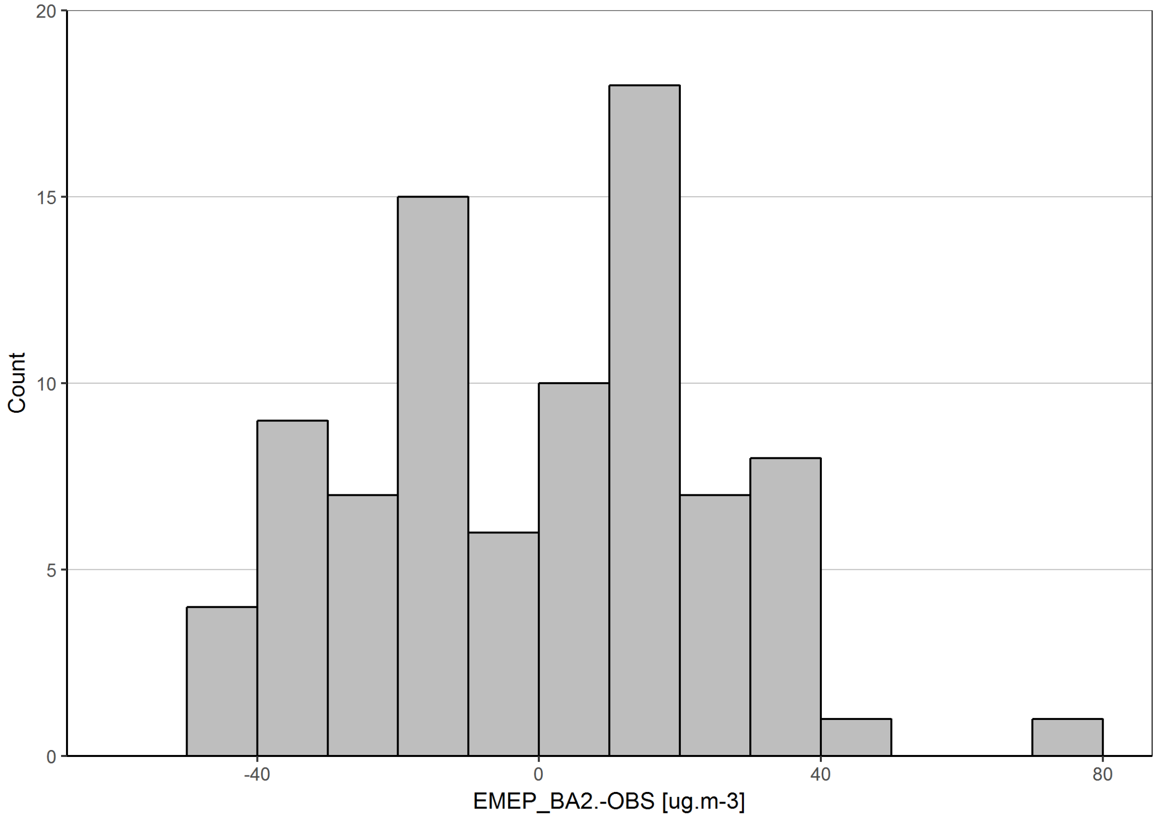

Figure 3.8. Bias distribution of original (upper), BA1 (middle) and BA2 (lower) adjusted modelled results of $PM_{2.5}$ concentration.

The influences of BA1 and BA2 on NMGE and RMSE, which reflect both systematic and unsystematic errors, are however different. BA1 slightly reduces NMGE and RMSE, while BA2 increases both slightly. Figure 3.8 presents the distribution of bias between observations and original (upper panel), BA1 (middle panel), and BA2 (lower panel) adjusted modelled results of $PM_{2.5}$ concentration. It can be seen that the bias between the observed and the originally modelled $PM_{2.5}$ concentrations spread from -60 to 60 μg/m^3, and are more distributed towards the left side.

BA1 and BA2 are both effective for making the bias distribution more balanced around the value zero. Applying BA1 can also make the bias distribution more concentrated around the value zero (see middle panel of Figure 3.8), while the bias distribution is more dispersed when BA2 is applied (see lower panel of Figure 3.8). From this point of view, BA1 shows a better effect for bias adjustment of the data than BA2.

As a more comprehensive bias adjustment technique, BA3 improves all the listed model performance evaluation metrics (see Table 3.5). Apart from MB, RMSE also substantially decreased from originally 22.37 to 8.1 μg/m^3. The correlation coefficient (r) is also improved from 0.49 to 0.64. Figure 3.9 presents the scatter plot of observations and BA3 adjusted modelled results of annual average PM2.5 concentrations in 86 cities over China in 2010. Compared with Figure 3.7, it can be seen that after BA3 adjustment there are no data points located below the y = 0.5x line, and all the data points are more adjacent to the y = x line.

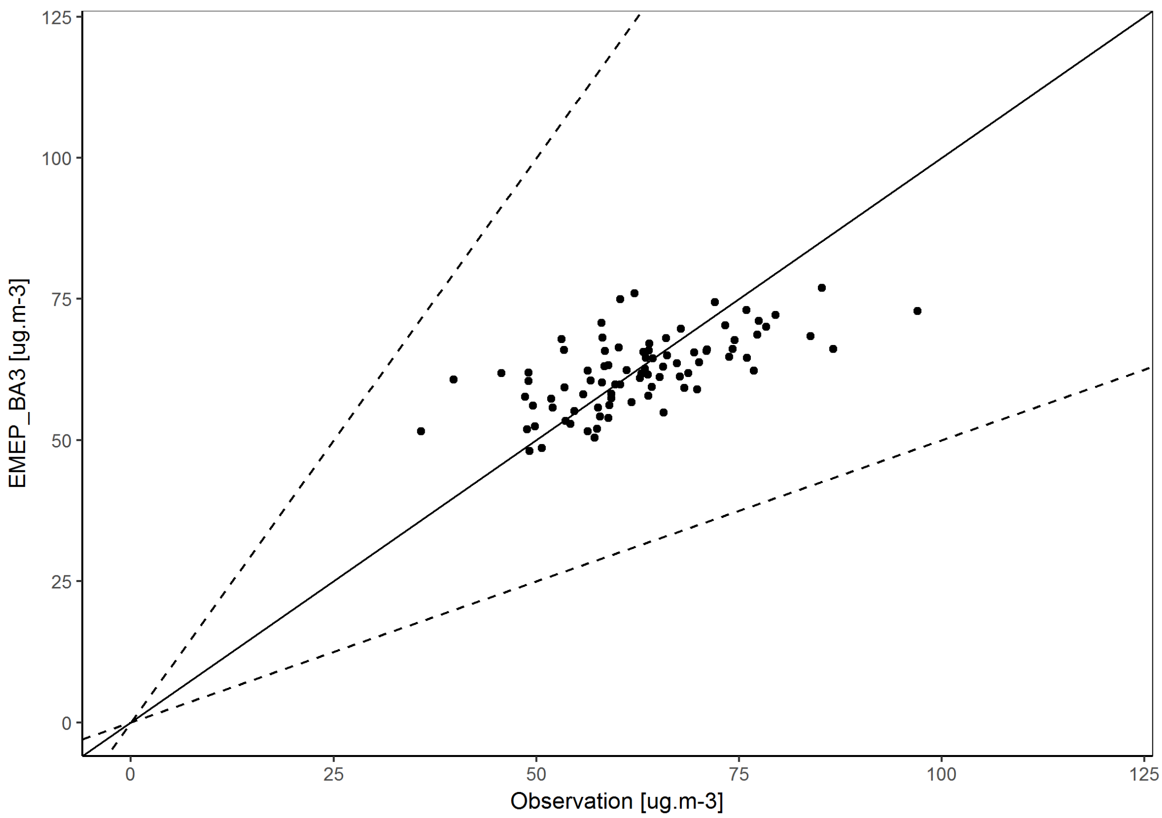

Figure 3.9. Scatter plot of observations and BA3 adjusted modelled results of annual average PM2.5 concentration in 86 cities over China.

It can be concluded that all the three investigated bias adjustment methods are capable of reducing to some extent the bias between observed and simulated annual average $PM_{2.5}$ concentration in China. With no need of other supplementary data, the applications of BA1 and BA2 are simple and time-efficient. BA3 can simultaneously reduce modelling bias and improve correlation between observed and simulated $PM_{2.5}$ concentration records. However, BA3 requires more input data, such as meteorological data and population density which have influence on PM concentration and composition.

BA1 is found to be effective for improving all the considered model evaluation metrics except for the correlation coefficient. Considering that projection of future meteorological and population density data may introduce new uncertainties, BA1 is applied in the next steps. A sensitivity analysis investigating the influences of the three bias adjustment techniques on the results of health impact assessment is presented in section 4.1.

3.3 Health effects of air pollution

With the estimated $PM_{2.5}$ concentration level and the CRFs discussed before, YOLL due to $PM_{2.5}$ pollution are analysed for all the identified scenarios. Firstly, the health effects caused by $PM_{2.5}$ pollution in 2010 (BL) and 2030 (BAU) are presented, then the obtainable health benefits of policy scenarios compared to BAU in 2030 are discussed.

3.3.1 Health impacts of $PM_{2.5}$ pollution in BL 2010 and BAU 2030

Results show that long-term exposure to $PM_{2.5}$ concentration levels under the scenario BL and BAU would reduce the life expectancy of people at different ages by 8.6-18.6 and 7.5-16.4 months in China. 8.2 and 13.4 million YOLL are estimated to be related to $PM_{2.5}$ pollution nationwide in BL 2010 and BAU 2030, respectively.

The results presented in this chapter are calculated using bias adjusted (applying BA1 as described in section 3.2.2) $PM_{2.5}$ concentration and the nonlinear CRF. The nonlinear CRF is chosen here as it covers the entire exposure range, with special consideration of the substantial variation of $PM_{2.5}$ concentration in all the grids over China (see Figure 3.5). A sensitivity analysis of different bias adjustment techniques and CRFs are discussed in section 4.

3.3.1.1 Loss of life expectancy from exposure to $PM_{2.5}$

It is estimated that long-term exposure to $PM_{2.5}$ concentration of 2010 and BAU 2030 in China will reduce the life expectancy of people at different ages by 8.6-18.6 and 7.5-16.4 months, respectively. Taking differences of life expectancy at birth as representative indicator, substantial spatial variation of LLE attributable to $PM_{2.5}$ is observed for both 2010 (0-26.9 months) and 2030 (0-24.7 months) as shown in Figure 3.10.

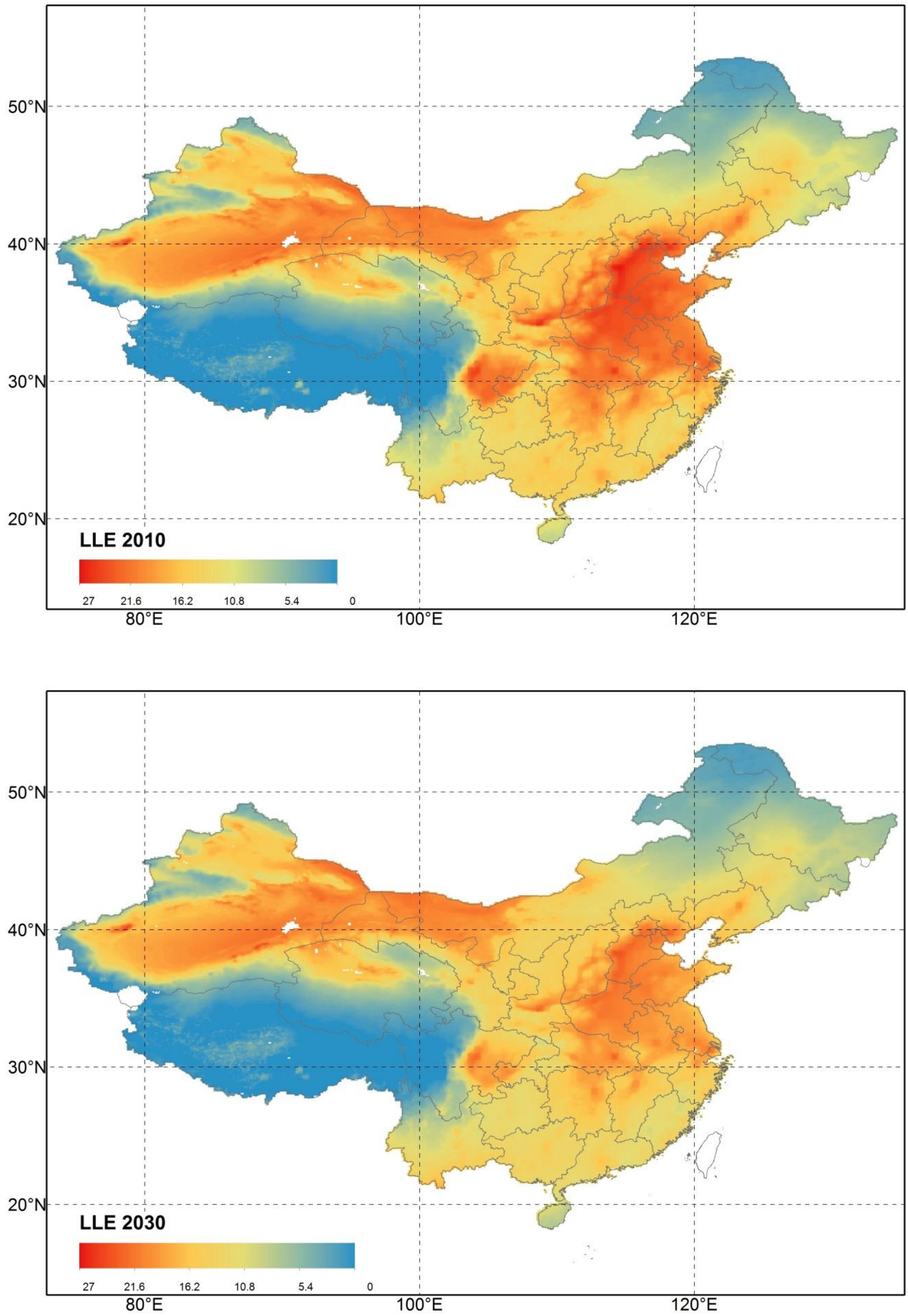

Figure 3.10. Loss of life expectancy (LLE) attributable to $PM_{2.5}$ under BL 2010 and BAU 2030 (unit: month).

The estimated LLE are consistent with other estimates, e.g. 16.5 months from Global Burden of Disease (GBD) Study 2010 (Lim et al., 2012; Lozano et al., 2012), 3-5 years in cities north of Huai River in China (Chen et al., 2013), 8.0-22.2 months under pollution level in 2004 and 2013 in China (Ma et al., 2016).

Higher LLE are estimated for eastern and northwest China owing to higher pollution levels. As the PWC of $PM_{2.5}$ is estimated to decrease from 49.7 μg/m^3 in 2010 to 39.6 μg/m^3 in BAU 2030 (see Table 3.3), LLE attributable to $PM_{2.5}$ is also calculated to decrease over China especially in polluted regions where higher reductions of air pollutants emission are forecasted. Improvement of air quality from 2010 to BAU 2030 can lead to a maximum of 4.4 months gain of life expectancy among all the grids in China (see Figure S1).

3.3.1.2 Years of life lost from exposure to $PM_{2.5}$

The YOLL attributable to long-term $PM_{2.5}$ exposure in China are 8.2 and 13.4 million in 2010 and BAU 2030, respectively. Figure 3.11 displays the spatial distribution of attributable YOLL in 2010 and 2030. Higher YOLL and changes are observed in eastern China, especially around big cities with high pollution level and population density (see also Figure S2). Figure 3.12 displays the distribution of attributable YOLL and population exposed to different levels of $PM_{2.5}$ concentration in 2010 and BAU 2030. The distributions of $PM_{2.5}$ concentration in all the grids (1-141 μg/m^3 in 2010; 1-108 μg/m^3 in 2030) are divided into 500 logarithmically spaced bins. The bin-width-normalized sum of attributable YOLL and population for the grids in each concentration bin is then calculated.

The population-$PM_{2.5}$ distribution in 2010 has a broad peak between 30-50 μg/m^3, and has two sharp peaks around 70 and 100 μg/m^3 (see Figure 3.12). The population-$PM_{2.5}$ distribution in 2030 has a similar shape as that in 2010, but it is shifted to the left side of the x-axis (lower $PM_{2.5}$ concentration). As health risks increase with $PM_{2.5}$ concentration, the YOLL-$PM_{2.5}$ distribution is skewed to the right of the population-$PM_{2.5}$ distribution. The YOLL-$PM_{2.5}$ distribution in 2030 has a larger area than that of 2010, which represents an increase of total attributable YOLL.

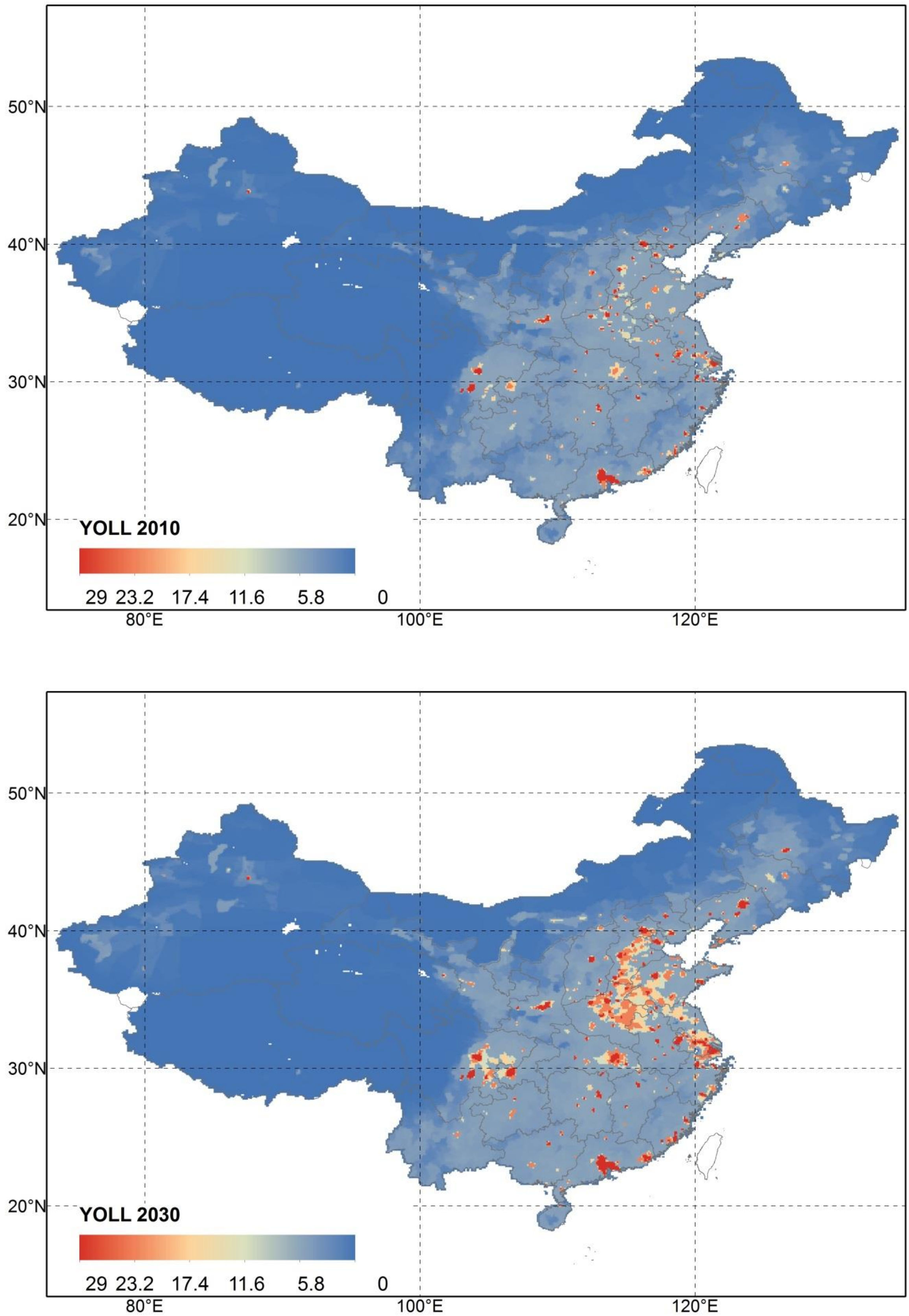

Figure 3.11. Years of life lost (YOLL) attributable to $PM_{2.5}$ in BL 2010 and BAU 2030 (unit: 10^3 years).

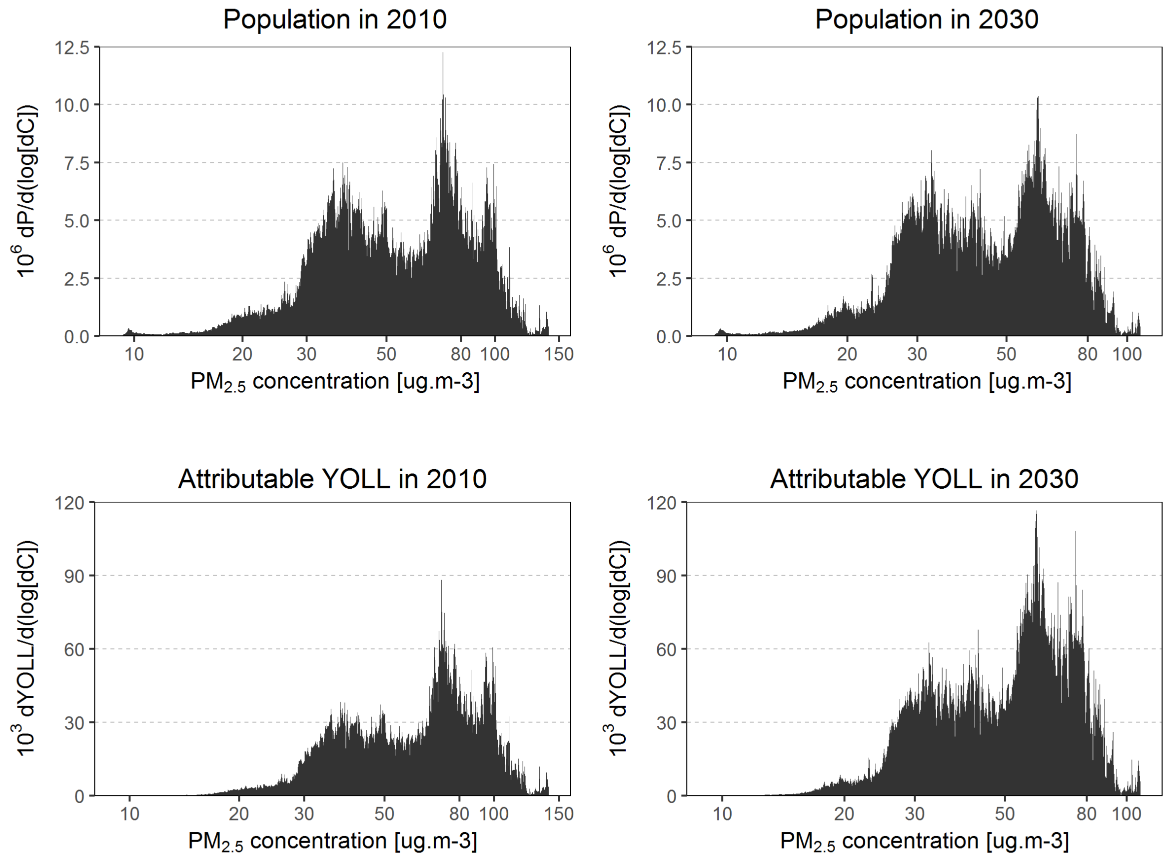

Figure 3.12. Distributions of population and YOLL to $PM_{2.5}$ concentration in BL 2010 and BAU 2030.

Based on the YOLL-$PM_{2.5}$ distribution, the total YOLL attributable to $PM_{2.5}$ exposure are segmented into four equal groups (Quartiles of YOLL: 2.06 million per group in 2010, 3.35 million per group in 2030). The corresponding $PM_{2.5}$ concentration levels and the exposed population are also listed for each quartile as shown in Table 3.6.

The attributable YOLL per thousand population (YOLL/k pop) is around 1.8 times higher for quartile 4 than for quartile 1 for both years. In 2010, 25% of YOLL attributable to $PM_{2.5}$ are experienced by 19% (35%) of population who live in areas with $PM_{2.5}$ concentration higher than 81 μg/m^3 (lower than 41 μg/m^3). A similar figure can be seen for 2030. 79% (67%) of population living in areas with $PM_{2.5}$ concentration higher than 35 μg/m^3, national secondary $PM_{2.5}$ standard of China, experience 87% (77%) of total attributable YOLL in 2010 (2030). Regions with $PM_{2.5}$ concentration higher than 75 μg/m^3 acount for 26% (10%) of population and 34% (13%) of YOLL attributable to $PM_{2.5}$ exposure in China in 2010 (2030).

Table 3.6. Targeting population of concentration-based quartiles of YOLL in BL 2010 and BAU 2030.

Year	Quartiles	$PM_{2.5}$ concentration		Population		Attributable YOLL	
		range	mean	million	% of total	million	per k pop
2010	1	0-41.4	22.2	463.6	34.6	2.06	4.44
	2	41.4-64.7	52.2	336.2	25.1	2.06	6.13
	3	64.7-81.3	71.1	285.6	21.3	2.06	7.21
	4	81.3-140.2	94.7	255.4	19.0	2.06	8.07
2030	1	0-35.5	19.9	488.6	34.5	3.35	6.85
	2	35.5-53.2	43.3	355.2	25.1	3.35	9.42
	3	53.2-65.7	59.0	298.9	21.1	3.35	11.19
	4	65.7-107.9	73.4	272.9	19.3	3.35	12.26

3.3.1.3 Health impacts from $PM_{2.5}$ by province

The health impacts caused by $PM_{2.5}$ pollution are also analysed at provincial level. Figure 3.13 shows the YOLL per thousand population experienced by the population living under $PM_{2.5}$ pollution in 31 provinces (provinces, municipalities, and autonomous regions) in mainland China in BL 2010 and BAU 2030. The red coloured provinces (Henan, Beijing, Hebei, and Tianjin) are the areas with highest $PM_{2.5}$ pollution in China, and are consequently experiencing higher health impacts from $PM_{2.5}$ per unit population (ca. 8 YOLL/k pop in 2010, 12 YOLL/k pop in BAU 2030).

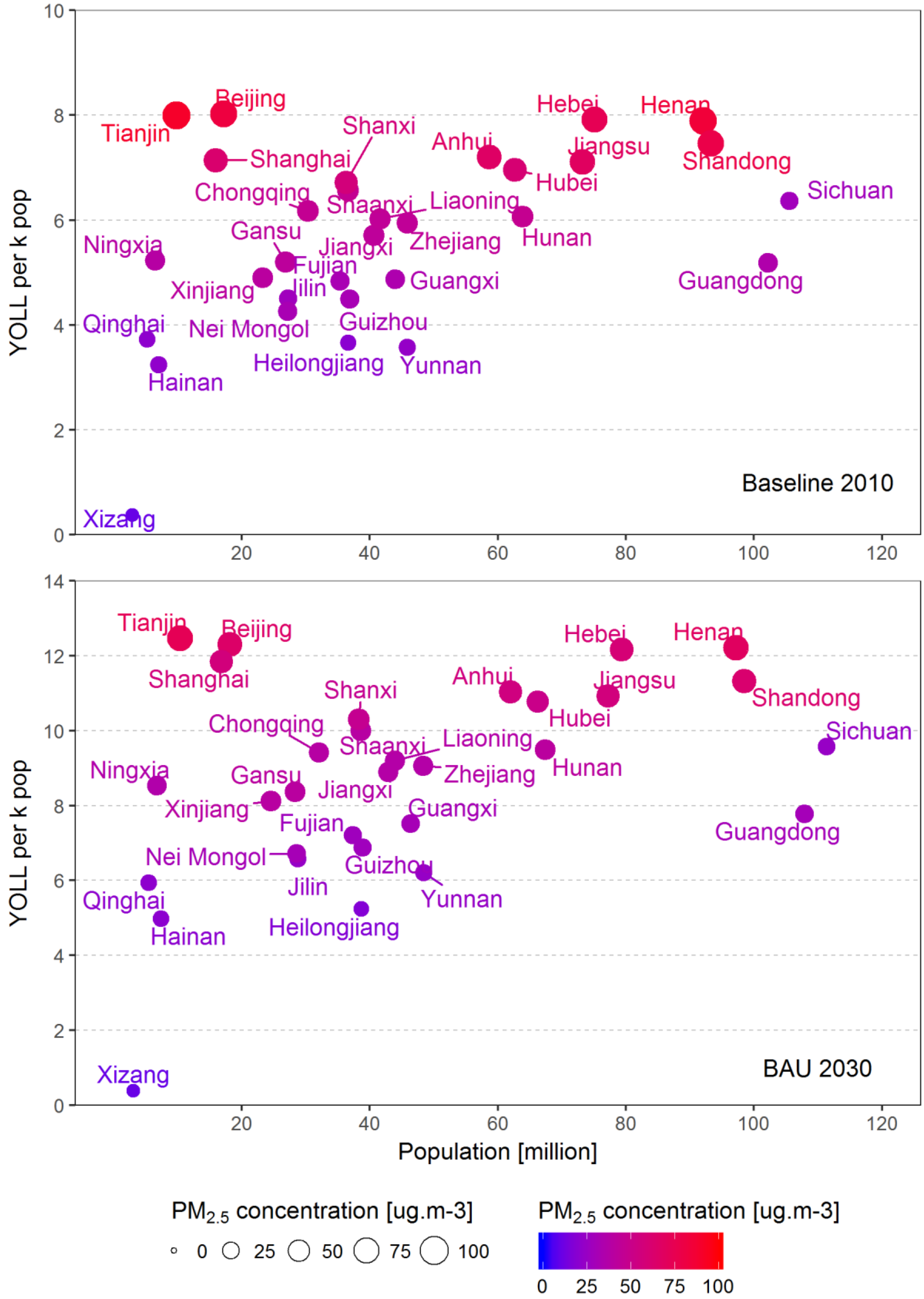

Figure 3.13. YOLL per thousand population and PM2.5 concentration in BL 2010 and BAU 2030 in Chinese provinces.

Metropolitan clusters, such as BTH, PRD, and YRD region, are the focus areas of haze pollution in China. The YOLL attributable to $PM_{2.5}$ in BTH region are 0.8 million in 2010 and 1.3 million in BAU 2030, which amount to 10% of total attributable YOLL in China. Comparing the most populous provinces in China (Henan, Shandong, Sichuan, and Guangdong), the Northern provinces (Henan and Shandong) have higher $PM_{2.5}$ pollution levels than the southern ones (Sichuan and Guangdong).

The population in Henan and Shandong is 10% less than that of Sichuan and Guangdong. However, the YOLL attributable to $PM_{2.5}$ in Henan and Shandong are 18% (21%) higher than that of Sichuan and Guangdong in 2010 (2030). Lower health impacts from $PM_{2.5}$ are observed for less economically developed provinces (Xizang, Hainan, Heilongjiang, and Yunnan). It can be seen by comparing the upper and lower panel of Figure 3.13 that $PM_{2.5}$ concentrations are predicted to decrease in most provinces from 2010 to BAU 2030, however, the attributable YOLL per thousand population are estimated to increase. The underlying causes to this situation are discussed in the next section.

3.3.1.4 Influences of population growth and ageing

It can be seen that even though the LLE attributable to $PM_{2.5}$ exposure in China decreased from 2010 to BAU 2030 (Figure 3.10), the corresponding YOLL increased (Figure 3.11) in most regions. LLE reflects the impacts of increased hazard rate caused by air pollution, and is estimated based on baseline incidence rates and relative risks. While YOLL, by definition (see Equation 2.9), depends not only on ambient $PM_{2.5}$ concentration, but also on the size and age structure of the exposed population.

The population in China is projected to increase from 1.34 billion in 2010 to 1.42 billion in 2030 with considerable population ageing (UN, 2015). The proportion of people aged over 50 will increase from 25% in 2010 to 40% in 2030 as can be seen in Figure 3.14. In order to examine how the population change will overshadow the YOLL reduction from emission reduction of BAU 2030 compared with that of 2010, a sensitivity analysis of population growth and age structure change on YOLL attributable to $PM_{2.5}$ exposure in BAU 2030 is conducted.

The YOLL attributable to $PM_{2.5}$ exposure in BAU 2030 are calculated considering different assumptions on the target population: P1, population size and age structure are the same as that of 2010; P2, considering only population size increase not ageing; P3, considering only population ageing not population size increase; P3, real population projection of 2030 which considers both population growth and ageing. P1 demonstrates the impact of air pollution reduction isolated from population change.

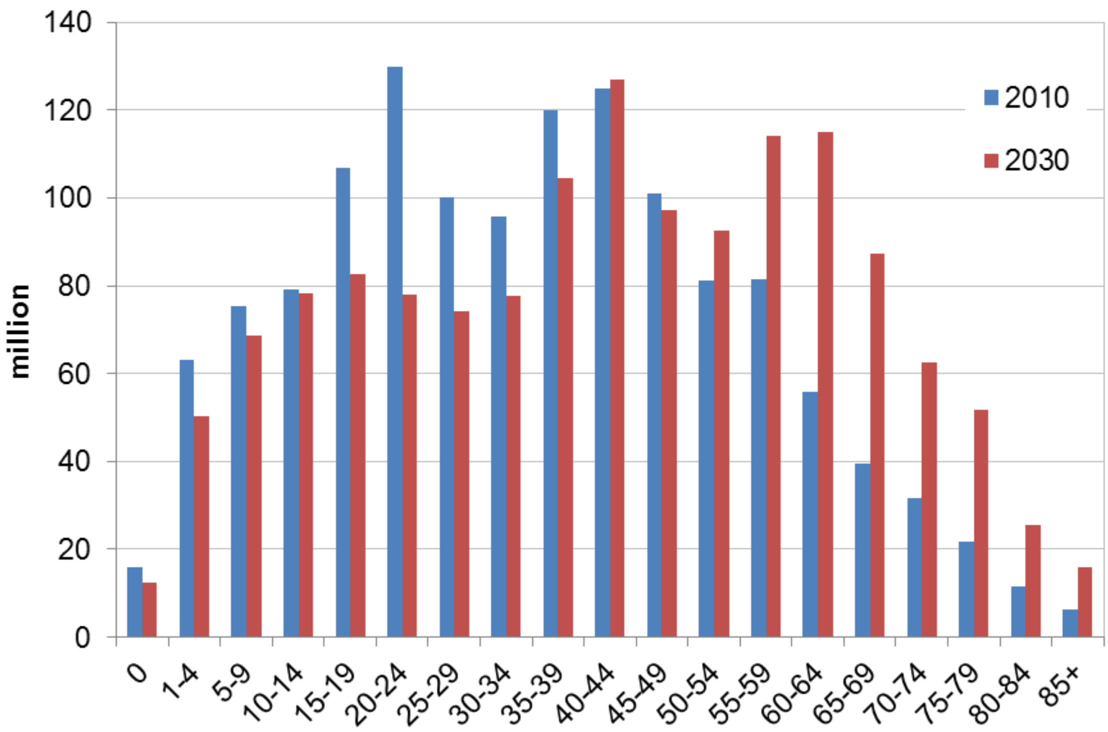

Figure 3.14. Age structure of population in China in 2010 and 2030.
Source: visualized by author based on UN (2015).

As is shown in Table 3.7, YOLL attributable to $PM_{2.5}$ is estimated to be 7.2 million in 2030 if no population change is projected, which represents a 12% decrease from those in 2010 (8.2 million). In P2, 6% population growth from 2010 to 2030 is considered, which will result in 5.6% higher YOLL attributable to $PM_{2.5}$ compared with those for P1. Considering population ageing (P3), the attributable YOLL of 2030 is estimated to be 12.7 million, 75.3% higher than that of P1. Combining population ageing and growth, the attributable YOLL in BAU 2030 will be increased by 85% compared with those for P1, and are 63% higher than those in 2010.

It is worth noting that changes in population size and age structure are not the only driving factors that affect the estimation of $PM_{2.5}$ induced YOLL from 2010 to 2030. Changes in wealth, health care, building technologies, and lifestyles (e.g.

smoking, exercise) are all potential impact factors. However, without reliable information on the changing patterns and the impact pathways, and more importantly, with the intention to isolate the impact of air pollution reduction, these factors are assumed to be the same in the policy scenarios as in the BL and BAU scenarios.

Table 3.7. Influences of population growth and age structure change on YOLL attributable to $PM_{2.5}$ in 2030.

Assumption on population	P1	P2	P3	P4
YOLL (million)	7.2	7.6	12.7	13.4
Increase of YOLL compared with P1	-	5.6%	75.3%	85.0%

Note: assumptions on population in 2030 compared with that of 2010: P1-identical population as that of 2010; P2-only population growth; P3-only age structure change; P4-consider both population growth and age structure change.

3.3.2 Health benefits of policy scenarios in 2030

3.3.2.1 Avoidable YOLL and LLE attributable to long-term $PM_{2.5}$ exposure

The estimates of reduced health damages that may be obtained by implementing the strategies considered in the policy scenarios (as discussed in section 3.1.2) are reported in this section. Compared with the BAU scenario, improvement of air quality under the MTFR, CLMT, and COMB scenarios may avoid 3.5, 0.9, and 4.0 million YOLL attributable to long-term exposure to $PM_{2.5}$.

Through adopting best available end-of-pipe air pollutants control technologies in the MTFR scenario, the LLE attributable to long-term $PM_{2.5}$ exposure of people in different age groups may be reduced by 2.03-4.29 months, compared to those in the BAU scenario. Health benefits of climate change mitigation strategies (represented in the CLMT scenario) are also significant although not as striking: the $PM_{2.5}$ induced LLE would be reduced by 0.5-1.0 months. By implementing both end-of-pipe technologies and climate change mitigation strategies (represented in the COMB scenario), the $PM_{2.5}$ induced LLE would be reduced by

2.3-4.8 months, which represent a 30% reduction compared with those in the BAU scenario.

3.3.2.2 Health benefits of policy scenarios by provinces

Health benefits of policy scenarios attributable to reduced $PM_{2.5}$ exposure vary substantially among Chinese provinces. Figure 3.15 presents the estimation of the avoided YOLL per million population in Chinese provinces related to the reduced levels of $PM_{2.5}$ concentration (represented by the colour and size of the data points) in the MTFR (upper panel), CLMT (middle panel), and COMB (lower panel) scenarios compared to the BAU scenario. The discussions of policy scenarios hereafter are all based on comparisons with the BAU scenario.

Under the MTFR scenario, $PM_{2.5}$ concentration in Chinese provinces can be reduced by 0.1-33 μg/m^3. Higher reductions are observed in Tianjin, Henan, and Beijing. While in provinces where $PM_{2.5}$ concentrations are relatively low in BAU, e.g. Xizang, Qinghai, and Hainan, lower $PM_{2.5}$ concentration reductions are predicted. Through implementing the policy measures in the MTFR scenario, $PM_{2.5}$ related provincial YOLL can be reduced by 800-278,000 years. Henan, Sichuan, and Guangdong are the provinces where highest benefits, in terms of total avoided YOLL attributable to long-term $PM_{2.5}$ exposure, are observed. They are the most populous provinces in China, improving the air quality in these provinces can yield highest total benefits.

Avoided YOLL per million population give indication of obtainable health benefits from reduced $PM_{2.5}$ concentration for a standardized population, which helps to look exclusively at the impact of $PM_{2.5}$ exposure. Under MTFR, the avoided YOLL per million population of Chinese provinces range between 0.3 and 4.7 mainly concentrated around 2.5, as is shown in the upper panel of Figure 3.15. Shanghai, Beijing, and Tianjin are the provinces with highest per capita YOLL avoided. It can be seen that the $PM_{2.5}$ concentration reduction in Shanghai is smaller than that in Tianjin, while the per capita YOLL avoided is estimated to be higher in Shanghai than that in Tianjin. This reflects the nonlinearity of the concentration-response relationships.

As has been discussed in section 3.2.1, $PM_{2.5}$ concentration reductions are predicted to be more significant in the eastern provinces (see Figure 3.6). The corresponding YOLL avoided per capita in these provinces are also projected to be larger. In BTH region, the avoided YOLL attributable to $PM_{2.5}$ are 0.33, 0.11, and 0.36 million in 2030 in the MTFR, CLMT, and COMB scenarios respectively, which correspond to over 9% of total avoided YOLL in each scenario. Provinces in YRD region (Shanghai, Jiangsu, and Zhejiang) have a population of 150 million (11% of total population in China) in 2030.

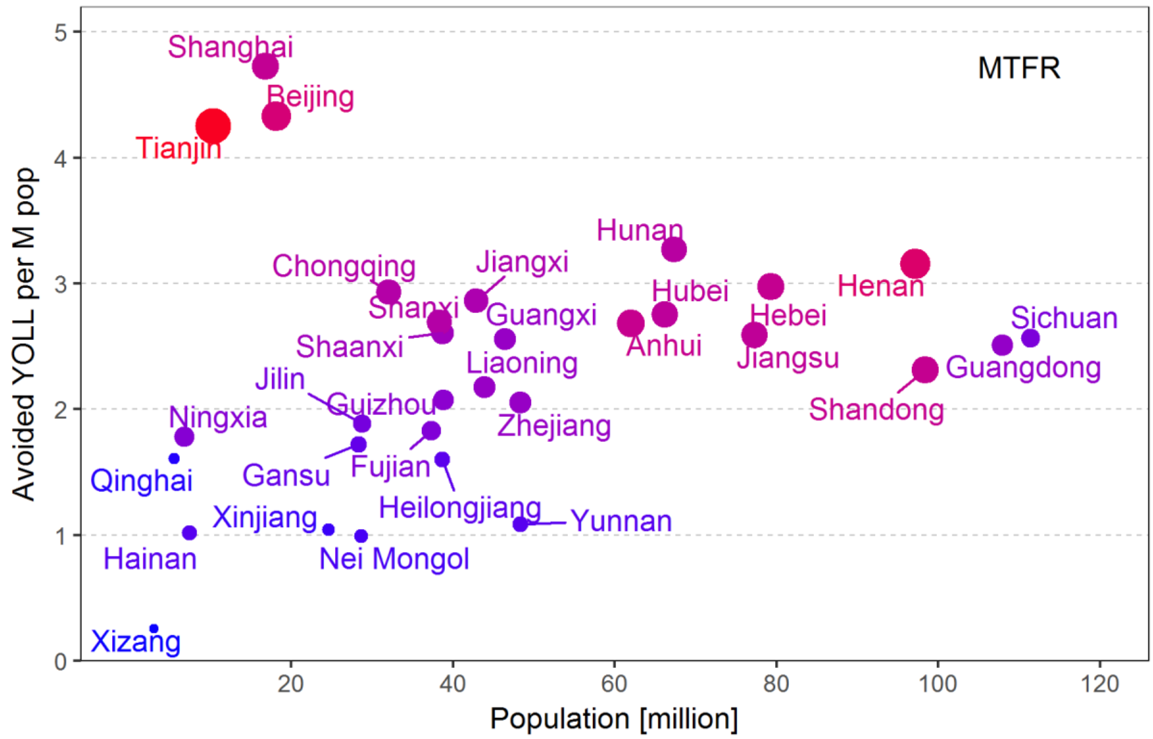

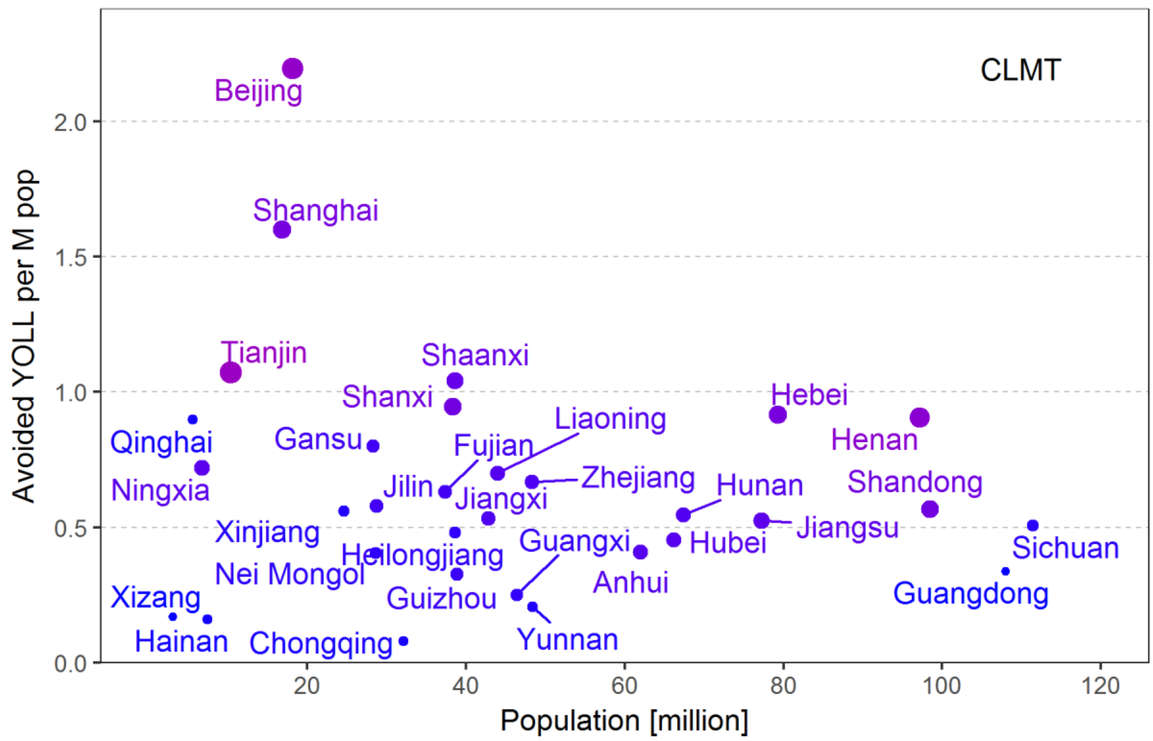

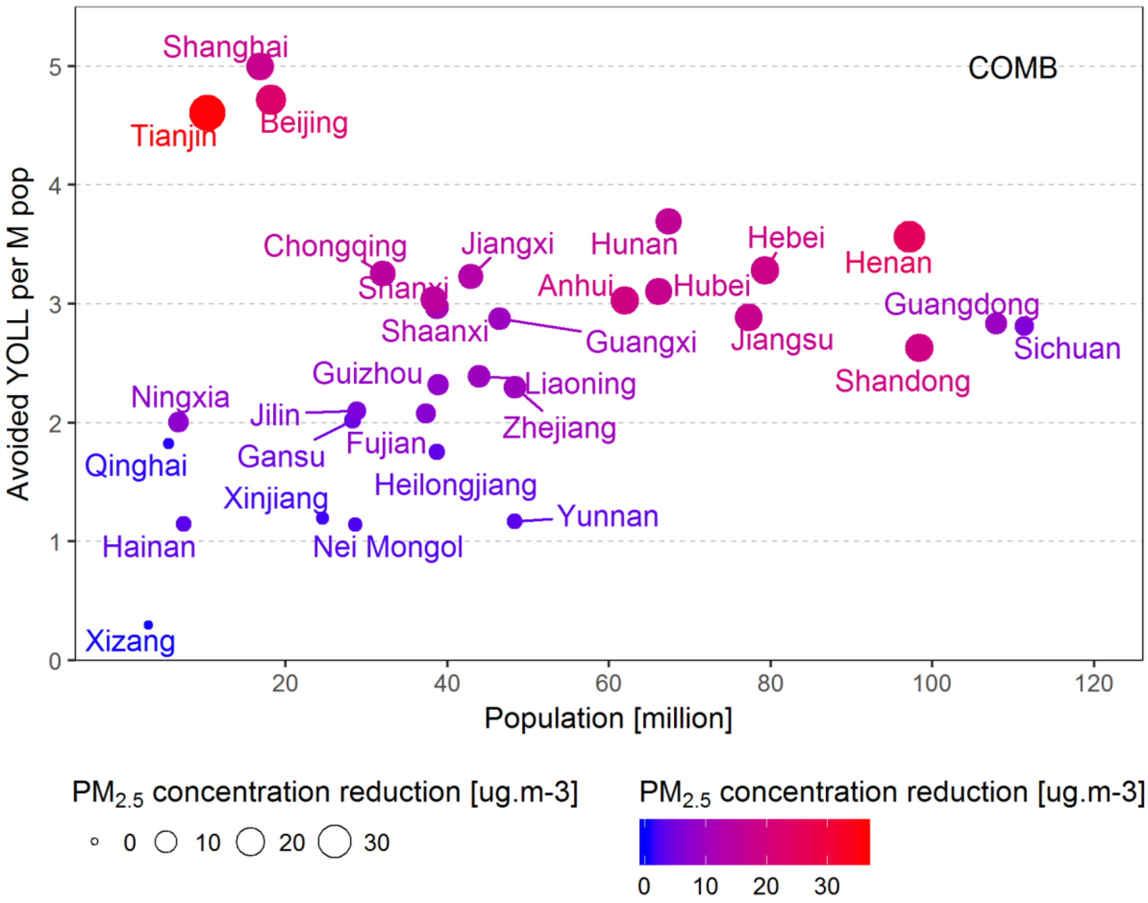

Figure 3.15. Avoided YOLL per million population and $PM_{2.5}$ concentration reduction under the MTFR, CLMT, and COMB scenarios compared to the BAU scenario in Chinese provinces in 2030.

Policy measures in MTFR, CLMT, and COMB may avoid 0.47 (13% of total avoided YOLL), 0.14 (16%), and 0.51 (13%) million YOLL attributable to $PM_{2.5}$ in YRD in 2030. The top three provinces with highest avoided YOLL attributable to $PM_{2.5}$ are: Henan, Sichuan and Guangdong in MTFR; Henan, Hebei, and Shanghai in CLMT; Henan, Guangdong, and Sichuan in COMB. These provinces are the most populous and industrialized regions in China. With relatively higher pollution levels, they are predicted to have higher potentials of air pollution control, which can yield considerable health benefits.

3.4 Monetary valuation of integrated impacts

The damage costs due to long-term exposure to $PM_{2.5}$ in China in 2010 and 2030, as well as the health benefits from reduced air pollution and GHG mitigation benefits obtained from implementing the control options considered in the policy scenarios are measured in monetary terms applying the methodology described in section 2.2.5. Firstly, the valuation of health effects attributable to $PM_{2.5}$ in BL 2010 and BAU 2030 is conducted, the integrated benefits of considered policy scenarios are presented and analysed, and then the policy implications drawn from this study are discussed.

3.4.1 Damage costs due to air pollution in BL and BAU

Long-term exposure to $PM_{2.5}$ is estimated to be related to 8.3 and 13.4 million YOLL in BL 2010 and BAU 2030. Considering the VOLY estimated for China in 2010 and 2030, the related damage costs are 136.8 (85.7, 490.3) billion EUR_{2010} in 2010 and 588.7 (368.0, 2111.4) billion EUR_{2010} in BAU 2030, which amount to about 3.9% (2.5%, 14.1%) of China's GDP in 2010 and 5.2% (3.2%, 18.5%) of GDP in 2030. Under current legislation, the per capita damage costs related to $PM_{2.5}$ in China are predicted to increase more than four times from 102.0 (63.9, 365.6) EUR_{2010}/cap in 2010 to 415.9 (259.9, 1491.6) EUR_{2010}/cap in 2030.

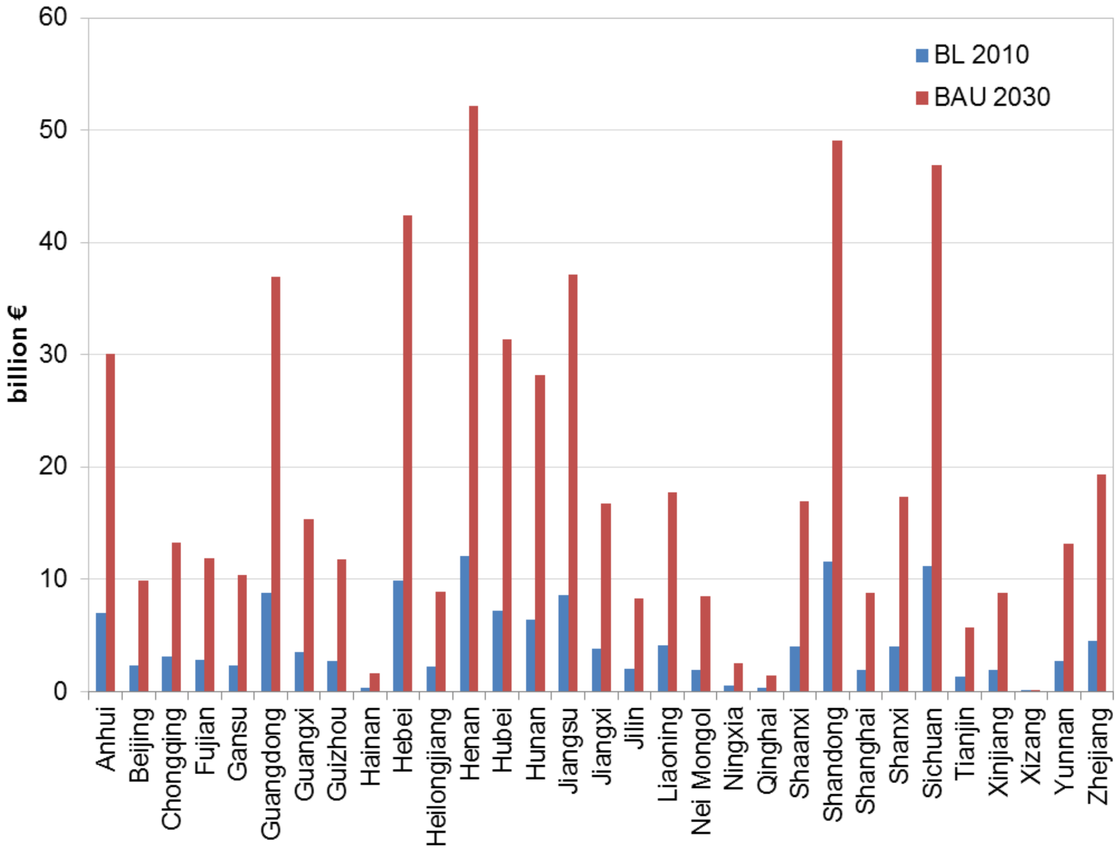

Figure 3.16. Provincial damage costs as a result of $PM_{2.5}$ pollution in BL 2010 and BAU 2030.

Figure 3.16 shows the damage costs (central value) as a result of $PM_{2.5}$ pollution in Chinese provinces in BL 2010 and BAU 2030. In all the provinces $PM_{2.5}$ related damage costs are projected to increase from BL 2010 to BAU 2030. Smaller damage costs are observed in less developed and populated provinces in both years, such as Xizang, Qinghai, Hainan, and Ningxia. High $PM_{2.5}$ related damage costs are estimated in provinces with denser population, such as Henan, Shandong, Sichuan, Hebei, Jiangsu, and Guangdong, which contributed to more than 45% of total damage costs across China in both years.

Owing to high $PM_{2.5}$ pollution levels, BTH region is estimated to experience the highest per capita damage costs attributable to long-term $PM_{2.5}$ exposure of around 130 EUR_{2010}/cap in 2010 and 540 EUR_{2010}/cap in 2030. The above analysis and results show an urgent demand in more stringent air pollution control policies for China. The effectiveness of the designed policy scenarios in terms of reducing damage costs caused by air pollution and climate change compared to the BAU scenario is demonstrated in the next section.

3.4.2 Integrated benefits of policy scenarios

The avoidable health effects in different scenarios are presented in section 3.3.2. The monetary health benefits calculated by multiplying avoidable YOLL with VOLY are listed in Table 3.8. The results show that the health benefits (central values) from MTFR, CLMT, and COMB are 156, 38, and 174 billion EUR_{2010}, respectively, which are about 1.4, 0.3, and 1.5% of GDP in 2030.

Table 3.8. Monetary values of health benefits and GHG reduction benefits in policy scenarios compared with BAU in 2030 (billion EUR_{2010}).

Scenario	Health benefits			GHG reduction benefits		
	Lower	Central	Upper	Lower	Central	Upper
MTFR	97.34	155.75	558.58	12.82	29.48	46.14
CLMT	23.66	37.85	135.75	103.31	237.61	371.91
COMB	108.72	173.95	623.84	116.51	267.97	419.43

The benefits of climate change mitigation are calculated based on MAC and MDC as described in section 2.2.5. In 2030, the benefits from GHG mitigation in MTFR, CLMT, and COMB are around 30, 238, 268 billion EUR_{2010}, respectively, as can be seen in Table 3.8. The estimated GHG reduction benefits from policy scenarios amount to about 0.3, 2.1, and 2.4% of China's GDP in 2030.

The monetary integrated co-benefits of policy scenarios are summarized in Figure 3.17. The central values of the co-benefits of the MTFR, CLMT, and COMB scenarios are 185, 275, 442 billion EUR_{2010}, which represent 1.6, 2.4, 3.9% of GDP in 2030, respectively. These estimates are comparable with other studies (He et al., 2010; Hou et al., 2012; Huang et al., 2012; Xie et al., 2016; Zhang et al., 2013a). In MTFR, the health benefits are much higher than GHG reduction benefits as the end-of-pipe control technologies considered in MTFR are more effective for reducing emissions of air pollutants. In CLMT, the GHG reduction benefits are higher than health benefits since greater reductions in GHG emissions are expected when CCS installation, fuel saving and substitution are considered. In COMB, the health benefits and GHG reduction benefits are relatively comparable.

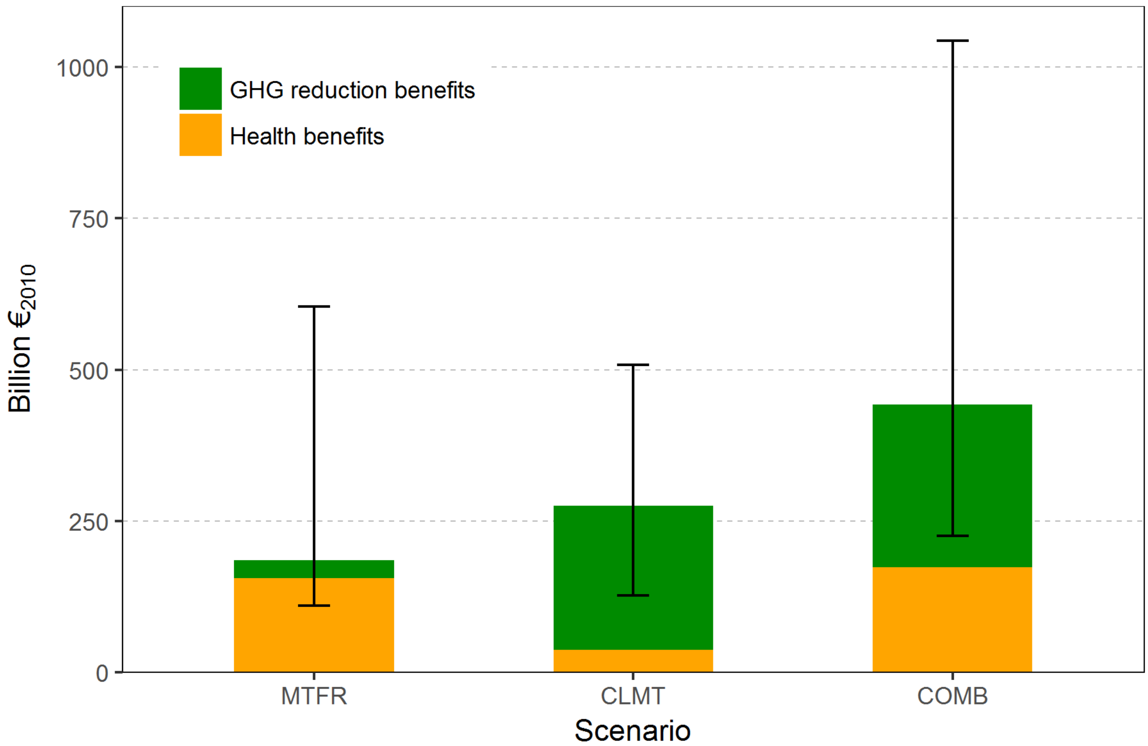

Figure 3.17. Co-benefits of policy scenarios in 2030.

Integrated benefits of policy scenarios vary substantially among provinces. Figure 3.18 presents the integrated benefits of the MTFR, CLMT, and COMB scenarios at provincial level in 2030 with the background colour showing the $PM_{2.5}$ concentration under the BAU scenario. It can be seen that eastern provinces (more populous and developed areas) incur higher co-benefits from policy scenarios, e.g. Shanghai (5.9, 3.7, and 4.1% of total co-benefits in China from MTFR, CLMT, and COMB, respectively), Guangdong (7.2, 6.1, and 6.9%), and Shandong (6.4, 7.3, and 7.1%), Henan (7.9, 7.1, and 7.3%). The economic benefits from all the three policy scenarios are relatively low in Xinjiang, Qinghai, and Xizang, provinces with lower emission and concentration levels.

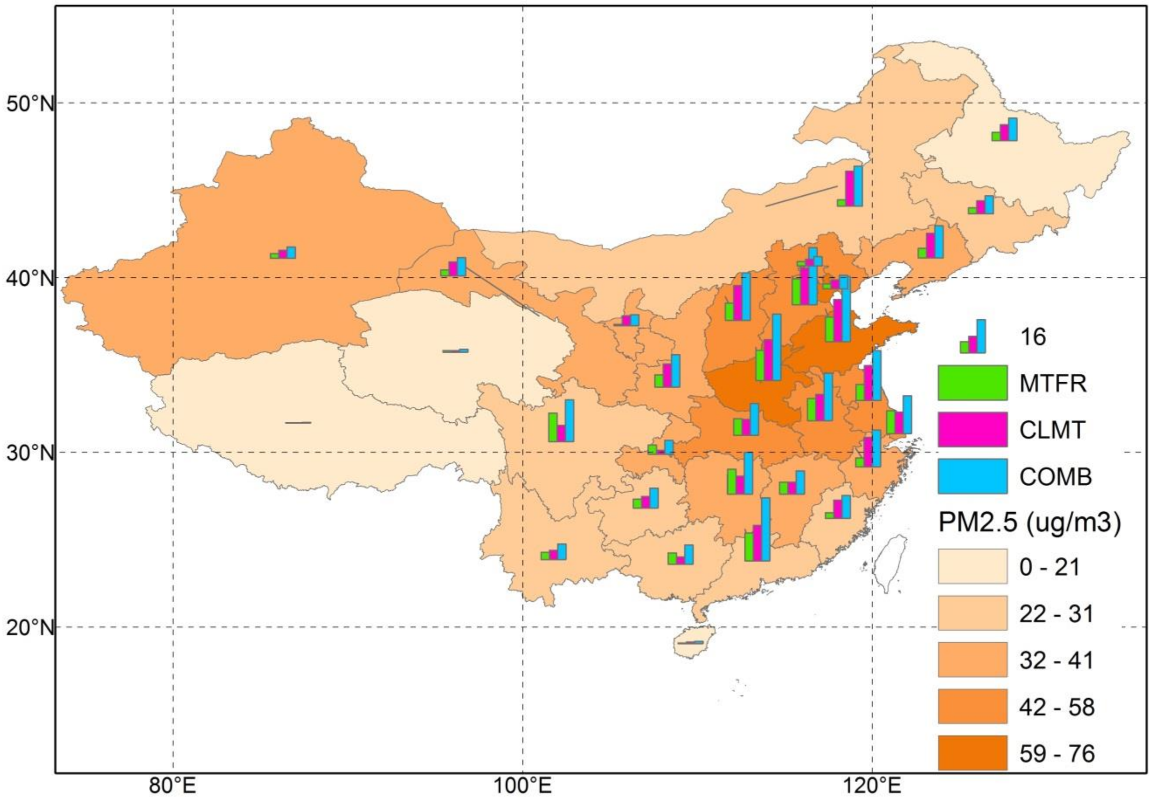

Figure 3.18. Provincial co-benefits of policy scenarios in 2030.

In most provinces, the co-benefits from CLMT are higher than those from MTFR, e.g. Nei Mongol (3.1 and 16.8 billion EUR_{2010} from MTFR and CLMT), Shanxi (8.2 and 16.4 billion EUR_{2010}), Jiangsu (7.6 and 16.8 billion EUR_{2010}), and Zhejiang (4.2 and 14.1 billion EUR_{2010}). The provinces in which co-benefits from MTFR are expected to be higher than those from CLMT are all in the southern of China and with relatively lower GHG emissions, e.g. Sichuan (13.7 and 7.8 billion

EUR_{2010} from MTFR and CLMT), Chongqing (4.4 and 1.9 billion EUR_{2010}), Guangxi (5.5 and 3.6 billion EUR_{2010}), and Hunan (12.0 and 8.6 billion EUR_{2010}).

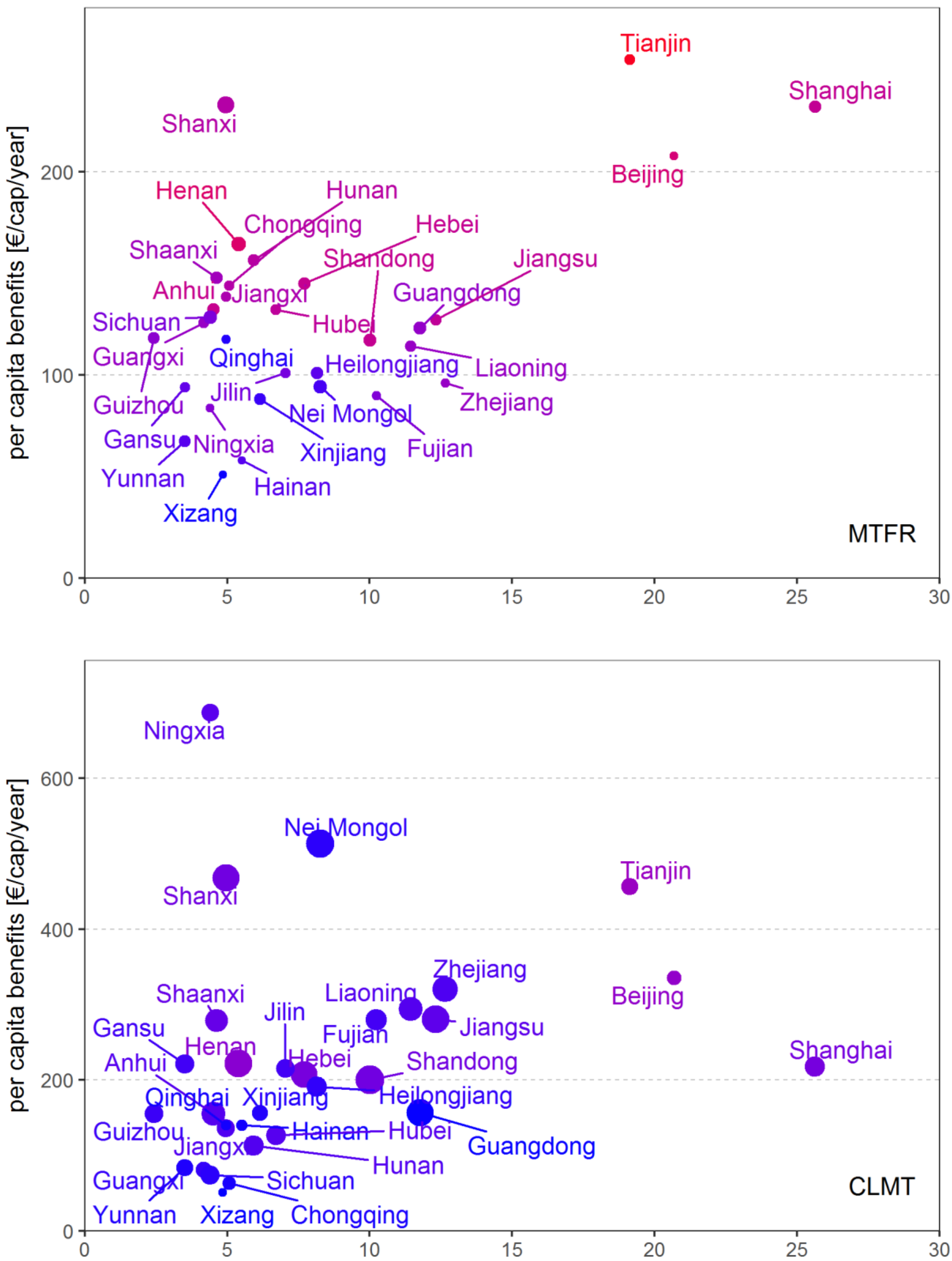

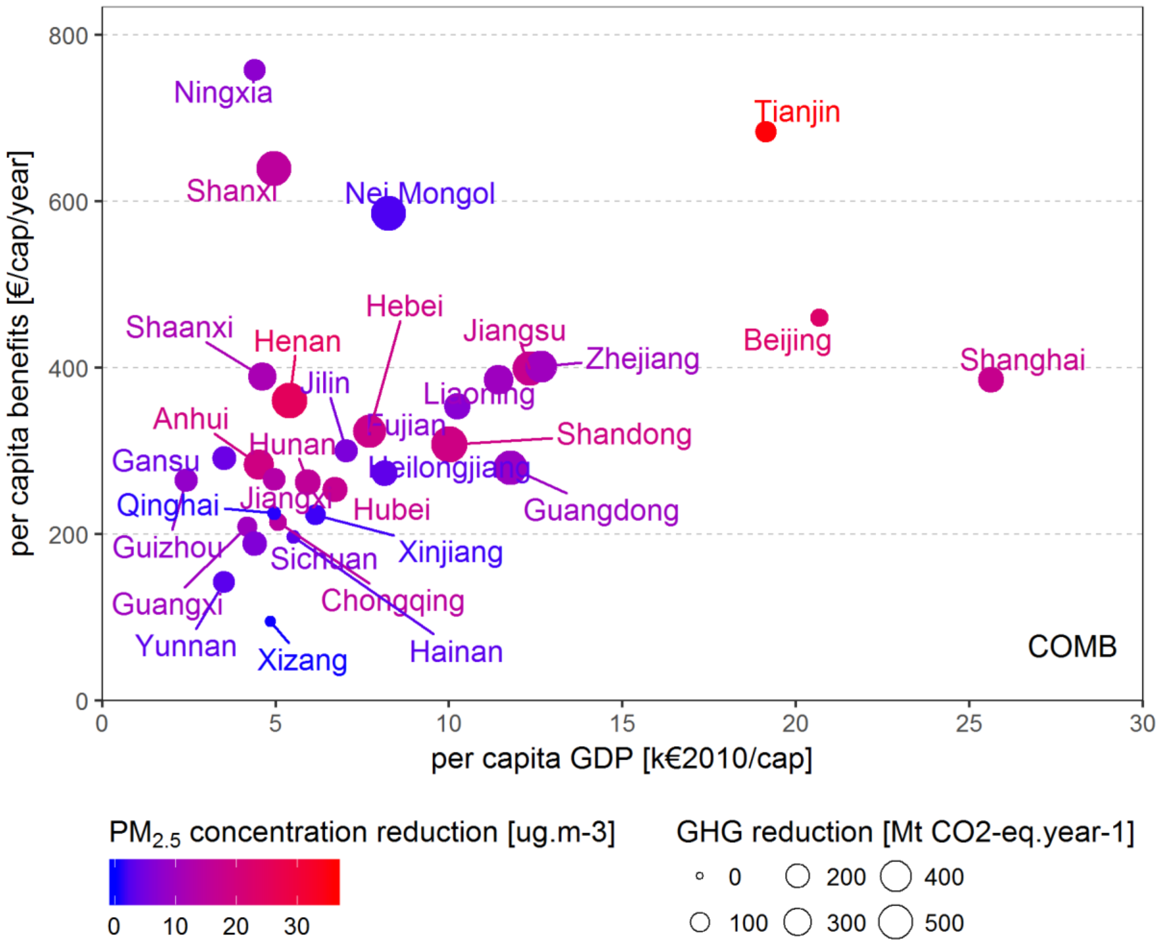

Figure 3.19. Co-benefits per capita under the MTFR, CLMT, and COMB scenarios compared to the BAU scenario in Chinese provinces in 2030.

To take a closer look at provincial benefits from policy scenarios, the per capita integrated co-benefits as a result of reduced $PM_{2.5}$ concentration and GHG emissions are presented in Figure 3.19. Figure S3 and Figure S4 show the data for health benefits and GHG reduction benefits separately. The statistics of provincial per capita co-benefits and the ratio between per capita co-benefits and per capita GDP are summarized in Table 3.9.

In MTFR, the per capita co-benefits from improved air quality and reduced GHG emissions of Chinese provinces range between 51.0 and 255.3 EUR_{2010}/cap. The provinces with highest per capita co-benefits are Tianjin, Shanxi, Shanghai, and Beijing, with 255.3, 232.9, 232.2, and 208.0 EUR_{2010} per capita co-benefits, which represent 1.3, 4.7, 0.9, and 1.0% of per capita provincial GDP in 2030, respectively.

In CLMT, the co-benefits are dominated by GHG reduction benefits. Owing to large amount of GHG emission reduction predicted in less populated provinces, e.g. Ningxia and Nei Mongol, the per capita co-benefits of these provinces are estimated to be high. As the per capita GDP of Ningxia and Nei Mongol are also relatively low, the per capita co-benefits from CLMT of these provinces amount to over 10% of provincial per capita GDP. For most provinces, the per capita co-benefits from CLMT are around 200 EUR_{2010}/cap in 2030.

Table 3.9. Statistics of provincial per capita co-benefits from policy scenarios in 2030.

Scenario	per capita co-benefits (EUR_{2010}/cap)				% of per capita GDP			
	mean	median	min	max	mean	median	min	max
MTFR	128.60	123.09	50.96	255.34	2.01	1.89	0.76	4.89
CLMT	226.55	199.91	50.48	687.50	3.44	2.54	0.85	15.62
COMB	335.54	291.79	95.04	757.75	5.18	4.20	1.50	17.22

In COMB, per capita co-benefits range between 95.0 and 757.8 EUR_{2010}/cap. The top provinces with highest per capita co-benefits from COMB are Ningxia (757.8 EUR_{2010}/cap), Tianjin (683.8 EUR_{2010}/cap), Shanxi (639.5 EUR_{2010}/cap), and Nei Mongol (585.4 EUR_{2010}/cap). In all the three policy scenarios, low co-benefits are observed in Xizang and Yunnan, which have relatively lower $PM_{2.5}$ concentration and GHG emissions and are therefore less sensitive to air quality management strategies.

3.4.3 Discussion and policy implications

Rapid economic growth and increase in energy consumption have caused severe air pollution in China. It is well recognized that benefits of abating air pollutants emissions and GHG emissions can be achieved spontaneously. Quantification of the economic impacts of air pollution and climate change effects in China has caused increasing scientific interests. Hou et al. (2012) reported that China suffered a health-related economic loss due to PM of 2.1% of China's GDP for the year 2009, and even greater than 4% of GDP in some area, which is a bit lower than what is found in this study for the year 2010.

Huang and Zhang (2013) found that the health benefits of achieving $PM_{2.5}$ air quality standard in BTH region account for 1.66-6.94% of regional GDP in 2009, a level quite similar to the findings of this study. A study (Huang et al., 2012) on the PRD region showed the economic loss of the health effects from PM pollution is 1.35% of the regional GDP in 2006. He et al. (2010) found that energy policies which may reduce 12-32% of air pollutant concentration and over 1400 Mt of CO_2 emissions in China can yield more than 100 billion US$ of health benefits in 2030, which are lower than the estimates of this study due to lower control targets.

This study focuses on the impacts of long-term exposure to $PM_{2.5}$ on mortality, which are often used as representative of health effects caused by air pollution (Apte et al., 2015; Boldo et al., 2006; Lee et al., 2015). However it is worth noting that there are several potential benefits from air pollution control measures that are not yet assessed explicitly in this study. One aspect is that control measures not only reduce $PM_{2.5}$ but also other air pollutants (e.g. NO_2 and O_3), and air pollution not only affects mortality but also morbidity. Additionally, reduced air pollution is usually also associated with ecosystem benefits (Bignal et al., 2007; Lovett et al., 2009).

The costs of air pollution control and climate change mitigation measures were not assessed in this study due to the difficulties in collecting cost parameters for variety of sectors. However, this study has developed a methodology to quantify the integrated impacts of environmental policies of China, which is a combination of emission estimation model, atmospheric model, and health and climate change mitigation benefit evaluation model. The analysis of this study provides solid evidence on the substantial benefits achievable from promoting air pollution control and climate change mitigation strategies in China.

Up to 2030, aggressive air pollution control and GHG reduction policies in China will lead to significant benefits in the aspects of health and climate change mitigation. Emissions of air pollutants in China can be reduced by 49-91% for the year 2030 by applying most up-to-date technical reduction technologies, which will lead to a 51% reduction of population-weighted $PM_{2.5}$ concentration compared with the 2010 level. The reduction of $PM_{2.5}$ exposure under the MTFR scenario is estimated to result in 3.5 million avoided YOLL in China compared to the BAU scenario, which corresponds to about 4.3 months of avoided LLE. The total health benefits are calculated to be around 156 billion EUR_{2010}, 1.4% of China's GDP in 2030.

Applying air pollutants reduction technologies can also reduce the GHG emissions by 5% in 2030. The corresponding GHG reduction benefits are estimated to be around 30 billion EUR_{2010}, which adds the total co-benefits up to 185 billion EUR_{2010}, 1.6% of China's GDP in 2030. MTFR might not be the most economic option when taking into account also the costs of the policies, but it provides valuable information about the magnitude of achievable benefits through implementing technical reduction technologies. Future technology development and economies of scale may improve the emission reduction potential and reduce the costs of the technologies.

GHG emission mitigation measures can reduce the GHG emission per GDP by 41% in 2030 compared to the BAU scenario, together with a 7-22% reduction of air pollutants. As a result of 30% reduction of population-weighted $PM_{2.5}$ concentration compared with the 2010 level, 0.9 million YOLL or 1.0 months of LLE can be avoided. The total co-benefits of CLMT account for 2.4% of China's GDP in 2030, 14% of which are health benefits from reduced air pollution. The CLMT scenario gives insights on the co-benefits for air pollution induced health impacts achievable through pursuing climate change mitigation targets.

By implementing simultaneously air pollutant reduction technologies and GHG mitigation measures, emissions of air pollutants and GHG are projected to reduce by 46-93% compared to the BAU scenario in 2030. Compared with the 2010 level, the population-weighted $PM_{2.5}$ concentration and the GHG emission per GDP can be reduced by 54 and 74%, respectively. The total integrated benefits are estimated to be around 442 billion EUR_{2010} (3.9% of China's GDP in 2030), in which health benefits and GHG reduction benefits account for 40 and 60%, respectively. As the problems of air pollution and climate change are quite interrelated, it is often the case that addressing them together will also be economically efficient (Dong et al., 2015; West et al., 2004).

Substantial provincial disparities exist in China in terms of emission and pollution levels. Provinces with higher estimated health and GHG reduction benefits from environmental policies are the ones with high population density and per capita

GDP values, e.g. Shanghai, Beijing, and Tianjin, and high energy intensity, e.g. Ningxia, Shanxi, and Nei Mongol. Smaller economic benefits are indicated in less developed and populated provinces, such as Xizang, Yunnan, Guizhou, and Hainan, owing to the fact that they have relatively lower base emission and pollution levels and less people that would benefit from improving air quality in these provinces.

However, this does not imply that less attention should be paid to emission and air pollution control in those provinces. Firstly, air pollution especially PM pollution is not a local environmental problem but a regional transboundary issue (Guo et al., 2014; Yang et al., 2011). Emissions from neighboring regions and regional transport of secondary aerosols add significant fine particle loads to local contributions. Moreover, it is normally more cost effective to employ mitigation technologies in less developed regions as they are in the lower end of the MAC curve (Dong et al., 2015; Yang and Lei, 2017).

Both air pollution control and climate change mitigation demand regional collaboration. The Chinese central government should set clear air pollution control targets and time schedule, and incorporate air quality improvement into the local government assessment indicators. Incentives and guidance should also be offered for the regional joint pollution prevention and control by the central government. Technological and financial aid should be provided for the less developed provinces by developed provinces who would benefit from air pollution abatement. Income gap between urban and rural residents should also be mitigated, and subsidies should be provided to promote cleaner energy in underdeveloped regions.

In less developed provinces, the energy efficiency and pollutants removal efficiencies are relatively low. Promoting advanced technologies and end-of-pipe control measures would be very efficient for reducing emissions from these regions. For more developed regions, the focus can be placed on pursuing better energy and industry structure, and enhancing energy and resource conservation. The current air pollutants emission charges in China are much lower than the marginal mitigation costs of pollutants. Increasing emission charges and strengthening supervision would improve emission reduction initiative and promote total amount control and trading of pollutant discharge.

Environmental education and public participation and supervision also play an important role in environmental management which would provide extensive support for building an environmental friendly society. Integrated assessment approach which addresses the health and climate change mitigation effects of environmental policies can help policy makers to select optimal policy options to achieve control targets. These analyses should be carried out before the environmental policies are actually implemented in order to avoid possible misleading decision-making and achieve maximum welfare gains.

4 Sensitivity and uncertainty analyses

The main objective of this study is to develop a methodology for estimating integrated benefits of air pollution control and climate change mitigation strategies in China and to identify the potential order of magnitude of the effects. However, in this kind of assessment many of the assumptions, input data, and models are associated with uncertainties. The assessment results are usually sensitive to some parameters and selected functions. Sensitivity analysis provides information on model structure and the influence of exogenous parameters. Moreover, knowledge of the uncertainties extends the results with confidence ranges which are important information for researchers and policy makers.

4.1 Sensitivity analysis

Sensitivity analyses of the simulation results are carried out with regard to two sets of parameters: the CRF for health impacts quantification and the bias adjustment techniques for modelled $PM_{2.5}$ concentration. As discussed in section 2.2.4.2, linear and log-linear form CRFs with lowest RR of all-cause mortality from existing U.S. cohort studies (Pope et al., 2002) and RR from a Chinese cohort study (Cao et al., 2011) are adopted to estimate health effects attributable to long-term $PM_{2.5}$ exposure.

The modelled $PM_{2.5}$ concentration from the EMEP model (Simpson et al., 2012) appears to underestimate annual average $PM_{2.5}$ values compared with monitored data. The influence of three bias adjustment techniques (as illustrated in section 3.2.2) are explored and compared with original modelled results without bias adjustment.

The results of the sensitivity analysis are summarized in Table 4.1. Generally, it can be seen that for all the policy scenarios the central value of health benefits using the nonlinear CRF is lower than that using the U.S. linear and log-linear CRFs, and higher than that using the Chinese CRFs. The influences of bias adjustment techniques show different patterns when using different CRFs. For the nonlinear CRF, health benefits of policy scenarios with bias adjustment for modelled $PM_{2.5}$ are generally smaller than or similar to those without bias adjustment (see Figure 4.1).

Table 4.1. Sensitivity analysis of CRFs and bias adjustment techniques on health benefits from policy scenarios in 2030.

Scenario	BA approach	Health benefits (billion EUR_{2010})				
		Nonlinear	Linear	Log-linear	Linear	Log-linear
		(Burnett et al., 2014)	(Pope et al., 2002)		(Cao et al., 2011)	
MTFR	BA1	155.75	312.91	369.89	56.34	58.10
	BA2	168.21	317.20	376.23	57.13	58.89
	BA3	157.15	337.85	395.73	60.93	62.88
	No BA	193.43	292.33	331.15	55.34	56.64
CLMT	BA1	37.85	103.90	129.92	17.55	18.26
	BA2	41.75	111.04	138.58	18.53	19.29
	BA3	50.01	125.61	150.65	22.05	22.84
	No BA	45.91	97.02	115.64	17.30	17.86
COMB	BA1	173.95	339.64	399.32	61.54	63.41
	BA2	187.94	343.58	405.22	62.29	64.14
	BA3	173.29	365.11	426.12	66.14	68.21
	No BA	217.30	316.85	357.22	60.32	61.69

As reflected by the shape of the nonlinear CRF, RR values for chronic mortality at high concentrations are lower than the values at low concentrations. Adjusting the underestimation of modelled concentration would result in lower health benefits from one unit concentration reduction.

It can be seen in Figure 4.1 that the central values of health benefits estimated by applying BA1 and BA3 (BA2) are about 20% (13%) lower than those without bias adjustment (No BA) for the MTFR and COMB scenarios. For the CLMT scenario, applying BA1 and BA2 would reduce the health benefits results by 10-18%. The health benefits estimated applying BA3 are slightly higher than those without bias adjustment.

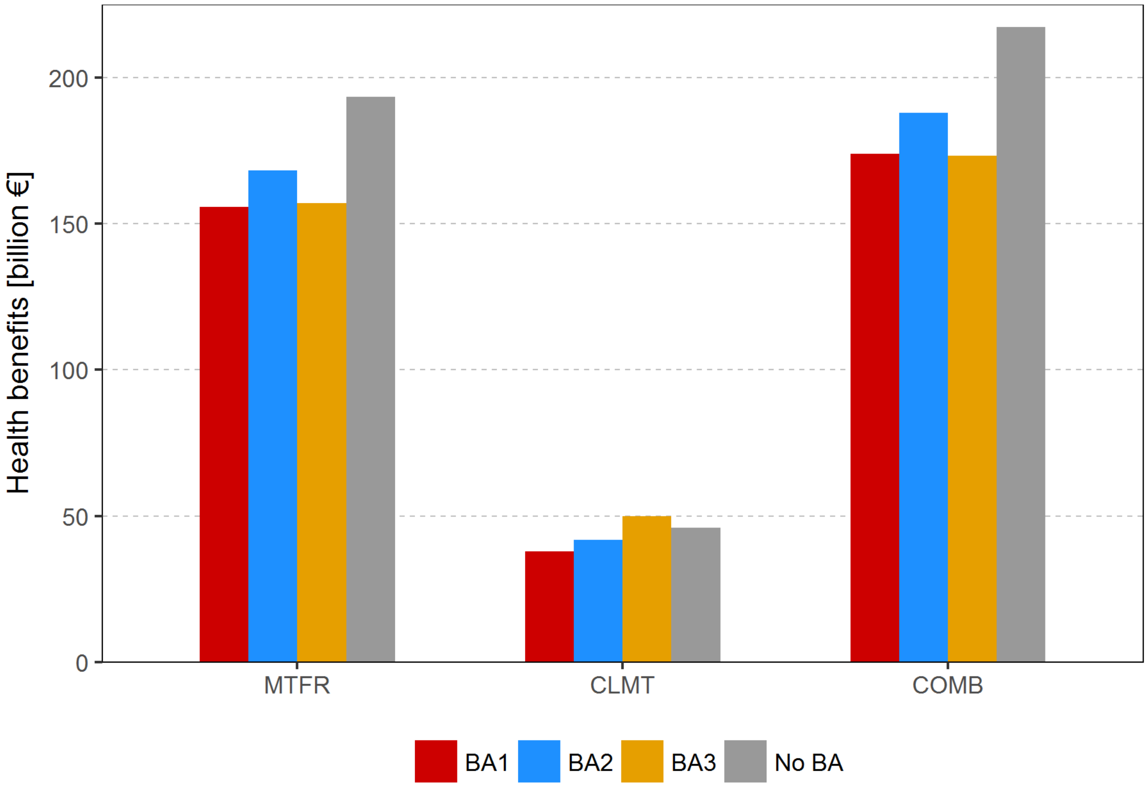

Figure 4.1. Health benefits of policy scenarios estimated with the nonlinear CRF and different bias adjustment methodologies.

However, when the linear or log-linear CRF is used, applying bias adjustment would increase the estimated health benefits from the policy scenarios as can be seen in Table 4.1. For example, using the log-linear CRF from the U.S. cohort study, applying BA3 would increase the estimated health benefits from policy scenarios by 20-30% compared with those without bias adjustment, followed by BA2 (13-20%) and BA1 (12%). When the CRF from the Chinese cohort study is used, the estimated health benefits appear to be less sensitive to bias adjustment techniques. The central values of health benefits of policy scenarios estimated with bias adjustment are in most of case less than 8% higher than those without bias adjustment.

Figure 4.2 shows the sensitivity of health benefits resulting from improved air quality to the shape of CRFs when BA1 is applied. Unlike bias adjustment discussed above, the shape of CRFs affects the estimation results in a consistent manner no matter which bias adjustment technique is applied. Therefore, hereafter the results applying BA1 are taken as examples.

It can be seen from Figure 4.2 that the health benefits of the MTFR scenario are around 156 billion EUR_{2010} using the nonlinear CRF, which are about half of those using the CRF from the U.S. cohort study (linear U.S. and log-linear U.S.), and 2.7 times of those using the Chinese CRF (linear China and log-linear China). Similar characteristics can be observed for the results of the CLMT and COMB scenarios.

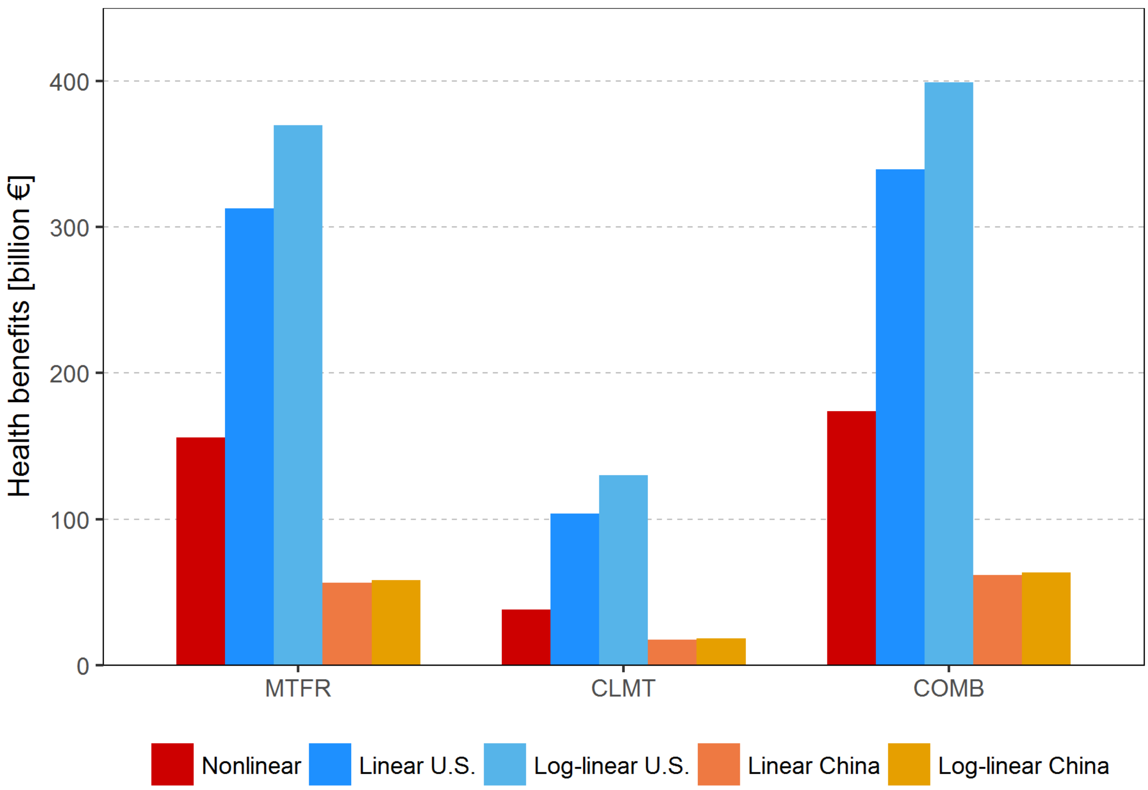

Figure 4.2. Health benefits of policy scenarios estimated with different CRFs.

The linear shape of CRF is commonly used as a simplified representation of the log-linear shape of CRF (Kan and Chen, 2004; Zhang et al., 2010). The analyses of this study show that when a low RR value is used (e.g. the Chinese CRF), the results using linear and log-linear functions are similar. However, when a higher RR value is used (e.g. the U.S. CRF) the estimated health benefits from improved air quality using log-linear function could be more than 20% higher than those using linear function.

It can be concluded that the estimation of health effects caused by $PM_{2.5}$ is quite sensitive to the selected CRF. It is meaningful to take a closer look at this issue, e.g. not only on aggregated but also on spatially distributed results. Figure 4.3 shows the spatial distribution of LLE attributable to long-term $PM_{2.5}$ exposure in BAU 2030 scenario using the log-linear U.S. and Chinese CRFs, which can be compared with the results using the nonlinear (lower panel of Figure 3.10) and linear CRFs (Figure S5).

The results estimated using the log-linear U.S. CRF (upper panel of Figure 4.3) show that long-term exposure to $PM_{2.5}$ under the BAU scenario can cause up to 81.4 months LLE in polluted area. However when the Chinese CRF is used (lower panel of Figure 4.3), the highest $PM_{2.5}$ related LLE among all the grids is 11.8 months. The differences between the results estimated using higher and lower CRFs are generally bigger in more polluted grids. The LLE attributable to $PM_{2.5}$ estimated using the U.S. CRF is over 3.5 times higher than that using the Chinese CRF in most of the grids, with a maximum ratio of 6.

The distributions of YOLL attributable to $PM_{2.5}$ in the BAU scenario estimated using the linear and log-linear CRFs are presented in Figure 4.4, which can be compared with Figure 3.12. It can be seen that the Chinese CRF reflects the lowest health response to $PM_{2.5}$ along the whole spectrum of $PM_{2.5}$ concentration. The health effects calculated using the U.S. CRF are similar to or even a bit smaller than those using the nonlinear CRF at low $PM_{2.5}$ concentrations, but much higher than the nonlinear CRF at high concentration levels (e.g. higher than 55 $\mu g/m^3$).

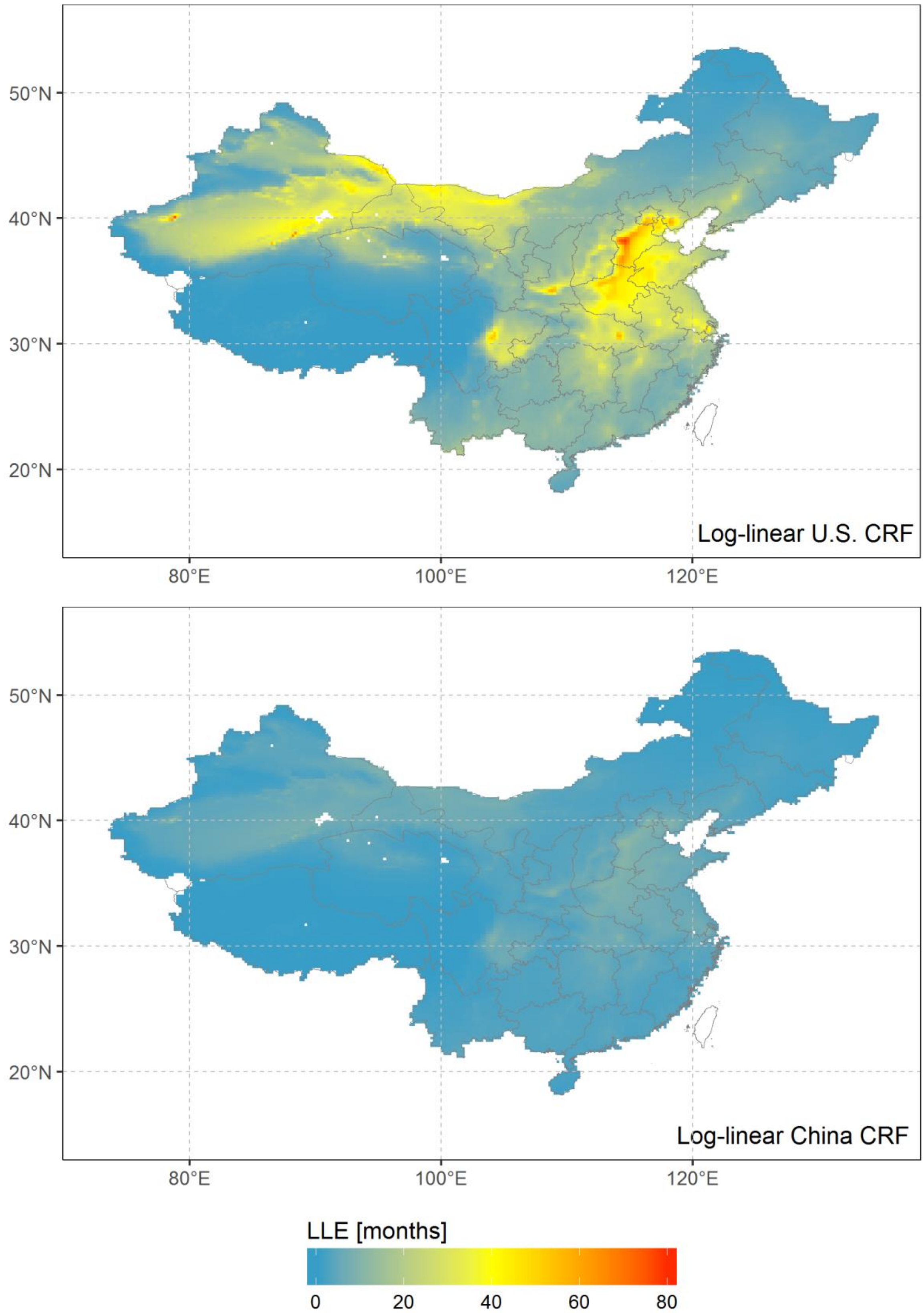

Figure 4.3. LLE attributable to $PM_{2.5}$ in BAU 2030 estimated using the log-linear CRFs (compare with Figure 3.10).

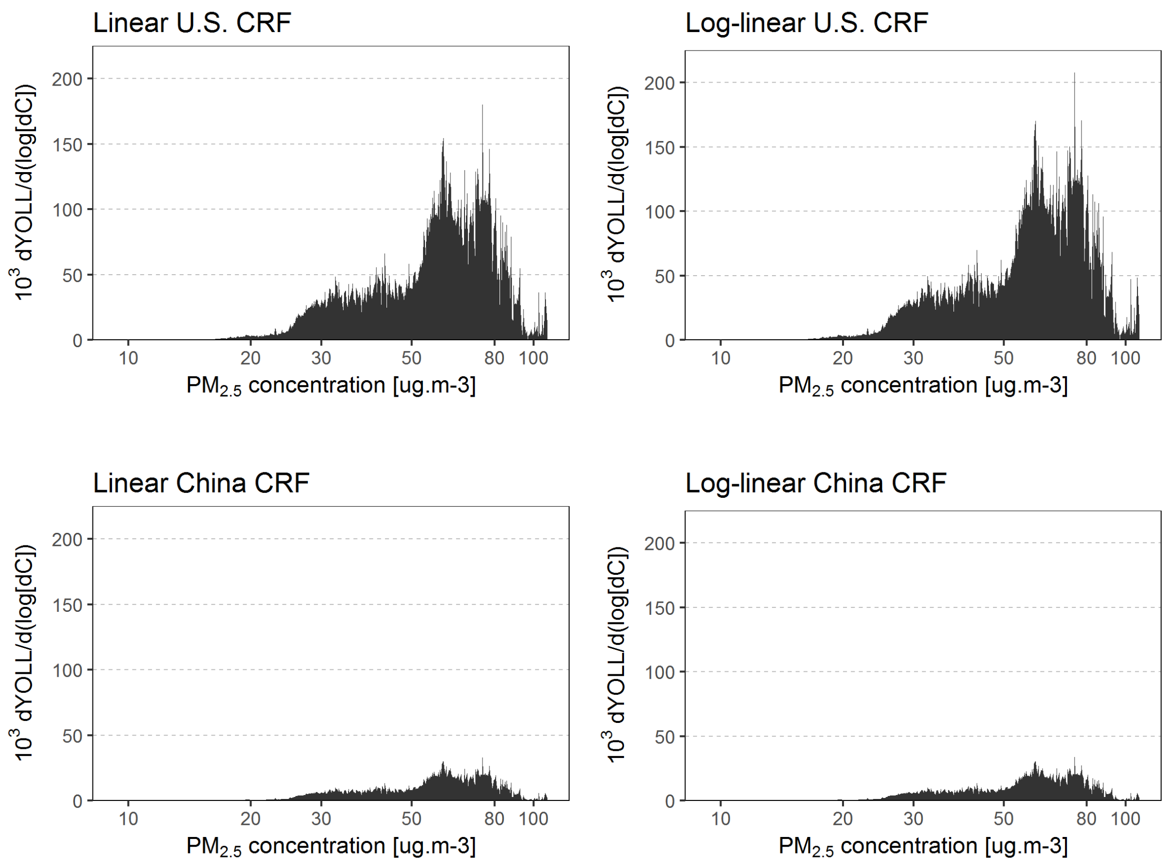

Figure 4.4. Distributions of YOLL attibutable to $PM_{2.5}$ in BAU 2030 estimated using different CRFs (compare with Figure 3.12).

The quartiles of YOLL attributable to $PM_{2.5}$ as well as the corresponding concentration range and the exposed population in the BAU scenario calculated with the linear and log-linear CRFs are summarized in Table 4.2. The total YOLL attributable to $PM_{2.5}$ in the BAU scenario calculated using the linear U.S., log-linear U.S., linear Chinese, log-linear Chinese, and nonlinear CRF are 15.9, 17.6, 3.1, 3.2, and 13.4 million, respectively.

Even though big differences can be observed for the YOLL calculated using the different linear and log-linear CRFs, the $PM_{2.5}$ concentration and population correspond to each quartile of YOLL are quite similar. This can be explained by the intrinsic characteristics of the linear and log-linear CRFs.

It can be seen from Table 4.2 that for the first (fourth) quartile, 25% (25%) of YOLL attributable to $PM_{2.5}$ are experienced by 46-50% (11-13%) of population who live in areas with concentration levels lower than 45 μg/m^3 (higher than 71 μg/m^3). The attributable YOLL per thousand population for the fourth quartile are 3 (2.5) times higher than those for the first quartile when the U.S. (Chinese) CRF is used. While for the nonlinear CRF, the ratio between YOLL per thousand population of the first and fourth YOLL quartile is 1.8 (see Table 3.6).

Table 4.2. Comparison of concentration-based quartiles of YOLL attributable to $PM_{2.5}$ in BAU 2030 using the linear and log-linear CRFs.

CRF	Quartiles	$PM_{2.5}$ concentration		Population		Attributable YOLL	
		range	mean	million	% of total	million	per k pop
Linear U.S.	1	0-43.7	22.6	687.3	48.6	3.98	5.79
	2	43.7-59.5	51.9	320.9	22.7	3.98	12.39
	3	59.5-72.1	64.4	229.5	16.2	3.98	17.33
	4	72.1-107.9	78.5	177.9	12.6	3.98	22.36
Log-linear U.S.	1	0-45.4	23.0	718.5	50.8	4.40	6.12
	2	45.4-60.1	53.2	308.5	21.8	4.40	14.25
	3	60.1-73.2	65.2	229.0	16.2	4.40	19.20
	4	73.2-107.9	79.5	159.6	11.3	4.40	27.54
Linear China	1	0-42.2	22.1	654.1	46.2	0.78	1.19
	2	42.2-58.6	50.6	326.9	23.1	0.78	2.38
	3	58.6-71.4	63.6	244.6	17.3	0.78	3.18
	4	71.4-107.9	78.0	190.0	13.4	0.78	4.10

CRF	Quartiles	$PM_{2.5}$ concentration		Population		Attributable YOLL	
		range	mean	million	% of total	million	per k pop
Log-linear China	1	0-42.4	22.2	659.2	46.6	0.79	1.20
	2	42.4-58.6	50.7	321.8	22.7	0.79	2.46
	3	58.6-71.4	63.6	244.6	17.3	0.79	3.24
	4	71.4-107.9	78.0	190.0	13.4	0.79	4.17

(Pope et al., 2009) indicates that the exposure-response relationship between mortality and $PM_{2.5}$ concentration is steeper at low levels of exposure than that at higher exposures. This issue is also reflected by the considerable difference between the U.S. CRF and the Chinese CRF. The U.S. CRF is representative for annual ambient average concentrations from approximately 5 to 30 μg/m^3 (Pope et al., 2002). The average $PM_{2.5}$ concentration considered in the Chinese cohort study is about 90 μg/m^3 (Cao et al., 2011). For local studies, these linear CRFs could be used if the ambient concentration levels fall within the range which is considered in the corresponding cohort study.

The linear CRFs can be directly applied to calculate the change in health risks caused by change in concentration levels. However using the U.S. CRF (the Chinese CRF) for regions with high (low) pollution levels would lead to overestimation (underestimation). For regional studies, especially when the regional differences of $PM_{2.5}$ concentration levels are considerable as is the case for this study, the nonlinear CRF should be adopted as it captures the declining marginal mortality effect from lower to higher concentrations.

It is worth noting that CRFs are normally provided with confidence intervals, which means that the calculated results have confidence ranges. In order to show the results more clearly and precisely, in the above discussion only the central values are used. A comprehensive uncertainty analysis of the integrated assessment will be presented in the next section. The sensitivity analyses bring insights on how the biases of the concentration data and the choice of CRFs would affect the $PM_{2.5}$ related health impact assessment.

4.2 Uncertainty analysis

Assessing the integrated impacts of environmental policies is a comprehensive mission. It pulls considerable amount of data, information, and models together from various fields, and therefore the uncertainties of the results are expected to be larger than those of most physical and chemical experiments. With the purpose of providing information on the robustness of the results and conclusions, an uncertainty analysis is conducted, which analyses the error ranges of parameters from various sources and modelling stages and finally quantifies the overall uncertainties.

4.2.1 Methodologies of uncertainty analysis

The analytical approach for uncertainty assessment of multiplicative models developed by Spadaro and Rabl (2008) is adopted in this study. It is transparent and convenient for testing different assumptions about the various sources of uncertainty, and is less time and resource consuming than the traditional Monte Carlo approach. Firstly, the uncertainties of each input parameter and component are identified. The uncertainties are expressed either as confidence intervals or geometric standard deviation (σ_g) with distribution functions (e.g. triangular distribution, normal distribution, lognormal distribution).

In impact assessment, the final results are a product of factors whose distributions are very commonly lognormal (Limpert et al., 2001). Spadaro and Rabl (2008) suggest that the confidence intervals of benefit estimates are multiplicative, as the distributions are close to lognormal which can be characterized in terms of geometric mean μ_g and geometric standard deviation σ_g. When the lower and upper limits of the 68% confidence interval (CI) (or 95% CI) of a variable z are known, the geometric mean and geometric standard deviation of the distribution can be estimated by:

$$\mu_g = \sqrt{z_{0.68u} z_{0.68l}} \text{ or } \sqrt{z_{0.95u} z_{0.95l}} \qquad \text{Equation 4.1}$$

$$\sigma_g = \sqrt{z_{0.68u}/z_{0.68l}} \text{ or } \sqrt[4]{z_{0.95u}/z_{0.95l}}$$ Equation 4.2

Where,

μ_g= geometric mean of variable z.

σ_g= geometric standard deviation of variable z.

$z_{0.68u}, z_{0.68l}, z_{0.95u}, z_{0.95l}$= the upper and lower limits of the 68% and 95% CI of variable z.

Once the uncertainties in the source categories are determined, they are combined to get the overall uncertainty. For multiplicative factors (x_i), e.g. emission rate of pollutant, change of concentration due to emission, slope of CRF, and VOLY, Equation 4.3 and Equation 4.4 can be derived for the uncertainty of the product (y).

$$\mu_{gy} = \mu_{gx1}\mu_{gx2} \cdots \mu_{gxn}$$ Equation 4.3

$$[\ln(\sigma_{gy})]^2 = [\ln(\sigma_{gx1})]^2 + [\ln(\sigma_{gx2})]^2 + \cdots + [\ln(\sigma_{gxn})]^2$$ Equation 4.4

Where,

μ_g= geometric mean of a variable.

σ_g= geometric standard deviation of a variable.

For the combination of impacts on health and climate change, the approach for estimating the uncertainty of the sum suggested by Spadaro and Rabl (2008) is adopted. Two estimates for the geometric standard deviation of the sum are calculated, which represent respectively over- and underestimation. The average of the two estimates is then used as the final estimate. Spadaro and Rabl (2008) have validated the approach with Monte Carlo calculations, and suggested that it produces good approximation. The details of the applied equations are listed in Table S1.

Uncertainties exist at every step of the integrated assessment due to the lack of data and knowledge of specific information. In the following, the uncertainties of each component (emission modelling, concentration modelling, health impact assessment, monetary valuation) are quantified. Applying the above presented methodology, the uncertainties of individual components are aggregated to provide an estimate of the overall uncertainty for the entire model.

4.2.2 Uncertainties of emission modelling

To quantify the uncertainties of the emission data, the approach suggested in the 2006 IPCC Guidelines for National Greenhouse Gas inventories (IPCC, 2006) is followed, which mainly consists of determining the uncertainty ranges of individual variables and parameters, aggregating the uncertainties of individual component to the total inventory, and determining the uncertainty in the trend.

According to Equation 2.1 the main variables used in emission modelling is activity data (e.g. energy consumption) and emission factors (uncontrolled emission factors, and penetrations and removal efficiencies of control technologies). Estimating the underlying uncertainties is normally based on periodic emission measurements, empirical data from literature and other documented data, or expert judgement (IPCC, 2006). As the national emission inventory used in this study involves big amount of data and assumptions, it is very difficult to collect specific uncertainty data. The uncertainty ranges for activity data and emission factors suggested in the EMEP/EEA Air Pollutant Emission Inventory Guidebook (EEA, 2016) are considered.

The developed emission scenarios rely on the energy projection from the Energy Technology Perspectives 2012 (IEA, 2012). The uncertainties of energy statistics as well as socio-economic drivers for China are suggested to be in the order of 5 to 10%. For emission factors, the uncertainty ranges depend on the specific air pollutant and emission source. Five categories of uncertainty ranges (A: 10-30%, B: 20-60%, C: 50-200%, D: 100-300%, E: order of magnitude) are used considering the volume of measurements and representativeness. The detailed descriptions and numbers can be found in the uncertainties chapter of EEA (2016).

4.2.3 Uncertainties of concentration modelling

In this study the results of two atmospheric models, the MSC-W EMEP model and the parameterized TM5 model, are used to estimate the baseline $PM_{2.5}$ concentration and concentration changes under policy scenarios. Considering the complexity of atmospheric models, a range of two to five is often cited for the geometric standard deviation of modelled results. This study focuses on long-term exposure to $PM_{2.5}$, therefore annual average concentration levels are used, which are considered to have greater accuracy than short-term (e.g. daily, hourly concentration) values (Jin et al., 2010).

The comparisons of annual average concentrations between modelled and monitored data conducted in this study show that the agreement is within a factor of two for most of the cities. Owing to the lack of data and especially for future scenarios, comparison with measurement data is not practical. Spadaro and Rabl (2008) analysed the uncertainties related to the main processes considered in atmospheric models: dispersion of primary pollutants, formation of secondary pollutants, and the effect of background emissions on chemical transformation.

Table 4.3. Assumptions on the uncertainties of concentration modelling.

Process	Geometric standard deviation (σ_g)
Dispersion of non-reactive primary pollutants	1.5
Dispersion of sulfur dioxide and sulphates	1.7
Dispersion of NO_x and nitrates	1.7
Formation of sulphates from SO_2	1.2
Formation of nitrates from NO_x	1.4
Effect of background emissions on the formation of sulphates from SO_2	1.05
Effect of background emissions on the formation of nitrates from NO_x	1.15

Source: (Spadaro and Rabl, 2008)

Bias adjustment would reduce the uncertainties of modelled concentrations. However, it is difficult to estimate the resulting uncertainty reduction quantitatively, especially for future scenarios. To avoid underestimating the uncertainty, the suggested uncertainty levels for atmospheric models are maintained. The uncertainties are expressed as geometric standard deviation (σ_g) as summarized in Table 4.3. Applying Equation 4.4, the total geometric standard deviation (σ_g) is calculated to be 1.50 for primary PM, 1.76 for sulphates, and 1.90 for nitrates.

4.2.4 Uncertainties of health impact assessment

The uncertainties of health impact assessment stem from the uncertainties of population data, health data (baseline incidence rate), CRF, and the calculation of YOLL. Population and mortality data are collected routinely. For a rather short timescale (e.g. 20 years), the uncertainty arises from projection of population is predicted to be small compared to other factors. Leksell and Rabl (2001) show that estimates of impacts from changes in hazards are relatively insensitive to variations in assumptions about future baseline incidence rates. Following the recommendations of Holland (2014), a ±5% range with triangular distribution is applied to population data and mortality rate.

The confidence intervals of CRFs for health impacts are normally reported for 95% probability, which are almost symmetric around the mean value. Spadaro and Rabl (2008) argue that a Gaussian distribution could be assumed for RR, and $\mu \pm 2\sigma$ (μ: mean; σ: standard deviation) is approximately the 95% CI. The geometric standard deviation σ_g can be calculated by Equation 4.5.

$$\sigma_g = \sqrt{\frac{\mu + \sigma}{\mu - \sigma}} \qquad \text{Equation 4.5}$$

The calculated σ_g of CRFs used in this study is summarized in Table 4.4, which is similar to the calculation of other studies (Roos, 2017; Spadaro and Rabl, 2008). When the changes in age-specific mortality rate caused by air pollution are identified, the next step is to determine the corresponding LLE and YOLL. Leksell and Rabl (2001) examined the dependency of LLE on the demographics of a population and the variation of RR with age, and found that the effects are relatively small. The suggested σ_g of 1.3 is applied for the calculation of the YOLL for a given mortality risk.

Table 4.4. Geometric standard deviation σ_g of concentration-response functions.

CRF	ALRI	COPD	IHD	LC	STOKE	All-cause	
	(Burnett et al., 2014)					(Pope et al., 2002)	(Cao et al., 2011)
σ_g	1.79	1.78	1.93	1.66	1.77	1.60	1.95

4.2.5 Uncertainties of monetary valuation

The economic valuation of non-market goods, e.g. life expectancy and climate change, involves a much higher uncertainty than the valuation of goods with market prices. In this study the economic costs of GHG and VOLY have direct influence on the final results. Studies on the costs of climate change (Du et al., 2015; Yang and Lei, 2017; Zhang and Yu, 2016) and mortality (Aunan et al., 2004; Hammitt and Zhou, 2006; He and Wang, 2010; Wang and Mullahy, 2006) show large variations, which reflect on one hand the dependency of the costs on sampling population and period and on the other hand the uncertainty of the methodologies.

VOLY expresses the WTP value to avoid a life year loss, which is difficult to monetize with a high degree of certainty. The transferring of estimates from a base year to future years and between populations with different income levels involves assumptions on economic development (e.g. growth rate of GDP per capita), discounting rate (reflecting time preference), and income elasticity. This leads to some additional uncertainties. Following the suggestions of Spadaro and Rabl (2008), a lognormal distribution with σ_g of 2 is applied for the valuation of YOLL (VOLY).

Regarding climate change effects, as discussed in section 2.2.5.2, some of the potentially important impacts are very difficult to assess, e.g. catastrophic climate change impacts, impacts on ecosystem, and shifts in population and farming centres. The monetary valuation of climate change impacts is considered to have significant uncertainties due to the facts like inaccurate estimation of GHG emissions, natural variability of climate, the potential for unpredicted or unrecognized factors, and incomplete understanding of the total climate system (IPCC, 2014).

The uncertainty of abatement costs estimation is relatively smaller than that of damage costs (Calvin et al., 2009; Kuik et al., 2009). However, in the process of policy-making, there is no information about whether the optimal reduction target is set. Moreover, future technology innovation and economies of scales may affect the cost of abatement options, which are difficult to foresee. For the purpose of this study, a full consideration of the uncertainties is preferred. Based on the review of Tol (2005, 2008), a lognormal distribution with geometric standard deviation of 5 is assumed as an estimate of the uncertainty of climate change costs.

4.2.6 Overall uncertainties

To evaluate the total uncertainty of the damage costs of $PM_{2.5}$, the geometric standard deviations (σ_g) of the above presented components are combined by applying Equation 4.4. The total σ_g of $PM_{2.5}$ related damage costs is around 3, which is consistent with result of a Monte Carlo analysis conducted by Roos (2017) for the overall uncertainty of economic costs of air pollution. The estimated uncertainties of damage costs of $PM_{2.5}$ and GHG are then combined to get the overall uncertainty of the integrated impacts applying the methodology described in section 4.2.1.

The overall uncertainty depends on the contribution of each type of impacts (from improved air quality and reduced GHG emissions) to integrated benefits. The estimated confidence intervals of integrated benefits from policy scenarios compared to the BAU scenario in 2030 are presented in Table 4.5. It can be seen that the σ_g of integrated benefits is smaller than that of both $PM_{2.5}$ related health benefits and GHG reduction benefits for the MTFR and COMB scenarios. For the CLMT scenario, in which the GHG reduction benefits dominate the integrated benefits, the total σ_g of integrated benefits is smaller than that of GHG reduction benefits and a bit higher than that of $PM_{2.5}$ related health benefits.

The estimation of overall uncertainties covered the full chain of integrated assessment of environmental policies. Most sources of uncertainties, e.g. the uncertainty of data and parameters, the structural uncertainty of model, and unpredictability, are considered. Though it is difficult or impossible to include all uncertainties, the contribution of variables with relatively small error ranges can be neglected considering the quadric combination of σ_g expressed by Equation 4.4. It is axiomatic that even though integrated assessment is with substantial uncertainty, approximately a factor of 3, it is way better than unknown in the absence of such analysis. More encouragingly the penalty of choosing the wrong value from the large uncertainty range is found to be small in practice (Rabl et al., 2005).

Table 4.5. Overall uncertainty of integrated benefits (unit: billion EUR_{2010}) from policy scenarios.

Scenario	μ_g	σ_g	95% CI	68% CI
MTFR	239.9	2.4	(41.5, 1387.8)	(99.7, 577.0)
CLMT	353.1	3.3	(32.9, 3789.4)	(107.8, 1156.7)
COMB	619.5	2.7	(87.2, 4403.5)	(232.4, 1651.7)

Note: μ_g: geometric mean; σ_g: geometric standard deviation.

5 Conclusions and outlook

5.1 Conclusions and remarks

China is facing severe challenges of air pollution as well as GHG emissions due to rapid increase of energy consumption and vehicle numbers, industrialization and urbanization. It has been widely proven by scientific research that air pollution is a major environmental risk to health (Guo et al., 2013; Pope, 2000). In recent years, with the progress of a series of epidemiological research methods, health risks caused by air pollution, especially $PM_{2.5}$, attracted increasing attention and interest.

Due to the rising awareness of environmental protection and increasing international pressure, the Chinese government has set a series of targets and plans for air pollution control and climate change mitigation (Jin et al., 2016; Xu et al., 2014). Air pollution and climate change are closely linked to each other as they are largely affected by similar sources and may interact with each other through atmospheric chemical reactions (Swart et al., 2004). However, current policy-making in China rarely takes these two issues into consideration simultaneously.

Continued reductions in air pollution and GHG emissions are essential, as they pose serious threats to both people's health and the environment in China and across the world. Under such circumstances, the estimation of health risks and climatic effects of recent environmental policies is informative for future development. Integrated assessment of different policy pathways, which takes into account all relevant benefits, damages, and costs, plays an important role in informing the policy-making process. Integrated assessment models have been widely developed and applied in developed countries (Friedrich et al., 2011; Sabel et al., 2016; USEPA, 2004), while limited research has been conducted for China.

This study developed a methodology to analyse the integrated impacts of atmospheric environmental policies on human health and climate change in China. Emission estimation, air quality modelling, health impact assessment, and economic evaluation are synthesized following the full-chain impact pathway from sources of emissions via environmental quality changes to physical and economic impacts.

The newly developed framework supports the simultaneous assessment of the effects of air pollution control and climate change mitigation policies in terms of changes in emissions, concentration and exposure levels, and physical and economic impacts. For concentration modelling, the results of the advanced 3D Eulerian EMEP model and the parameterized TM5 model are integrated, which on one hand leads to the generation of concentration maps with high spatial resolution for the baseline (BL) and business as usual (BAU) scenarios and on the other hand supports concentration modelling of massive policy scenarios.

Though the underestimation of $PM_{2.5}$ concentrations by large-scale atmospheric models is generally observed, no previous study has conducted a systematic bias adjustment especially for China. In this study, the integrated assessment methodology is expanded with a bias adjustment approach which reduces the bias between observed and simulated annual average $PM_{2.5}$ concentration in China. To investigate the effects of different concentration-response functions (CRFs) and fulfil various simulations needs, the extended methodology enables choices of linear and nonlinear CRFs.

Through the integration of the life table method for quantification of health impacts in terms of years of life lost (YOLL) and the income elasticity method for transferring monetary values between different economies, the improved methodology allows monetary estimation and aggregation of health risks and climate change effects. Furthermore, a systematic methodology of full chain uncertainty analysis is incorporated, which to the author's knowledge is one of the first attempts to quantify overall uncertainties of an integrated assessment in China.

Following the impact pathway approach, a quantitative assessment of the economic health and climatic benefits from improved air quality and reduced GHG emissions under different present and future scenarios in China is conducted. Considering current legislations, emissions of SO_2, NO_x, and PM will be reduced by 20-40% from 2010 (BL) to 2030 (BAU), which is simulated to result in a 20% reduction of population-weighted concentration (PWC) of $PM_{2.5}$. However, these reductions are not enough to offset the impacts of economic and population growth.

Results show that air pollution, more specifically exposure to $PM_{2.5}$, caused 8.2 million YOLL in 2010 in China. This number will be further increased to 13.4

million YOLL in 2030 if no additional control measures are implemented. The value of a life year lost (VOLY) due to air pollution, which expresses the society's collective willingness-to-pay to avoid a small probability of losing a life year, is estimated to be 16,600 (10,400-59,500) EUR_{2010} for the year 2010, and 44,000 (27,500-157,800) EUR_{2010} for 2030 considering income growth. The central values of the estimated health damage costs are 136.8 and 588.7 billion EUR_{2010} in 2010 and BAU 2030, which amount to about 3.9 and 5.2% of China's GDP of the identical year, respectively.

The impacts of more stringent policy scenarios are investigated. Compared with the BAU scenario, aggressive end-of-pipe control policies, i.e. adopting the maximum technically feasible reduction technologies (the MTFR scenario), in China can reduce the emissions of SO_2, NO_x, PM, and VOC by 49-91% in 2030. Climate change mitigation policies (the CLMT scenario) in terms of improving energy efficiency, increasing renewable energy use, and deploying CCS systems can reduce 48% of the CO_2 emissions in 2030. Emissions of air pollutants can be simultaneously reduced by 8-22%. If these measures are jointly implemented (the COMB scenario), GHG emissions can be reduced by 46%, and emissions of air pollutants will be reduced by 62-93% compared with BAU.

Emission reduction of air pollutants in the MTFR, CLMT, and COMB scenarios are predicted to reduce the PWC of $PM_{2.5}$ in 2030 by 38, 12, and 42% compared with those under the BAU scenario, respectively. Compared with the BAU scenario, improved air quality under the MTFR, CLMT, and COMB scenarios may avoid 3.5, 0.9, and 4.0 million YOLL attributable to long-term exposure to $PM_{2.5}$. The achievable health benefits from the MTFR, CLMT, and COMB scenarios are around 156, 38, and 174 billion EUR_{2010}, respectively, which account for 1.4, 0.3, and 1.5% of China's GDP in 2030.

Additionally, significant GHG reduction benefits can be obtained. To quantify the economic benefits of climate change mitigation, the external costs of GHG are estimated to be 15 to 54 EUR_{2010}/t $CO_{2\text{-eq}}$ in China for the year 2030. Compared to the BAU scenario, the economic benefits of GHG mitigation under MTFR, CLMT, and COMB are 29 (13-46), 238 (103-372), and 268 (117-419) billion EUR_{2010}, with the central estimates amounting to about 0.3, 2.1, and 2.4% of China's GDP in 2030, respectively. The results clearly show that policies intending to reduce GHG emissions are also effective in improving air quality, and vice versa. In the COMB scenario, the health benefits from improved air quality and GHG reduction benefits are relatively comparable.

Clear provincial disparities on emissions, concentration levels, and attainable benefits from policy measures exist in China. Higher emissions and consequently higher YOLL attributable to $PM_{2.5}$ exposure are observed in eastern China, especially around big cities with high pollution levels and population density. Provinces with higher estimated health benefits from air pollution control policies are the ones with large population and emissions, e.g. Henan, Sichuan, and Guangdong. Higher GHG reduction benefits from climate change mitigation measures are estimated for provinces with higher energy production bases such as Nei Mongol and Shanxi.

Higher per capita health benefits from policy measures are estimated for big cities with high population density, e.g. Shanghai, Beijing, and Tianjin. Provinces with higher per capita GHG reduction benefits are the ones with high energy intensity such as Ningxia, Nei Mongol, and Shanxi. Smaller economic benefits are indicated in less developed and populated provinces, such as Xizang, Yunnan, Guizhou, and Hainan, owing to the fact that they have relatively lower base emission and pollution levels and less people that would benefit from improved air quality in these provinces.

Sensitivity analyses of the simulation results are carried out with regard to two sets of parameters: CRFs for health impact assessment and bias adjustment techniques for $PM_{2.5}$ concentration modelling. Results show that health benefits of air pollution control policies estimated using the nonlinear CRF are about half of those using the CRF from U.S. cohort study, and 2.7 times of those using the CRF from a Chinese cohort study. For local studies, the U.S. or Chinese CRFs could be used if the ambient concentration levels fall within the range which is considered in the corresponding cohort study. However, for large scale regional analysis especially when the regional differences of $PM_{2.5}$ concentration levels are considerable as is the case for this study, the nonlinear CRF should be adopted as it captures the declining marginal mortality effect from lower to higher concentrations.

Three bias adjustment approaches, i.e. an additive correction of the mean bias (BA1), a multiplicative ratio correction (BA2), and a linear regression correction (BA3) are investigated in this study. All the three investigated bias adjustment methods are capable of reducing to some extent the bias between observed and simulated annual average $PM_{2.5}$ concentration in China. The performance of BA1 is relatively better than that of BA2, and it does not demand projection of supplementary data as is the case for BA3. Compared with CRFs, bias adjustment techniques have smaller influences on the results. Depending on the shape of the selected CRF, health benefits of policy scenarios estimated with bias adjustment can be a bit higher or lower than those without bias adjustment.

The uncertainties of such integrated assessment estimated in this work are much larger than those of most physical and chemical experiments. With the purpose of providing information on the robustness of the results to better support rational decision-making, an uncertainty analysis is conducted. Analysing the error ranges of parameters from various sources and modelling stages (e.g. emission and concentration modelling, health impact assessment, monetary valuation) the overall uncertainties of the final results are quantified.

The overall uncertainty of monetized integrated benefits from improved air quality and reduced GHG emissions in terms of geometric standard deviation is around 2.4-3.3, which is similar to previous estimates (Roos, 2017; Spadaro and Rabl, 2008). The integrated benefits, i.e. the total health benefits and GHG reduction benefits, of the MTFR, CLMT, and COMB scenarios in 2030 are 239.9 (95% CI: 41.5, 1387.8), 353.1 (32.9, 3789.4), and 619.5 (87.2, 4403.5) billion EUR_{2010}, respectively.

Although $PM_{2.5}$ is often considered as the main indicator of ambient air pollution in health impact assessment, as is the case in this study, there may be additional health effects due to exposure to other air pollutants (e.g. NO_2 and O_3). Chronic mortality is chosen as the representative health endpoint in this study to derive YOLL attributable to $PM_{2.5}$ exposure. In addition to mortality, air pollution can also cause increased morbidity (Héroux et al., 2015; Li et al., 2015). The overall health benefits achievable from improved air quality may thus be higher than the estimation in this study.

The integrated assessment methodology developed in this study enables the consideration of air pollution induced health effects and GHG related climatic effects in the process of environmental policy development in China. The reduction potential and integrated benefits from policy measures estimated in this study provide valuable policy insights for China and other developing countries.

The contribution of integrated assessment to the optimization of policy options and avoidance of possible misleading decision-making is self-evident. Previous experience in atmospheric environmental management in China has shown that reducing the emissions of a single pollutant at a time can be neither effective nor efficient for improving air quality. Concentration- and impact-oriented policy-making supported by integrated assessment can maximize social benefits.

Health benefits and GHG reduction benefits achievable from environmental quality improvement are substantial, which is favorable to recover the implementation costs of various environmental policies. A comprehensive consideration of economic impacts from air pollution induced health effects and climate change, a win-win strategy, supports the identification and framing of optimum environmental policies. End-of-pipe air pollutants control measures (e.g. installation of FGD and SCR) are effective for China's air pollution control and bring significant health benefits although their impacts on GHG reduction are relatively small.

Deploying CCS systems in power generation and industrial sectors can greatly reduce GHG emissions which can bring more benefits on the long-term. Many GHG mitigation measures, such as improving energy efficiencies, co-generation of heat and power, and promotion of solar and hydro power, provide substantial health benefits as well. Recognition of the integrated benefits would give priorities to such policies with the largest synergies.

Substituting coal with biomass is implemented as an effective measure to reduce GHG emissions and improve energy security. However, it may not be an optimal option for cities with high PM pollution levels as biomass burning may bring additional pressure on local air quality. Careful considerations should also be given to electric vehicle promotion. Promoting electric vehicles in China can only be an effective pollution control measure instead of a pollution transfer measure when the energy mix for power generation is simultaneously improved. Synergistic reduction of air pollution and GHG emissions is the most efficient way to combat air pollution and climate change.

The integrated benefits at the provincial level indicate that provinces with high population density and high energy intensity would benefit more from air pollution control and GHG reduction. However, this is not to say that less attention should be paid to emission and air pollution control in other regions as air pollution especially $PM_{2.5}$ pollution is more a regional transboundary issue than a local environmental problem (Guo et al., 2014; Yang et al., 2011). Joint prevention and control of regional air pollution should be promoted which enables extensive regional cooperation and exchange of experience and resources.

5.2 Outlook

The results of this study open up several interesting opportunities for future work. Firstly assessment of the costs of policy measures is not included in this study due to the difficulties in collecting various cost parameters of policy implementation in China. Through comparison of costs and benefits, a cost-benefit analysis can be conducted which helps to quantify the net benefits (benefits minus costs) of different control options and identify the most cost-effective measures.

Secondly, due to data and methodology constraints, the health impact assessment in this study only considered chronic mortality caused by exposure to ambient $PM_{2.5}$. With the improvement of data availability and model quality, the scope of the analysis could be extended to cover more air pollutants (e.g. O_3, NO_2), both mortality and morbidity (e.g. hospital admission, acute and chronic diseases), and ecological impacts (e.g. loss of biodiversity).

Air pollution and its health effects vary substantially with microenvironments (e.g. urban and rural, outdoor and indoor), time (e.g. season, daytime), characteristics of the exposed population (e.g. sex, employment status). However, due to the unavailability of sophisticated exposure models, the annual average ambient $PM_{2.5}$ concentration in each grid is used for exposure assessment in this study. With the development of exposure assessment models, indoor exposure and human mobility patterns could be considered for health impacts evaluation.

Owing to the limitation of data sources, some important parameters used in the evaluation process, such as VOLY and MDC, are derived from European studies and the same values are applied for the whole country. The same age structure and baseline health data are assumed for the population in all the grids across China. The analysis would be improved through supplementary analysis of regional and local parameters considering different demographic structure and economic development.

Furthermore, it would be interesting to investigate a broader range of air pollution control and GHG reduction policies. The developed methodology can be used to investigate the integrated impacts of single policies and diverse measures embedded in scenarios, and analyse how various proposals would interact with current environmental policies. Analyses about how to achieve maximum benefits with certain costs constraints or how to fulfill a certain objective (e.g. an ambient concentration limit) with the least costs possible would help Chinese policy makers to achieve optimal balance between economic development and environmental protection.

China has been moving forward to improve urban air quality and reduce carbon intensity. The improvements of economic structure, technology, and policy tools have led to significant economic benefits for China and even other regions. With air pollution levels remaining well above recommended thresholds especially in big cities, future actions are needed and, as this study has shown, will bring substantial benefits. In order to realize the strategic requirements of sustainable development, environmental policy-making should carefully consider the impacts of economic development and energy consumption on human health and the environment.

References

Amann, M., Bertok, I., Borken, J., Chambers, A., Cofala, J., Dentener, F., Heyes, C., Hoglund, L., Klimont, Z., Purohit, P., Rafaj, P. and Schöpp, W.: GAINS-Asia: A Tool to Combat Air Pollution and Climate Change Simutaneously, Methodology., 2008.

Amann, M., Bertok, I., Borken-Kleefeld, J., Cofala, J., Heyes, C., Höglund-Isaksson, L., Klimont, Z., Nguyen, B., Posch, M., Rafaj, P., Sandler, R., Schöpp, W., Wagner, F. and Winiwarter, W.: Cost-effective control of air quality and greenhouse gases in Europe: Modeling and policy applications, Environ. Model. Softw., 26(12), 1489–1501, doi:10.1016/j.envsoft.2011.07.012, 2011.

Anthoff, D., Hepburn, C. and Tol, R. S. J.: Equity weighting and the marginal damage costs of climate change, Ecol. Econ., 68(3), 836–849, doi:10.1016/j.ecolecon.2008.06.017, 2009.

Apte, J. S., Marshall, J. D., Cohen, A. J. and Brauer, M.: Addressing Global Mortality from Ambient PM2.5, Environ. Sci. Technol., 49(13), 8057–8066, doi:10.1021/acs.est.5b01236, 2015.

Aunan, K., Fang, J., Vennemo, H., Oye, K. and Seip, H.: Co-benefits of climate policy—lessons learned from a study in Shanxi, China, Energy Policy [online] Available from: http://www.sciencedirect.com/science/article/pii/S0301421503001563 (Accessed 26 August 2014), 2004.

Aunan, K., Fang, J., Hu, T., Seip, H. M. and Vennemo, H.: Climate Change and Air Quality—Measures with Co-Benefits in China, Environ. Sci. Technol., 40(16), 4822–4829, doi:10.1021/es062994k, 2006.

Bessagnet, B., Pirovano, G., Mircea, M., Cuvelier, C., Aulinger, A., Calori, G., Ciarelli, G., Manders, A., Stern, R., Tsyro, S., García Vivanco, M., Thunis, P., Pay, M.-T., Colette, A., Couvidat, F., Meleux, F., Rouïl, L., Ung, A., Aksoyoglu, S., Baldasano, J. M., Bieser, J., Briganti, G., Cappelletti, A., D'Isidoro, M., Finardi, S., Kranenburg, R., Silibello, C., Carnevale, C., Aas, W., Dupont, J.-C., Fagerli, H., Gonzalez, L., Menut, L., Prévôt, A. S. H., Roberts, P. and White, L.: Presentation of the EURODELTA III intercomparison exercise – evaluation of the chemistry transport models' performance on criteria pollutants and joint analysis with meteorology, Atmos. Chem. Phys., 16(19), 12667–12701, doi:10.5194/acp-16-12667-2016, 2016.

Bickel, P. and Friedrich, R.: ExternE - Externalities of Energy, Methodology 2005 Update, Luxemburg. [online] Available from: http://www.externe.info/externe_d7/sites/default/files/methup05a.pdf, 2005.

Bignal, K. L., Ashmore, M. R., Headley, A. D., Stewart, K. and Weigert, K.: Ecological impacts of air pollution from road transport on local vegetation, Appl.

Geochemistry, 22(6), 1265–1271, doi:10.1016/j.apgeochem.2007.03.017, 2007.

Böhringer, C., Carbone, J. and Rutherford, T.: Embodied Carbon Tariffs, Cambridge, MA., 2011.

Boldo, E., Medina, S., Le Tertre, A., Hurley, F., Mücke, H.-G., Ballester, F., Aguilera, I. and Group, D. E. on behalf of the A.: Apheis: Health Impact Assessment of Long-term Exposure to PM2.5 in 23 European Cities, Eur. J. Epidemiol., 21(6), 449–458, doi:10.1007/s10654-006-9014-0, 2006.

Bollen, J., van der Zwaan, B., Brink, C. and Eerens, H.: Local air pollution and global climate change: A combined cost-benefit analysis, Resour. Energy Econ., 31(3), 161–181, doi:10.1016/J.RESENEECO.2009.03.001, 2009.

Brauer, M., Amann, M., Burnett, R. T., Cohen, A., Dentener, F., Ezzati, M., Henderson, S. B., Krzyzanowski, M., Martin, R. V, Van Dingenen, R., van Donkelaar, A. and Thurston, G. D.: Exposure assessment for estimation of the global burden of disease attributable to outdoor air pollution., Environ. Sci. Technol., 46(2), 652–60, doi:10.1021/es2025752, 2012.

Bruce, J. P., Lee, H. and Haites, E. F.: Climate change 1995: economics and social dimensions of climate chage, Cambridge University Press, Cambridge, UK., 1996.

Brunekreef, B.: Air pollution and life expectancy: is there a relation?, Occup. Environ. Med., 54(11), 781–4 [online] Available from: http://www.ncbi.nlm.nih.gov/pubmed/9538349 (Accessed 12 June 2017), 1997.

Brunekreef, B.: Health effects of air pollution observed in cohort studies in Europe, J Expo Sci Env. Epidemiol, 17, doi:10.1038/sj.jes.7500628, 2007.

Burnett, R. T., Arden Pope, C., Ezzati, M., Olives, C., Lim, S. S., Mehta, S., Shin, H. H., Singh, G., Hubbell, B., Brauer, M., Ross Anderson, H., Smith, K. R., Balmes, J. R., Bruce, N. G., Kan, H., Laden, F., Prüss-Ustün, A., Turner, M. C., Gapstur, S. M., Diver, W. R. and Cohen, A.: An integrated risk function for estimating the global burden of disease attributable to ambient fine particulate matter exposure, Environ. Health Perspect., 122(4), 397–403, doi:10.1289/ehp.1307049, 2014.

Calvin, K., Patel, P., Fawcett, A., Fisher-Vanden, K., Edmonds, J., Kim, S. H., Sands, R. and Wise, M.: The distribution and magnitude of emissions mitigation costs in climate stabilization under less than perfect international cooperation: SGM results, Energy Econ., 31, S187–S197, doi:10.1016/J.ENECO.2009.06.014, 2009.

Cao, J., Yang, C., Li, J., Chen, R., Chen, B., Gu, D. and Kan, H.: Association between long-term exposure to outdoor air pollution and mortality in China: A cohort study, J. Hazard. Mater., 186(2–3), 1594–1600, doi:10.1016/j.jhazmat.2010.12.036, 2011.

Chae, Y. and Park, J.: Quantifying costs and benefits of integrated environmental strategies of air quality management and greenhouse gas reduction in the Seoul

Metropolitan Area, Energy Policy, 39(9), 5296–5308, doi:10.1016/J.ENPOL.2011.05.034, 2011.

Chang, J. C. and Hanna, S. R.: Air quality model performance evaluation, Meteorol. Atmos. Phys., 87(1–3), 167–196, doi:10.1007/s00703-003-0070-7, 2004.

Chen, B., Hong, C. and Kan, H.: Exposures and health outcomes from outdoor air pollutants in China, Toxicology, 198(1–3), 291–300, doi:10.1016/J.TOX.2004.02.005, 2004.

Chen, C., Chen, B., Wang, B. and Huang, C.: Low-carbon energy policy and ambient air pollution in Shanghai, China: a health-based economic assessment., Sci. … [online] Available from: http://europepmc.org/abstract/MED/17207519 (Accessed 13 June 2013), 2007.

Chen, D., Liu, X., Lang, J., Zhou, Y., Wei, L., Wang, X. and Guo, X.: Estimating the contribution of regional transport to PM 2.5 air pollution in a rural area on the North China Plain, Sci. Total Environ., 583, 280–291, doi:10.1016/j.scitotenv.2017.01.066, 2017.

Chen, H., Goldberg, M. S. and Villeneuve, P. J.: A systematic review of the relation between long-term exposure to ambient air pollution and chronic diseases., Rev. Environ. Health, 23(4), 243–97 [online] Available from: http://www.ncbi.nlm.nih.gov/pubmed/19235364 (Accessed 12 June 2017), 2008.

Chen, Y., Ebenstein, A., Greenstone, M. and Li, H.: Evidence on the impact of sustained exposure to air pollution on life expectancy from China's Huai River policy., Proc. Natl. Acad. Sci. U. S. A., 110(32), 12936–41, doi:10.1073/pnas.1300018110, 2013.

CIESIN: Gridded Population of the World, Version 3 (GPWv3): Population Count Grid, Future Estimates, [online] Available from: http://dx.doi.org/10.7927/H42B8VZZ (Accessed 16 May 2016), 2005.

Cifuentes, L., Borja-Aburto, V. H., Gouveia, N., Thurston, G. and Davis, D. L.: Assessing the health benefits of urban air pollution reductions associated with climate change mitigation (2000-2020): Santiago, São Paulo, México City, and New York City., Environ. Health Perspect., 109 Suppl(Suppl 3), 419–25 [online] Available from: http://www.ncbi.nlm.nih.gov/pubmed/11427391 (Accessed 7 October 2017), 2001.

Cohen, A. J., Ross Anderson, H., Ostro, B., Pandey, K. D., Krzyzanowski, M., Künzli, N., Gutschmidt, K., Pope, A., Romieu, I., Samet, J. M. and Smith, K.: The global burden of disease due to outdoor air pollution., J. Toxicol. Environ. Health. A, 68(13–14), 1301–7, doi:10.1080/15287390590936166, 2006.

Denby, B.: Guidance on the Use of Models for the European Air Quality Directive, ETC/ACC report version 6.2. [online] Available from: http://www.calidaddelaire.es/descargas/Model_guidance_v5_1a.pdf, 2010.

Desaigues, B., Rabl, A., Ami, D., My, K. B., Masson, S., Salomon, M.-A. and

Santoni, L.: Monetary valuation of air pollution mortality: current Practice, Research Needs and Lessons from a Contingent valuation. [online] Available from: http://citeseerx.ist.psu.edu/viewdoc/download;jsessionid=359F4525C39772F19C4D7E683A8308B4?doi=10.1.1.321.5024&rep=rep1&type=pdf, 2004.

Desaigues, B., Ami, D., Bartczak, A., Braun-Kohlová, M., Chilton, S., Czajkowski, M., Farreras, V., Hunt, A., Hutchison, M., Jeanrenaud, C., Kaderjak, P., Máca, V., Markiewicz, O., Markowska, A., Metcalf, H., Navrud, S., Nielsen, J. S., Ortiz, R., Pellegrini, S., Rabl, A., Riera, R., Scasny, M., Stoeckel, M.-E., Szántó, R. and Urban, J.: Economic valuation of air pollution mortality: A 9-country contingent valuation survey of value of a life year (VOLY), Ecol. Indic., 11(3), 902–910, doi:10.1016/j.ecolind.2010.12.006, 2011.

Dickerson, R. R., Li, C., Li, Z., Marufu, L. T., Stehr, J. W., McClure, B., Krotkov, N., Chen, H., Wang, P., Xia, X., Ban, X., Gong, F., Yuan, J. and Yang, J.: Aircraft observations of dust and pollutants over northeast China: Insight into the meteorological mechanisms of transport, J. Geophys. Res., 112(D24), D24S90, doi:10.1029/2007JD008999, 2007.

Djalalova, I., Wilczak, J., McKeen, S., Grell, G., Peckham, S., Pagowski, M., DelleMonache, L., McQueen, J., Tang, Y. and Lee, P.: Ensemble and bias-correction techniques for air quality model forecasts of surface O3 and PM2.5 during the TEXAQS-II experiment of 2006, Atmos. Environ., 44(4), 455–467, doi:10.1016/j.atmosenv.2009.11.007, 2010.

Dong, H., Dai, H., Dong, L., Fujita, T., Geng, Y., Klimont, Z., Inoue, T., Bunya, S., Fujii, M. and Masui, T.: Pursuing air pollutant co-benefits of CO2 mitigation in China: A provincial leveled analysis, Appl. Energy, 144, 165–174, doi:10.1016/j.apenergy.2015.02.020, 2015.

Du, L., Hanley, A. and Wei, C.: Marginal Abatement Costs of Carbon Dioxide Emissions in China: A Parametric Analysis, Environ. Resour. Econ., 61(2), 191–216, doi:10.1007/s10640-014-9789-5, 2015.

Dudek, D., Golub, A. and Strukova, E.: Ancillary Benefits of Reducing Greenhouse Gas Emissions in Transitional Economies, World Dev., 31(10), 1759–1769, doi:10.1016/S0305-750X(03)00139-6, 2003.

EEA: EMEP/EEA air pollutant emission inventory guidebook - 2016 — European Environment Agency. [online] Available from: https://www.eea.europa.eu/publications/emep-eea-guidebook-2016 (Accessed 27 September 2017), 2016.

Friedrich, R.: Integrated Assessment of Policies for Reducing Health Impacts Caused by Air Pollution, in Environmental Determinants of Human Health, edited by J. M. Pacyna and E. G. Pacyna, pp. 117–132, Springer, Cham., 2016.

Friedrich, R., Kuhn, A., Bessagnet, B., Blesl, M., Bruchof, D., Cowie, H. and Fantke, P.: Methods and results of the HEIMTSA/INTARESE Common Case Study. [online] Available from: http://www.integrated-assessment.eu/eu/index.html, 2011.

Fu, J. S., Hsu, N. C., Gao, Y., Huang, K., Li, C., Lin, N.-H. and Tsay, S.-C.: Evaluating the influences of biomass burning during 2006 BASE-ASIA: a regional chemical transport modeling, Atmos. Chem. Phys., 12(9), 3837–3855, doi:10.5194/acp-12-3837-2012, 2012.

Geng, Y., Ma, Z., Xue, B., Ren, W., Liu, Z. and Fujitac, T.: Co-benefit evaluation for urban public transportation sector – a case of Shenyang, China, J. Clean. Prod., 58, 82–91, doi:10.1016/J.JCLEPRO.2013.06.034, 2013.

Gielen, D. and Chen, C.: The CO2 emission reduction benefits of Chinese energy policies and environmental policies:: A case study for Shanghai, period 1995–2020, Ecol. Econ., 39(2), 257–270, doi:10.1016/S0921-8009(01)00206-3, 2001.

Gregg, J. S., Andres, R. J. and Marland, G.: China: Emissions pattern of the world leader in CO_2 emissions from fossil fuel consumption and cement production, Geophys. Res. Lett., 35(8), L08806, doi:10.1029/2007GL032887, 2008.

Guan, D., Su, X., Zhang, Q., Peters, G. P., Liu, Z., Lei, Y. and He, K.: The socioeconomic drivers of China's primary PM 2.5 emissions, Environ. Res. Lett., 9(2), 24010, doi:10.1088/1748-9326/9/2/024010, 2014.

Guo, S., Hu, M., Zamora, M. L., Peng, J., Shang, D., Zheng, J., Du, Z., Wu, Z., Shao, M., Zeng, L., Molina, M. J. and Zhang, R.: Elucidating severe urban haze formation in China., Proc. Natl. Acad. Sci. U. S. A., 111(49), 17373–8, doi:10.1073/pnas.1419604111, 2014.

Guo, Y., Li, S., Tian, Z., Pan, X., Zhang, J. and Williams, G.: The burden of air pollution on years of life lost in Beijing, China, 2004-08: retrospective regression analysis of daily deaths., BMJ, 347(dec09_7), f7139, doi:10.1136/bmj.f7139, 2013.

Hammitt, J. K. and Robinson, L. A.: The Income Elasticity of the Value per Statistical Life: Transferring Estimates between High and Low Income Populations, J. Benefit-Cost Anal., 2(1), 1–29, doi:10.2202/2152-2812.1009, 2011.

Hammitt, J. K. and Zhou, Y.: The Economic Value of Air-Pollution-Related Health Risks in China: A Contingent Valuation Study, Environ. Resour. Econ., 33(3), 399–423, doi:10.1007/s10640-005-3606-0, 2006.

Hart, J. E., Garshick, E., Dockery, D. W., Smith, T. J., Ryan, L. M. and Laden, F.: Long-term ambient multipollutant exposures and mortality, Am J Respir Crit Care Med, 183, doi:10.1164/rccm.200912-1903OC, 2011.

Hasanbeigi, A., Lobscheid, A., Lu, H., Price, L. and Dai, Y.: Quantifying the co-benefits of energy-efficiency policies: A case study of the cement industry in Shandong Province, China, Sci. Total Environ., 458–460, 624–636, doi:10.1016/j.scitotenv.2013.04.031, 2013.

He, J. and Wang, H.: The value of statistical life : a contingent investigation in China, The World Bank., 2010.

He, K., Lei, Y., Pan, X., Zhang, Y., Zhang, Q. and Chen, D.: Co-benefits from energy policies in China, Energy, 35(11), 4265–4272, doi:10.1016/j.energy.2008.07.021, 2010.

HEI: Health Effects Institute, Reanalysis of the Harvard Six Cities Study and the American Cancer Society Study of Particulate Air Pollution and Mortality. [online] Available from: https://www.healtheffects.org/publication/reanalysis-harvard-six-cities-study-and-american-cancer-society-study-particulate-air (Accessed 27 June 2017), 2001.

Heinrich, J., Thiering, E., Rzehak, P., Kramer, U., Hochadel, M. and Rauchfuss, K. M.: Long-term exposure to NO2 and PM10 and all-cause and cause-specific mortality in a prospective cohort of women, Occup Env. Med, 70, doi:10.1136/oemed-2012-100876, 2013.

Héroux, M.-E., Anderson, H. R., Atkinson, R., Brunekreef, B., Cohen, A., Forastiere, F., Hurley, F., Katsouyanni, K., Krewski, D., Krzyzanowski, M., Künzli, N., Mills, I., Querol, X., Ostro, B. and Walton, H.: Quantifying the health impacts of ambient air pollutants: recommendations of a WHO/Europe project., Int. J. Public Health, 60(5), 619–27, doi:10.1007/s00038-015-0690-y, 2015.

Hoegh-Guldberg, O. and Bruno, J. F.: The impact of climate change on the world's marine ecosystems., Science, 328(5985), 1523–8, doi:10.1126/science.1189930, 2010.

Hoek, G., Krishnan, R. M., Beelen, R., Peters, A., Ostro, B. and Brunekreef, B.: Long-term air pollution exposure and cardio-respiratory mortality: a review, Env. Heal., 12, doi:10.1186/1476-069X-12-43, 2013.

Holland, M.: Implementation of the HRAPIE Recommendations for European Air Pollution CBA work. [online] Available from: http://ec.europa.eu/environment/air/pdf/CBA HRAPIE implement.pdf, 2014.

Hope, C.: Discount rates, equity weights and the social cost of carbon, Energy Econ., 30(3), 1011–1019, doi:10.1016/j.eneco.2006.11.006, 2008.

Horálek, J., de Smet, P., Kurfürst, P., de Leeuw, F. and Benešová, N.: European air quality maps of PM and ozone for 2011 and their uncertainty, ETC/ACM Technical Paper 2013/13. [online] Available from: http://acm.eionet.europa.eu/reports/ETCACM_TP_2013_13_spatAQmaps_2011, 2013.

Hou, Q., An, X., Wang, Y., Tao, Y. and Sun, Z.: An assessment of China's PM10-related health economic losses in 2009, Sci. Total Environ., 435–436, 61–65, doi:10.1016/j.scitotenv.2012.06.094, 2012.

Huang, D. and Zhang, S.: Health benefits evaluation for PM2.5 pollution control in Beijing-Tianjin-Hebei region of China, China Environ. Sci., 33(1), 166–174, 2013.

Huang, D., Xu, J. and Zhang, S.: Valuing the health risks of particulate air pollution in the Pearl River Delta, China, Environ. Sci. Policy, 15(1), 38–47, doi:10.1016/j.envsci.2011.09.007, 2012.

Huang, R.-J., Zhang, Y., Bozzetti, C., Ho, K.-F., Cao, J.-J., Han, Y., Daellenbach, K. R., Slowik, J. G., Platt, S. M., Canonaco, F., Zotter, P., Wolf, R., Pieber, S. M., Bruns, E. A., Crippa, M., Ciarelli, G., Piazzalunga, A., Schwikowski, M., Abbaszade, G., Schnelle-Kreis, J., Zimmermann, R., An, Z., Szidat, S., Baltensperger, U., Haddad, I. El and Prévôt, A. S. H.: High secondary aerosol contribution to particulate pollution during haze events in China, Nature, doi:10.1038/nature13774, 2014.

IEA: Energy Technology Perspectives 2012, OECD Publishing, Paris., 2012.

IEA: CO2 Emissions From Fuel Combustion Highlights 2016. [online] Available from: http://www.iea.org/publications/freepublications/publication/co2-emissions-from-fuel-combustion-highlights-2016.html (Accessed 9 October 2017), 2016.

IMF: International Monetary Fund, World Economic Outlook, [online] Available from: https://www.imf.org/external/pubs/ft/weo/2016/01/weodata/index.aspx, 2016.

IPCC: 2006 IPCC Guidelines for National Greenhouse Gas Inventories,Volume 1-General Guidance and Reporting. [online] Available from: http://www.ipcc-nggip.iges.or.jp/public/2006gl/vol1.html (Accessed 27 September 2017), 2006.

IPCC: IPCC Fifth Assessment Report: Climate Change 2014, Cambridge, UK. [online] Available from: https://www.ipcc.ch/report/ar5/, 2014.

Jin, L., Brown, N. J., Harley, R. A., Bao, J.-W., Michelson, S. A. and Wilczak, J. M.: Seasonal versus episodic performance evaluation for an Eulerian photochemical air quality model, J. Geophys. Res., 115(D9), 2156–2202, doi:10.1029/2009JD012680, 2010.

Jin, Y., Andersson, H. and Zhang, S.: Air Pollution Control Policies in China: A Retrospective and Prospects., Int. J. Environ. Res. Public Health, 13(12), doi:10.3390/ijerph13121219, 2016.

Kan, H. and Chen, B.: Particulate air pollution in urban areas of Shanghai, China: health-based economic assessment, Sci. Total Environ., 322(1–3), 71–79, doi:10.1016/j.scitotenv.2003.09.010, 2004.

Kan, H., Chen, B., Chen, C., Fu, Q. and Chen, M.: An evaluation of public health impact of ambient air pollution under various energy scenarios in Shanghai, China, Atmos. Environ. [online] Available from: http://www.sciencedirect.com/science/article/pii/S1352231003008008 (Accessed 13 June 2013), 2004.

Kang, D., Mathur, R. and Trivikrama Rao, S.: Assessment of bias-adjusted PM2.5 air quality forecasts over the continental United States during 2007, Geosci. Model Dev., 3(1), 309–320, doi:10.5194/gmd-3-309-2010, 2010.

Klimont, Z., Cofala, J., Xing, J., Wei, W., Zhang, C., Wang, S., Kejun, J., Bhandari, P., Mathur, R., Purohit, P., Rafaj, P., Chambers, A., Amann, M. and Hao, J.: Projections of SO_2, NO_x and carbonaceous aerosols emissions in Asia, Tellus B Chem. Phys. Meteorol., 61(4), 602–617, doi:10.1111/j.1600-0889.2009.00428.x, 2009.

Klimont, Z., Smith, S. J. and Cofala, J.: The last decade of global anthropogenic sulfur dioxide: 2000–2011 emissions, Environ. Res. Lett., 8(1), 14003, doi:10.1088/1748-9326/8/1/014003, 2013.

Klimont, Z., Kupiainen, K., Heyes, C., Purohit, P., Cofala, J., Rafaj, P., Borken-Kleefeld, J. and Schöpp, W.: Global anthropogenic emissions of particulate matter including black carbon, Atmos. Chem. Phys. Discuss., 1–72, doi:10.5194/acp-2016-880, 2016.

Kuik, O., Brander, L. and Tol, R. S. J.: Marginal abatement costs of greenhouse gas emissions: A meta-analysis, Energy Policy, 37(4), 1395–1403, doi:10.1016/j.enpol.2008.11.040, 2009.

Kukkonen, J., Olsson, T., Schultz, D. M., Baklanov, A., Klein, T., Miranda, A. I., Monteiro, A., Hirtl, M., Tarvainen, V., Boy, M., Peuch, V.-H., Poupkou, A., Kioutsioukis, I., Finardi, S., Sofiev, M., Sokhi, R., Lehtinen, K. E. J., Karatzas, K., San José, R., Astitha, M., Kallos, G., Schaap, M., Reimer, E., Jakobs, H. and Eben, K.: A review of operational, regional-scale, chemical weather forecasting models in Europe, Atmos. Chem. Phys., 12(1), 1–87, doi:10.5194/acp-12-1-2012, 2012.

Kunzli, N., Medina, S., Kaiser, R., Quénel, P., Horak, F. and Studnicka, M.: Assessment of Deaths Attributable to Air Pollution: Should We Use Risk Estimates based on Time Series or on Cohort Studies?, Am. J. Epidemiol., 153(11), 1050–1055, doi:10.1093/aje/153.11.1050, 2001.

Künzli, N., Kaiser, R., Medina, S., Studnicka, M., Chanel, O., Filliger, P., Herry, M., Horak, F., Puybonnieux-Texier, V., Quénel, P., Schneider, J., Seethaler, R., Vergnaud, J. C. and Sommer, H.: Public-health impact of outdoor and traffic-related air pollution: A European assessment, Lancet, 356(9232), 795–801, doi:10.1016/S0140-6736(00)02653-2, 2000.

Lee, C. J., Martin, R. V., Henze, D. K., Brauer, M., Cohen, A. and Donkelaar, A. van: Response of Global Particulate-Matter-Related Mortality to Changes in Local Precursor Emissions, Environ. Sci. Technol., 49(7), 4335–4344, doi:10.1021/acs.est.5b00873, 2015.

Legates, D. R. and McCabe, G. J.: Evaluating the use of “goodness-of-fit” Measures in hydrologic and hydroclimatic model validation, Water Resour. Res., 35(1), 233–241, doi:10.1029/1998WR900018, 1999.

Leksell, I. and Rabl, A.: Air Pollution and Mortality: Quantification and Valuation of Years of Life Lost, Risk Anal., 21(5), 843–857, doi:10.1111/0272-4332.215156, 2001.

Lepeule, J., Laden, F., Dockery, D. and Schwartz, J.: Chronic exposure to fine particles and mortality: an extended follow-up of the Harvard Six Cities study from 1974 to 2009, Env. Heal. Perspect, 120, doi:10.1289/ehp.1104660, 2012.

Li, F., Liu, Y., Lü, J., Liang, L. and Harmer, P.: Ambient air pollution in China poses a multifaceted health threat to outdoor physical activity., J. Epidemiol. Community Health, 69(3), 201–4, doi:10.1136/jech-2014-203892, 2015.

Li, S., Williams, G. and Guo, Y.: Health benefits from improved outdoor air quality and intervention in China, Environ. Pollut., 214, 17–25, doi:10.1016/j.envpol.2016.03.066, 2016.

Liang, Q., Jaeglé, L., Jaffe, D. A., Weiss-Penzias, P., Heckman, A. and Snow, J. A.: Long-range transport of Asian pollution to the northeast Pacific: Seasonal variations and transport pathways of carbon monoxide, J. Geophys. Res. Atmos., 109(D23), doi:10.1029/2003JD004402, 2004.

Lim, S. S., Vos, T., Flaxman, A. D., Danaei, G., Shibuya, K., Adair-Rohani, H., AlMazroa, M. A., Amann, M., Anderson, H. R., Andrews, K. G., Aryee, M., Atkinson, C., Bacchus, L. J., Bahalim, A. N., Balakrishnan, K., Balmes, J., Barker-Collo, S., Baxter, A., Bell, M. L., Blore, J. D., Blyth, F., Bonner, C., Borges, G., Bourne, R., Boussinesq, M., Brauer, M., Brooks, P., Bruce, N. G., Brunekreef, B., Bryan-Hancock, C., Bucello, C., Buchbinder, R., Bull, F., Burnett, R. T., Byers, T. E., Calabria, B., Carapetis, J., Carnahan, E., Chafe, Z., Charlson, F., Chen, H., Chen, J. S., Cheng, A. T.-A., Child, J. C., Cohen, A., Colson, K. E., Cowie, B. C., Darby, S., Darling, S., Davis, A., Degenhardt, L., Dentener, F., Des Jarlais, D. C., Devries, K., Dherani, M., Ding, E. L., Dorsey, E. R., Driscoll, T., Edmond, K., Ali, S. E., Engell, R. E., Erwin, P. J., Fahimi, S., Falder, G., Farzadfar, F., Ferrari, A., Finucane, M. M., Flaxman, S., Fowkes, F. G. R., Freedman, G., Freeman, M. K., Gakidou, E., Ghosh, S., Giovannucci, E., Gmel, G., Graham, K., Grainger, R., Grant, B., Gunnell, D., Gutierrez, H. R., Hall, W., Hoek, H. W., Hogan, A., Hosgood, H. D., Hoy, D., Hu, H., Hubbell, B. J., Hutchings, S. J., Ibeanusi, S. E., Jacklyn, G. L., Jasrasaria, R., Jonas, J. B., Kan, H., Kanis, J. A., Kassebaum, N., Kawakami, N., Khang, Y.-H., Khatibzadeh, S., Khoo, J.-P., et al.: A comparative risk assessment of burden of disease and injury attributable to 67 risk factors and risk factor clusters in 21 regions, 1990–2010: a systematic analysis for the Global Burden of Disease Study 2010, Lancet, 380(9859), 2224–2260, doi:10.1016/S0140-6736(12)61766-8, 2012.

Limpert, E., Stahel, W. A. and Abbt, M.: Log-normal Distributions across the Sciences: Keys and CluesOn the charms of statistics, and how mechanical models resembling gambling machines offer a link to a handy way to characterize log-normal distributions, which can provide deeper insight into variability and probability—normal or log-normal: That is the question, Bioscience, 51(5), 341–352, doi:10.1641/0006-3568(2001)051[0341:lndats]2.0.co;2, 2001.

Liu, F., Klimont, Z., Zhang, Q., Cofala, J., Zhao, L., Huo, H., Nguyen, B., Schöpp, W., Sander, R., Zheng, B., Hong, C., He, K., Amann, M. and Heyes, C.: Integrating mitigation of air pollutants and greenhouse gases in Chinese cities: development of GAINS-City model for Beijing, J. Clean. Prod., 58, 25–33, doi:10.1016/J.JCLEPRO.2013.03.024, 2013.

Liu, F., Beirle, S., Zhang, Q., van der A, R. J., Zheng, B., Tong, D. and He, K.: NOx emission trends over Chinese cities estimated from OMI observations during 2005 to 2015, Atmos. Chem. Phys., 17(15), 9261–9275, doi:10.5194/acp-17-9261-2017, 2017.

Liu, S., Hu, M., Slanina, S., He, L.-Y., Niu, Y.-W., Bruegemann, E., Gnauk, T. and Herrmann, H.: Size distribution and source analysis of ionic compositions of aerosols in polluted periods at Xinken in Pearl River Delta (PRD) of China, Atmos. Environ., 42(25), 6284–6295, doi:10.1016/j.atmosenv.2007.12.035, 2008.

Lovett, G. M., Tear, T. H., Evers, D. C., Findlay, S. E. G., Cosby, B. J., Dunscomb, J. K., Driscoll, C. T. and Weathers, K. C.: Effects of Air Pollution on Ecosystems and Biological Diversity in the Eastern United States, Ann. N. Y. Acad. Sci., 1162(1), 99–135, doi:10.1111/j.1749-6632.2009.04153.x, 2009.

Lozano, R., Naghavi, M., Foreman, K., Lim, S., Shibuya, K., Aboyans, V., Abraham, J., Adair, T., Aggarwal, R., Ahn, S. Y., AlMazroa, M. A., Alvarado, M., Anderson, H. R., Anderson, L. M., Andrews, K. G., Atkinson, C., Baddour, L. M., Barker-Collo, S., Bartels, D. H., Bell, M. L., Benjamin, E. J., Bennett, D., Bhalla, K., Bikbov, B., Abdulhak, A. Bin, Birbeck, G., Blyth, F., Bolliger, I., Boufous, S., Bucello, C., Burch, M., Burney, P., Carapetis, J., Chen, H., Chou, D., Chugh, S. S., Coffeng, L. E., Colan, S. D., Colquhoun, S., Colson, K. E., Condon, J., Connor, M. D., Cooper, L. T., Corriere, M., Cortinovis, M., de Vaccaro, K. C., Couser, W., Cowie, B. C., Criqui, M. H., Cross, M., Dabhadkar, K. C., Dahodwala, N., De Leo, D., Degenhardt, L., Delossantos, A., Denenberg, J., Des Jarlais, D. C., Dharmaratne, S. D., Dorsey, E. R., Driscoll, T., Duber, H., Ebel, B., Erwin, P. J., Espindola, P., Ezzati, M., Feigin, V., Flaxman, A. D., Forouzanfar, M. H., Fowkes, F. G. R., Franklin, R., Fransen, M., Freeman, M. K., Gabriel, S. E., Gakidou, E., Gaspari, F., Gillum, R. F., Gonzalez-Medina, D., Halasa, Y. A., Haring, D., Harrison, J. E., Havmoeller, R., Hay, R. J., Hoen, B., Hotez, P. J., Hoy, D., Jacobsen, K. H., James, S. L., Jasrasaria, R., Jayaraman, S., Johns, N., Karthikeyan, G., Kassebaum, N., Keren, A., Khoo, J.-P., Knowlton, L. M., Kobusingye, O., Koranteng, A., Krishnamurthi, R., Lipnick, M., et al.: Global and regional mortality from 235 causes of death for 20 age groups in 1990 and 2010: a systematic analysis for the Global Burden of Disease Study 2010, Lancet, 380(9859), 2095–2128, doi:10.1016/S0140-6736(12)61728-0, 2012.

Luo, X., Caron, J., Karplus, V. J., Zhang, D. and Zhang, X.: Interprovincial migration and the stringency of energy policy in China, Energy Econ., 58, doi:10.1016/j.eneco.2016.05.017, 2016.

Ma, G., Wang, J., Yu, F., Guo, X., Zhang, Y. and Li, C.: Assessing the premature death due to ambient particulate matter in China’s urban areas from 2004 to 2013, Front. Environ. Sci. Eng., 10(5), 7, doi:10.1007/s11783-016-0849-7, 2016.

Maibach, M., Schreyer, C., Sutter, D., Essen, H. P. van, Boon, B. H., Smokers, R., Schroten, A., Doll, C., Pawlowska, B. and Bak, M.: Handbook on estimation of external costs in the transport sector Internalisation Measures and Policies for All external Cost of Transport (IMPACT), Delft, The Netherlands. [online] Available from:
https://ec.europa.eu/transport/sites/transport/files/themes/sustainable/doc/2008_c

osts_handbook.pdf, 2008.

Mao, X., Yang, S., Liu, Q., Tu, J. and Jaccard, M.: Achieving CO2 emission reduction and the co-benefits of local air pollution abatement in the transportation sector of China, Environ. Sci. Policy, 21, 1–13, doi:10.1016/J.ENVSCI.2012.03.010, 2012.

Matus, K., Yang, T., Paltsev, S., Reilly, J. and Nam, K.-M.: Toward integrated assessment of environmental change: air pollution health effects in the USA, Clim. Change, 88(1), 59–92, doi:10.1007/s10584-006-9185-4, 2008.

Matus, K., Nam, K. M., Selin, N. E., Lamsal, L. N., Reilly, J. M. and Paltsev, S.: Health damages from air pollution in China, Glob. Environ. Chang., 22(1), 55–66, doi:10.1016/j.gloenvcha.2011.08.006, 2012.

McKeen, S., Wilczak, J., Grell, G., Djalalova, I., Peckham, S., Hsie, E.-Y., Gong, W., Bouchet, V., Menard, S., Moffet, R., McHenry, J., McQueen, J., Tang, Y., Carmichael, G. R., Pagowski, M., Chan, A., Dye, T., Frost, G., Lee, P. and Mathur, R.: Assessment of an ensemble of seven real-time ozone forecasts over eastern North America during the summer of 2004, J. Geophys. Res., 110(D21), D21307, doi:10.1029/2005JD005858, 2005.

Mendelsohn, R., Emanuel, K., Chonabayashi, S. and Bakkensen, L.: The impact of climate change on global tropical cyclone damage, Nat. Clim. Chang., 2(3), 205–209, doi:10.1038/nclimate1357, 2012.

MEP: National Environmental Statistics Bulletin 2005. [online] Available from: http://www.mep.gov.cn/gzfw_13107/hjtj/qghjtjgb/, 2006.

MEP: National Environmental Statistics Bulletin 2010. [online] Available from: http://www.mep.gov.cn/gzfw_13107/hjtj/qghjtjgb/ (Accessed 8 October 2017), 2011.

MEP: Ambient air quality standards (GB3095-2012), Ministry of Environmental Protection of the People's Republic of China. [online] Available from: http://english.mep.gov.cn/Resources/standards/Air_Environment/quality_standard1/201605/t20160511_337502.shtml (Accessed 8 October 2017a), 2012.

MEP: Technical Regulation on Ambient Air Quality Index (AQI) (on Trial), HJ 633-201., edited by Ministry of Environmental Protection of the People's Republic of China, China Environmental Science Press, Beijing. [online] Available from: http://kjs.mep.gov.cn/hjbhbz/bzwb/dqhjbh/jcgfffbz/201203/t20120302_224166.htm, 2012b.

MHPRC: Ministry of Health of the People's Republic of China, China Public Health Statistical Yearbook 2011, Peking Union Medical College Press., 2011.

Miller, B. G. and Hurley, J. F.: Life table methods for quantitative impact assessments in chronic mortality., J. Epidemiol. Community Health, 57(3), 200–206, doi:10.1136/jech.57.3.200, 2003.

Monteiro, A., Ribeiro, I., Tchepel, O., Sá, E., Ferreira, J., Carvalho, A., Martins, Monteiro, A., Ribeiro, I., Tchepel, O., Sá, E., Ferreira, J., Carvalho, A., Martins, V., Strunk, A., Galmarini, S., Elbern, H., Schaap, M., Builtjes, P., Miranda, A. I. and Borrego, C.: Bias Correction Techniques to Improve Air Quality Ensemble Predictions: Focus on O3 and PM Over Portugal, Environ. Model. Assess., 18(5), 533–546, doi:10.1007/s10666-013-9358-2, 2013.

Næss, Ø., Nafstad, P., Aamodt, G., Claussen, B. and Rosland, P.: Relation between concentration of air pollution and cause-specific mortality: Four-year exposures to nitrogen dioxide and particulate matter pollutants in 470 neighborhoods in Oslo, Norway, Am. J. Epidemiol., 165(4), 435–443, doi:10.1093/aje/kwk016, 2007.

NBSC: China Statistical Yearbook on Environment 2014, edited by National Bureau of Statistics and Ministry of Environmental Protection of China, China Statistics Press, Beijing. [online] Available from: http://www.stats.gov.cn/ztjc/ztsj/hjtjzl/, 2015.

NBSC: China Energy Statistical Yearbook 2015, edited by National Bureau of Statistics of China, China Statistics Press, Beijing., 2016.

NDRC: National Development and Reform Commission, Special Plan for Medium and Long Term Energy Conservation, [online] Available from: http://www.ndrc.gov.cn/xwfb/t20050628_27571.htm (Accessed 1 June 2016), 2004.

NDRC: National Development and Reform Commission, Medium and Long Term Development Plan for Nuclear Power, [online] Available from: nyj.ndrc.gov.cn/zywx/W020071102318742621534.pdf (Accessed 16 June 2016), 2005.

NDRC: National Development and Reform Commission, Medium and Long Term Development Plan for Renewable Energy, [online] Available from: http://www.sdpc.gov.cn/zcfb/zcfbtz/2007tongzhi/t20070904_157352.htm (Accessed 15 June 2016a), 2007.

NDRC: National Development and Reform Commission, National Natural Gas Utilization Policy, [online] Available from: http://www.sdpc.gov.cn/zcfb/zcfbtz/2007tongzhi/t20070904_157244.htm (Accessed 15 June 2016b), 2007.

Nielsen, C. P. and Ho, M. S., Eds.: Clearer Skies Over China Reconciling Air Quality, Climate, and Economic Goals, The MIT Press., 2013.

OECD: Economic Outlook No 91- Long-term baseline projections, [online] Available from: https://stats.oecd.org/Index.aspx?DataSetCode=EO91_LTB, 2012.

OECD: OECD Factbook 2015-2016: Economic, Environmental and Social Statistics, [online] Available from: http://dx.doi.org/10.1787/factbook-2015-en, 2016.

Okagawa, A., Masui, T., Akashi, O., Hijioka, Y., Matsumoto, K. and Kainuma, M.:

Assessment of GHG emission reduction pathways in a society without carbon capture and nuclear technologies, Energy Econ., 34, S391–S398, doi:10.1016/J.ENECO.2012.07.011, 2012.

ORNL DAAC: Spatial Data Access Tool (SDAT), , doi:10.3334/ornldaac/1388, 2017.

Ottinger, R. L.: Environmental Costs of Electricity, Oceana Publications, New York., 1991.

Pan, X., Yue, W., He, K. and Tong, S.: Health benefit evaluation of the energy use scenarios in Beijing, China, Sci. Total Environ., 374(2), 242–251, doi:10.1016/j.scitotenv.2007.01.005, 2007.

Patz, J. A., Campbell-Lendrum, D., Holloway, T. and Foley, J. A.: Impact of regional climate change on human health, Nature, 438(7066), 310–317, doi:10.1038/nature04188, 2005.

Pearce, D.: The Social Cost of Carbon and its Policy Implications, Oxford Rev. Econ. Policy, 19(3), 362–384, doi:10.1093/oxrep/19.3.362, 2003.

Peng, W., Yang, J., Wagner, F. and Mauzerall, D. L.: Substantial air quality and climate co-benefits achievable now with sectoral mitigation strategies in China, Sci. Total Environ., 598, 1076–1084, doi:10.1016/j.scitotenv.2017.03.287, 2017.

Pirovano, G., Balzarini, A., Bessagnet, B., Emery, C., Kallos, G., Meleux, F., Mitsakou, C., Nopmongcol, U., Riva, G. M. and Yarwood, G.: Investigating impacts of chemistry and transport model formulation on model performance at European scale, Atmos. Environ., 53, 93–109, doi:10.1016/j.atmosenv.2011.12.052, 2012.

Pope, C. A.: Epidemiology of fine particulate air pollution and human health: biologic mechanisms and who’s at risk?, Environ. Health Perspect., (Suppl 4), 713–23 [online] Available from: http://www.ncbi.nlm.nih.gov/pubmed/10931790 (Accessed 12 June 2017), 2000.

Pope, C. A. and Dockery, D. W.: Health effects of fine particulate air pollution: lines that connect, J. Air Waste Manage. Assoc., 56(6), 709–742, doi:10.1080/10473289.2006.10464485, 2006.

Pope, C. A., Burnett, R. T., Thun, M. J., Calle, E. E., Krewski, D., Ito, K. and Thurston, G. D.: Lung Cancer, Cardiopulmonary Mortality, and Long-term Exposure to Fine Particulate Air Pollution, JAMA, 287(9), 1132–1141, doi:10.1001/jama.287.9.1132, 2002.

Pope, C. A., Burnett, R. T., Krewski, D., Jerrett, M., Shi, Y., Calle, E. E. and Thun, M. J.: Cardiovascular Mortality and Exposure to Airborne Fine Particulate Matter and Cigarette Smoke: Shape of the Exposure-Response Relationship, Circulation, 120(11), 941–948, doi:10.1161/CIRCULATIONAHA.109.857888, 2009.

Prank, M., Sofiev, M., Tsyro, S., Hendriks, C., Semeena, V., Vazhappilly Francis, X., Butler, T., Denier van der Gon, H., Friedrich, R., Hendricks, J., Kong, X., Lawrence, M., Righi, M., Samaras, Z., Sausen, R., Kukkonen, J. and Sokhi, R.: Evaluation of the performance of four chemical transport models in predicting the aerosol chemical composition in Europe in 2005, Atmos. Chem. Phys., 16(10), 6041–6070, doi:10.5194/acp-16-6041-2016, 2016.

Preiss, P., Roos, J. and Friedrich, R.: Assessment of health impacts of coal fired power stations in Germany-by applying EcoSenseWeb, Stuttgart. [online] Available from: http://www.greenpeace.de/files/publications/130401_deliverable_ier_to_greenpeace_de_0.pdf, 2013.

Puett, R. C., Schwartz, J., Hart, J. E., Yanosky, J. D., Speizer, F. E. and Suh, H.: Chronic particulate exposure, mortality, and coronary heart disease in the nurses' health study, Am J Epidemiol, 168, doi:10.1093/aje/kwn232, 2008.

Puett, R. C., Hart, J. E., Yanosky, J. D., Paciorek, C. J., Schwartz, J. and Suh, H.: Chronic fine and coarse particulate exposure, mortality and coronary heart disease in the nurses' health study, Env. Heal. Perspect, 117, doi:10.1289/ehp.0900572, 2009.

Rabl, A., Spadaro, J. V. and Zwaan, B. van der: Uncertainty of Air Pollution Cost Estimates: To What Extent Does It Matter?, Environ. Sci. Technol., 39(2), 399–408, doi:10.1021/ES049189V, 2005.

Rabl, A., Spadaro, J. V. and Holland, M.: How Much Is Clean Air Worth? Calculating the Benefits of Pollution Control, Cambridge University Press, Cambridge., 2014.

Rafaj, P., Schöpp, W., Russ, P., Heyes, C. and Amann, M.: Co-benefits of post-2012 global climate mitigation policies, Mitig. Adapt. Strateg. Glob. Chang., 18(6), 801–824, doi:10.1007/s11027-012-9390-6P, 2013.

Rao, S., Klimont, Z., Leitao, J., Riahi, K., van Dingenen, R., Reis, L. A., Calvin, K., Dentener, F., Drouet, L., Fujimori, S., Harmsen, M., Luderer, G., Heyes, C., Strefler, J., Tavoni, M. and van Vuuren, D. P.: A multi-model assessment of the co-benefits of climate mitigation for global air quality, Environ. Res. Lett., 11(12), 124013, doi:10.1088/1748-9326/11/12/124013, 2016.

Reis, S., Nitter, S. and Friedrich, R.: Innovative approaches in integrated assessment modelling of European air pollution control strategies – Implications of dealing with multi-pollutant multi-effect problems, Environ. Model. Softw., 20(12), 1524–1531, doi:10.1016/J.ENVSOFT.2004.07.019, 2005.

Rohde, R. A. and Muller, R. A.: Air Pollution in China: Mapping of Concentrations and Sources., PLoS One, 10(8), e0135749, doi:10.1371/journal.pone.0135749, 2015.

Roos, J.: Ermittlung und Bewertung von vermiedenen Gesundheitsschäden im Rahmen der Technikbewertung, Universität Stuttgart, http://dx.doi.org/10.18419/OPUS-9177, 20 April., 2017.

Rosenzweig, C., Karoly, D., Vicarelli, M., Neofotis, P., Wu, Q., Casassa, G., Menzel, A., Root, T. L., Estrella, N., Seguin, B., Tryjanowski, P., Liu, C., Rawlins, S. and Imeson, A.: Attributing physical and biological impacts to anthropogenic climate change, Nature, 453(7193), 353–357, doi:10.1038/nature06937, 2008.

Sabel, C. E., Hiscock, R., Asikainen, A., Bi, J., Depledge, M., van den Elshout, S., Friedrich, R., Huang, G., Hurley, F., Jantunen, M., Karakitsios, S. P., Keuken, M., Kingham, S., Kontoroupis, P., Kuenzli, N., Liu, M., Martuzzi, M., Morton, K., Mudu, P., Niittynen, M., Perez, L., Sarigiannis, D., Stahl-Timmins, W., Tobollik, M., Tuomisto, J. and Willers, S.: Public health impacts of city policies to reduce climate change: findings from the URGENCHE EU-China project, Environ. Heal., 15(S1), S25, doi:10.1186/s12940-016-0097-0, 2016.

SCPRC: The State Council of the People's Republic of China, The state council executive meeting sets the GHGs (Greenhouse Gas) reduction target of China, (in Chinese) [online] Available from: http://www.gov.cn/ldhd/2009-11/26/content_1474016.htm (Accessed 19 June 2017), 2009.

SCPRC: The State Council of the People's Republic of China: The guidelines of promoting joint prevention and control policies and improving regional air quality, [online] Available from: http://www.gov.cn/xxgk/pub/govpublic/mrlm/201005/t20100513_56516.htm (Accessed 2 March 2017), 2010.

SCPRC: The State Council of the People's Republic of China: Integrated Work Plan for Energy Saving and Emission Reduction Duringthe Twelfth Five-Year Plan, [online] Available from: http://www.gov.cn/zwgk/2011-09/07/content_1941731.htm (Accessed 1 July 2016a), 2011.

SCPRC: The State Council of the People's Republic of China: The Twelfth Five-Year Plan for Environmental Protection, [online] Available from: http://www.gov.cn/zwgk/2011-12/20/content_2024895.htm (Accessed 5 February 2017b), 2011.

SCPRC: The State Council of the People's Republic of China: The Twelfth Five-Year Plan for National Economic and Social Development of the People's Republic of China, [online] Available from: http://www.gov.cn/2011lh/content_1825838.htm (Accessed 15 June 2016c), 2011.

SCPRC: The State Council of the People's Republic of China: The Twelfth Five-Year Plan for Energy Saving and Emission Reduction, [online] Available from: http://www.gov.cn/zwgk/2012-08/21/content_2207867.htm (Accessed 2 March 2017), 2012.

SCPRC: The State Council of the People's Republic of China: Air Pollution Prevention and Control Action Plan, [online] Available from: http://www.gov.cn/zwgk/2013-09/12/content_2486773.htm (Accessed 5 February 2017), 2013.

SCPRC: The State Council of the People's Republic of China: The Thirteenth

Five-Year Plan for Environmental Protection, [online] Available from: http://www.gov.cn/zhengce/content/2016-12/05/content_5143290.htm (Accessed 8 October 2017), 2016.

Silibello, C., D’Allura, A., Finardi, S., Bolignano, A. and Sozzi, R.: Application of bias adjustment techniques to improve air quality forecasts, Atmos. Pollut. Res., 6(6), 928–938, doi:10.1016/j.apr.2015.04.002, 2015.

Simpson, D., Benedictow, A., Berge, H., Bergström, R., Emberson, L. D., Fagerli, H., Flechard, C. R., Hayman, G. D., Gauss, M., Jonson, J. E., Jenkin, M. E., Nyíri, A., Richter, C., Semeena, V. S., Tsyro, S., Tuovinen, J.-P., Valdebenito, Á. and Wind, P.: The EMEP MSC-W chemical transport model – technical description, Atmos. Chem. Phys., 12(16), 7825–7865, doi:10.5194/acp-12-7825-2012, 2012.

Song, L., Gao, R., Li, Y. and Wang, G.: Analysis of China’s Haze Days in the Winter Half-Year and the Climatic Background during 1961–2012, Adv. Clim. Chang. Res., 5(1), 1–6, doi:10.3724/SP.J.1248.2014.001, 2014.

Spadaro, J. V. and Rabl, A.: Estimating the uncertainty of damage costs of pollution: A simple transparent method and typical results, Environ. Impact Assess. Rev., 28(2), 166–183, doi:10.1016/j.eiar.2007.04.001, 2008.

Stern, N.: The Stern Review on the Economic Effects of Climate Change, Cambridge University Press, Cambridge, UK. [online] Available from: http://webarchive.nationalarchives.gov.uk/20100407172811/http://www.hm-treasury.gov.uk/stern_review_report.htm, 2006.

Sun, J., Huang, L., Liao, H., Li, J. and Hu, J.: Impacts of Regional Transport on Particulate Matter Pollution in China: a Review of Methods and Results, Curr. Pollut. Reports, 3(3), 182–191, doi:10.1007/s40726-017-0065-5, 2017.

Swart, R., Amann, M., Raes, F. and Tuinstra, W.: A Good Climate for Clean Air: Linkages between Climate Change and Air Pollution. An Editorial Essay, Clim. Change, 66(3), 263–269, doi:10.1023/B:CLIM.0000044677.41293.39, 2004.

Tol, R. S. J.: The marginal damage costs of carbon dioxide emissions: an assessment of the uncertainties, Energy Policy, 33(16), 2064–2074, doi:10.1016/j.enpol.2004.04.002, 2005.

Tol, R. S. J.: The Social Cost of Carbon: Trends, Outliers and Catastrophes, Economics, 2, 2008–2025, doi:10.5018/economics-ejournal.ja.2008-25, 2008.

Tollefsen, P., Rypdal, K., Torvanger, A. and Rive, N.: Air pollution policies in Europe: efficiency gains from integrating climate effects with damage costs to health and crops, Environ. Sci. Policy, 12(7), 870–881, doi:10.1016/J.ENVSCI.2009.08.006, 2009.

UN: United Nations, Department of Economic and Social Affairs, Population Division, World Population Prospects: The 2015 Revision, custom data acquired via website., 2015.

USEPA: The Integrated Environmental Strategies Handbook: A Resource Guide for Air Quality Planning, Washington, DC. [online] Available from: http://unfccc.int/resource/cd_roms/na1/mitigation/Resource_materials/Integrated_Environmental_Strategies_Handbook_US_EPA/ies_comp_screen.pdf, 2004.

USEPA: United States Environmental Protection Agency: Particulate Matter (PM) Basics, [online] Available from: https://www.epa.gov/pm-pollution/particulate-matter-pm-basics (Accessed 12 October 2017), 2016.

Vautard, R., Builtjes, P. H. J., Thunis, P., Cuvelier, C., Bedogni, M., Bessagnet, B., Honoré, C., Moussiopoulos, N., Pirovano, G. and Schaap, M.: Evaluation and intercomparison of Ozone and PM10 simulations by several chemistry transport models over four European cities within the CityDelta project, Atmos. Environ., 41(1), 173–188, doi:10.1016/j.atmosenv.2006.07.039, 2007.

Vennemo, H., Aunan, K., He, J., Hu, T. and Li, S.: Benefits and costs to China of three different climate treaties, Resour. Energy Econ., 31(3), 139–160, doi:10.1016/J.RESENEECO.2009.03.003, 2009.

Voorhees, A. S., Wang, J., Wang, C., Zhao, B., Wang, S. and Kan, H.: Public health benefits of reducing air pollution in Shanghai: A proof-of-concept methodology with application to BenMAP, Sci. Total Environ., 485, 396–405, doi:10.1016/j.scitotenv.2014.03.113, 2014.

Wang, C., Zhou, X., Chen, R., Duan, X., Kuang, X. and Kan, H.: Estimation of the effects of ambient air pollution on life expectancy of urban residents in China, Atmos. Environ., 80, 347–351, doi:10.1016/j.atmosenv.2013.08.018, 2013a.

Wang, G., Huang, L., Gao, S., Gao, S. and Wang, L.: Measurements of PM10 and PM2.5 in urban area of Nanjing, China and the assessment of pulmonary deposition of particle mass, Chemosphere, 48(7), 689–695, doi:10.1016/S0045-6535(02)00197-2, 2002.

Wang, H. and Mullahy, J.: Willingness to pay for reducing fatal risk by improving air quality: A contingent valuation study in Chongqing, China, Sci. Total Environ., 367(1), 50–57, doi:10.1016/j.scitotenv.2006.02.049, 2006.

Wang, J., Mendelsohn, R., Dinar, A., Huang, J., Rozelle, S. and Zhang, L.: The impact of climate change on China's agriculture, Agric. Econ., 40(3), 323–337, doi:10.1111/j.1574-0862.2009.00379.x, 2009.

Wang, J., Hu, Z., Chen, Y., Chen, Z. and Xu, S.: Contamination characteristics and possible sources of PM10 and PM2.5 in different functional areas of Shanghai, China, Atmos. Environ., 68, 221–229, doi:10.1016/j.atmosenv.2012.10.070, 2013b.

Wang, S. and Hao, J.: Air quality management in China: Issues, challenges, and options, J. Environ. Sci., 24(1), 2–13, doi:10.1016/S1001-0742(11)60724-9, 2012.

Wang, S. X., Zhao, B., Cai, S. Y., Klimont, Z., Nielsen, C. P., Morikawa, T., Woo, J. H., Kim, Y., Fu, X., Xu, J. Y., Hao, J. M. and He, K. B.: Emission trends and mitigation options for air pollutants in East Asia, Atmos. Chem. Phys., 14(13), 6571–6603, doi:10.5194/acp-14-6571-2014, 2014.

Wang, X. and Smith, K. R.: Near-term Health Benefits of Greenhouse Gas Reductions: A Proposed Assessment Method and Application in Two Energy Sectors of China, World Health Organization Department of Protection of the Human Environment, Geneva, Switzerland. [online] Available from: https://digital.library.unt.edu/ark:/67531/metadc226706/ (Accessed 10 October 2017), 1999.

Wang, Y., Zhang, Q. Q., He, K., Zhang, Q. and Chai, L.: Sulfate-nitrate-ammonium aerosols over China: response to 2000–2015 emission changes of sulfur dioxide, nitrogen oxides, and ammonia, Atmos. Chem. Phys., 13(5), 2635–2652, doi:10.5194/acp-13-2635-2013, 2013c.

West, J. J., Osnaya, P., Laguna, I., Martínez, J. and Fernández, A.: Co-control of Urban Air Pollutants and Greenhouse Gases in Mexico City, Environ. Sci. Technol, 38(13), 3474–3481, doi:10.1021/ES034716G, 2004.

West, J. J., Smith, S. J., Silva, R. A., Naik, V., Zhang, Y., Adelman, Z., Fry, M. M., Anenberg, S., Horowitz, L. W. and Lamarque, J.-F.: Co-benefits of Global Greenhouse Gas Mitigation for Future Air Quality and Human Health., Nat. Clim. Chang., 3(10), 885–889, doi:10.1038/NCLIMATE2009, 2013.

WHO: Air quality guidelines - global update 2005, World Health Organization. [online] Available from: http://www.who.int/phe/health_topics/outdoorair/outdoorair_aqg/en/ (Accessed 28 June 2017), 2005.

WHO: Health risks of air pollution in Europe – HRAPIE project. Recommendations for concentration–response functions for cost–benefit analysis of particulate matter, ozone and nitrogen dioxide, World Health Organization. [online] Available from: http://www.euro.who.int/en/health-topics/environment-and-health/air-quality/publications/2013/health-risks-of-air-pollution-in-europe-hrapie-project.-recommendations-for-concentrationresponse-functions-for-costbenefit-analysis-of-particulate-matter,-ozone (Accessed 30 November 2017), 2013.

Wille, V. B.: Bewertung der Folgen des Klimawandels, Universität Stuttgart, unpublished., 2013.

World Bank: Cost of Pollution in China: economic estimates of physical damages, Washington, DC. [online] Available from: http://documents.worldbank.org/curated/en/782171468027560055/Cost-of-pollution-in-China-economic-estimates-of-physical-damages, 2007.

Xie, Y., Dai, H., Dong, H., Hanaoka, T. and Masui, T.: Economic Impacts from PM 2.5 Pollution-Related Health Effects in China: A Provincial-Level Analysis, Environ. Sci. Technol., 50(9), 4836–4843, doi:10.1021/acs.est.5b05576, 2016.

Xing, J., Wang, S. X., Chatani, S., Zhang, C. Y., Wei, W., Hao, J. M., Klimont, Z., Cofala, J. and Amann, M.: Projections of air pollutant emissions and its impacts on regional air quality in China in 2020, Atmos. Chem. Phys., 11(7), 3119–3136, doi:10.5194/acp-11-3119-2011, 2011.

Xing, J., Mathur, R., Pleim, J., Hogrefe, C., Gan, C.-M., Wong, D. C., Wei, C., Gilliam, R. and Pouliot, G.: Observations and modeling of air quality trends over 1990–2010 across the Northern Hemisphere: China, the United States and Europe, Atmos. Chem. Phys., 15(5), 2723–2747, doi:10.5194/acp-15-2723-2015, 2015.

Xu, B., Sun, Q., Wennersten, R. and Brandt, N.: An Analysis of China's Carbon Dioxide Mitigation Target, Sustain. Dev., 22(2), 113–121, doi:10.1002/sd.535, 2014.

Xu, Y. and Masui, T.: Local air pollutant emission reduction and ancillary carbon benefits of SO2 control policies: Application of AIM/CGE model to China, Eur. J. Oper. Res., 198(1), 315–325, doi:10.1016/J.EJOR.2008.07.048, 2009.

Yang, F., Tan, J., Zhao, Q., Du, Z., He, K., Ma, Y., Duan, F., Chen, G. and Zhao, Q.: Characteristics of PM2.5 speciation in representative megacities and across China, Atmos. Chem. Phys., 11(11), 5207–5219, doi:10.5194/acp-11-5207-2011, 2011.

Yang, G., Wang, Y., Zeng, Y., Gao, G. F., Liang, X., Zhou, M., Wan, X., Yu, S., Jiang, Y., Naghavi, M., Vos, T., Wang, H., Lopez, A. D. and Murray, C. J.: Rapid health transition in China, 1990–2010: findings from the Global Burden of Disease Study 2010, Lancet, 381(9882), 1987–2015, doi:10.1016/S0140-6736(13)61097-1, 2013a.

Yang, K. and Lei, Y.: The carbon dioxide marginal abatement cost calculation of Chinese provinces based on stochastic frontier analysis, Nat. Hazards, 85(1), 505–521, doi:10.1007/s11069-016-2582-8, 2017.

Yang, X., Teng, F. and Wang, G.: Incorporating environmental co-benefits into climate policies: A regional study of the cement industry in China, Appl. Energy, 112, 1446–1453, doi:10.1016/J.APENERGY.2013.03.040, 2013b.

Yu, L., Wang, G., Zhang, R., Zhang, L., Song, Y., Wu, B., Li, X., An, K. and Chu, J.: Characterization and source apportionment of PM2.5 in an urban environment in Beijing, Aerosol Air Qual. Res., 13(2), 574–583, doi:10.4209/aaqr.2012.07.0192, 2013.

Zeger, S. L., Dominici, F., McDermott, A. and Samet, J. M.: Mortality in the medicare population and chronic exposure to fine particulate air pollution in urban centers (2000--2005), Env. Heal. Perspect, 116, doi:10.1289/ehp.11449, 2008.

Zhang, D., Aunan, K., Martin Seip, H., Larssen, S., Liu, J. and Zhang, D.: The assessment of health damage caused by air pollution and its implication for policy making in Taiyuan, Shanxi, China, Energy Policy, 38(1), 491–502, doi:10.1016/j.enpol.2009.09.039, 2010.

Zhang, D., Rausch, S., Karplus, V. J. and Zhang, X.: Quantifying regional economic impacts of CO2 intensity targets in China, Energy Econ., 40, 687–701, doi:10.1016/j.eneco.2013.08.018, 2013a.

Zhang, J. and Wang, C.: Co-benefits and additionality of the clean development mechanism: An empirical analysis, J. Environ. Econ. Manage., 62(2), 140–154, doi:10.1016/J.JEEM.2011.03.003, 2011.

Zhang, M., Song, Y., Cai, X. and Zhou, J.: Economic assessment of the health effects related to particulate matter pollution in 111 Chinese cities by using economic burden of disease analysis, J. Environ. Manage., 88(4), 947–954, doi:10.1016/j.jenvman.2007.04.019, 2008.

Zhang, N. and Yu, Y.: Marginal abatement cost of pollutants for China: A nonparametric approach, Energy Sources, Part B Econ. Planning, Policy, 11(8), 753–759, doi:10.1080/15567249.2013.791896, 2016.

Zhang, Q., Streets, D. G., He, K., Wang, Y., Richter, A., Burrows, J. P., Uno, I., Jang, C. J., Chen, D., Yao, Z. and Lei, Y.: NO_x emission trends for China, 1995–2004: The view from the ground and the view from space, J. Geophys. Res., 112(D22), D22306, doi:10.1029/2007JD008684, 2007.

Zhang, Q., He, K. and Huo, H.: Policy Cleaning China's air, Nature, 484(7393), 161, doi:10.1038/484161a, 2012.

Zhang, R., Jing, J., Tao, J., Hsu, S.-C., Wang, G., Cao, J., Lee, C. S. L., Zhu, L., Chen, Z., Zhao, Y. and Shen, Z.: Chemical characterization and source apportionment of PM2.5 in Beijing: seasonal perspective, Atmos. Chem. Phys., 13(14), 7053–7074, doi:10.5194/acp-13-7053-2013, 2013b.

Zhao, B., Wang, S., Dong, X., Wang, J., Duan, L., Fu, X., Hao, J. and Fu, J.: Environmental effects of the recent emission changes in China: implications for particulate matter pollution and soil acidification, Environ. Res. Lett., 8(2), 24031, doi:10.1088/1748-9326/8/2/024031, 2013a.

Zhao, B., Wang, S. X., Liu, H., Xu, J. Y., Fu, K., Klimont, Z., Hao, J. M., He, K. B., Cofala, J. and Amann, M.: NO_x emissions in China: historical trends and future perspectives, Atmos. Chem. Phys., 13(19), 9869–9897, doi:10.5194/acp-13-9869-2013, 2013b.

Zhao, P., Dong, F., Yang, Y., He, D., Zhao, X., Zhang, W., Yao, Q. and Liu, H.: Characteristics of carbonaceous aerosol in the region of Beijing, Tianjin, and Hebei, China, Atmos. Environ., 71, 389–398, doi:10.1016/j.atmosenv.2013.02.010, 2013c.

Zhao, W., Kong, F. and Shen, W.: Co-benefits of local air pollutants and greenhouse gas reduction achieved by hydropower development in Xizang (Tibet) Autonomous Region, China, Chinese Geogr. Sci., 26(3), 304–313, doi:10.1007/s11769-016-0810-5, 2016.

Zhou, M., Wang, H., Zhu, J., Chen, W., Wang, L., Liu, S., Li, Y., Wang, L., Liu, Y., Yin, P., Liu, J., Yu, S., Tan, F., Barber, R. M., Coates, M. M., Dicker, D., Fraser, M., González-Medina, D., Hamavid, H., Hao, Y., Hu, G., Jiang, G., Kan, H., Lopez, A. D., Phillips, M. R., She, J., Vos, T., Wan, X., Xu, G., Yan, L. L., Yu, C., Zhao, Y., Zheng, Y., Zou, X., Naghavi, M., Wang, Y., Murray, C. J. L., Yang, G. and Liang, X.: Cause-specific mortality for 240 causes in China during 1990-2013: a systematic subnational analysis for the Global Burden of Disease Study 2013., Lancet (London, England), 387(10015), 251–72, doi:10.1016/S0140-6736(15)00551-6, 2016.

Appendixes

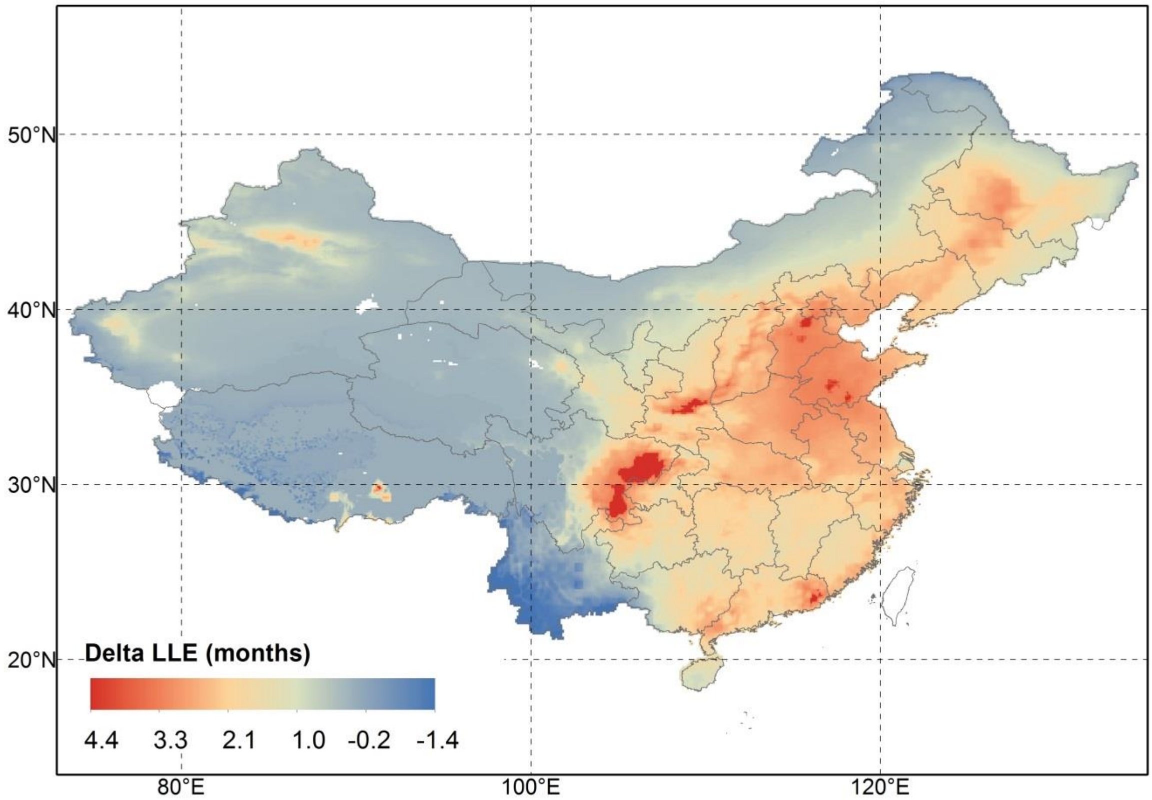

Figure S1. Differences of $PM_{2.5}$ attributable LLE (months) between Baseline 2010 and BAU 2030.

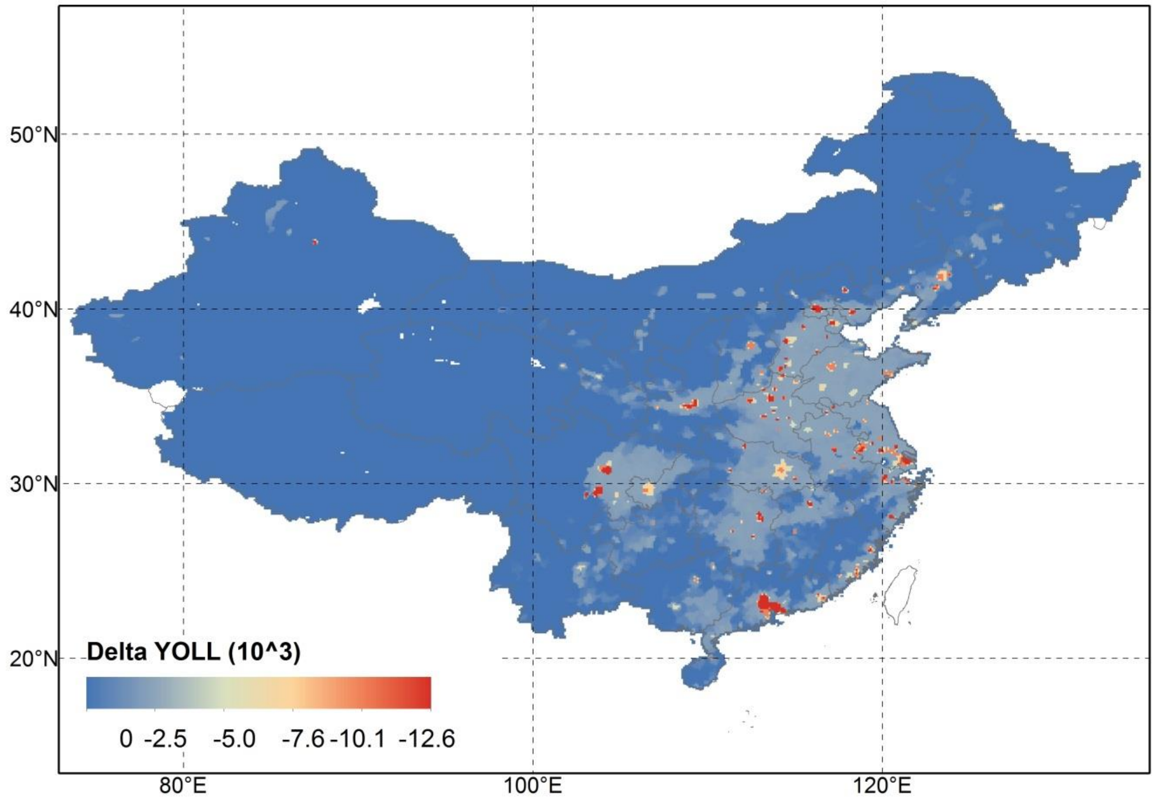

Figure S2. Differences of $PM_{2.5}$ attributable YOLL (10^3) between Baseline 2010 and BAU 2030.

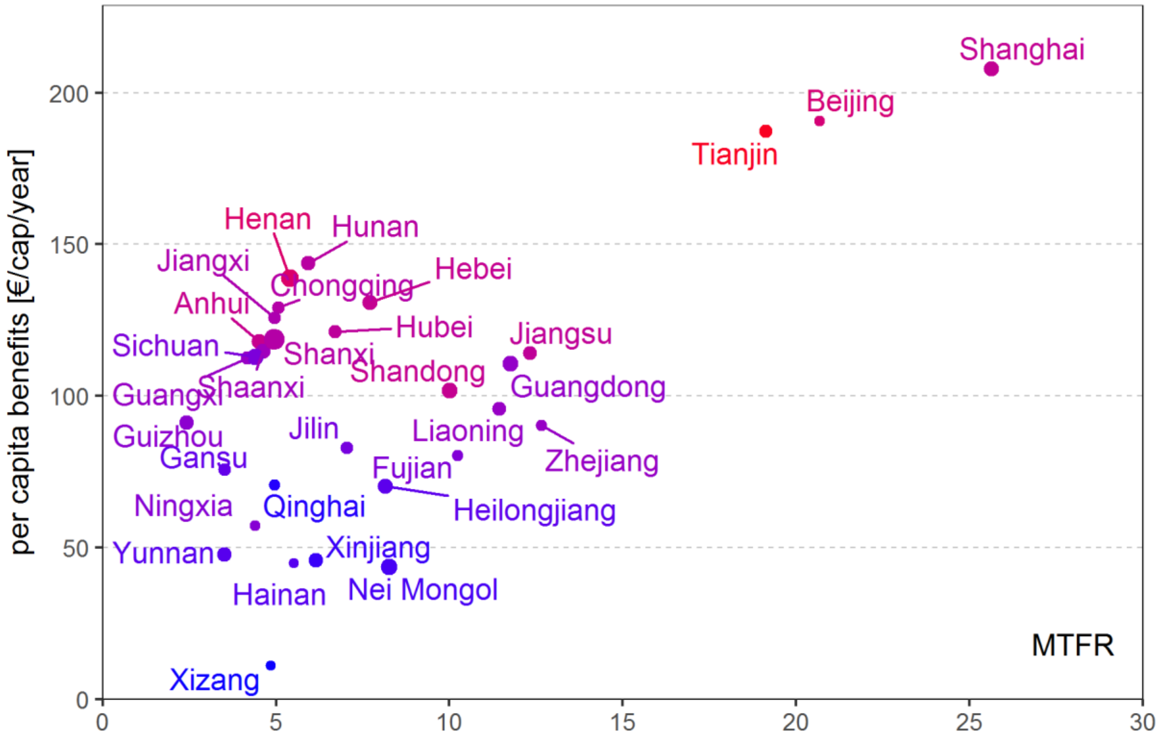

per capita benefits [€/cap/year]
MTFR
Shanghai
Beijing
Tianjin
Henan
Hunan
Jiangxi
Chongqing
Hebei
Anhui
Hubei
Jiangsu
Sichuan
Shanxi
Shandong
Guangxi
Shaanxi
Guangdong
Guizhou
Jilin
Liaoning
Gansu
Zhejiang
Fujian
Ningxia
Qinghai
Heilongjiang
Yunnan
Xinjiang
Hainan
Nei Mongol
Xizang

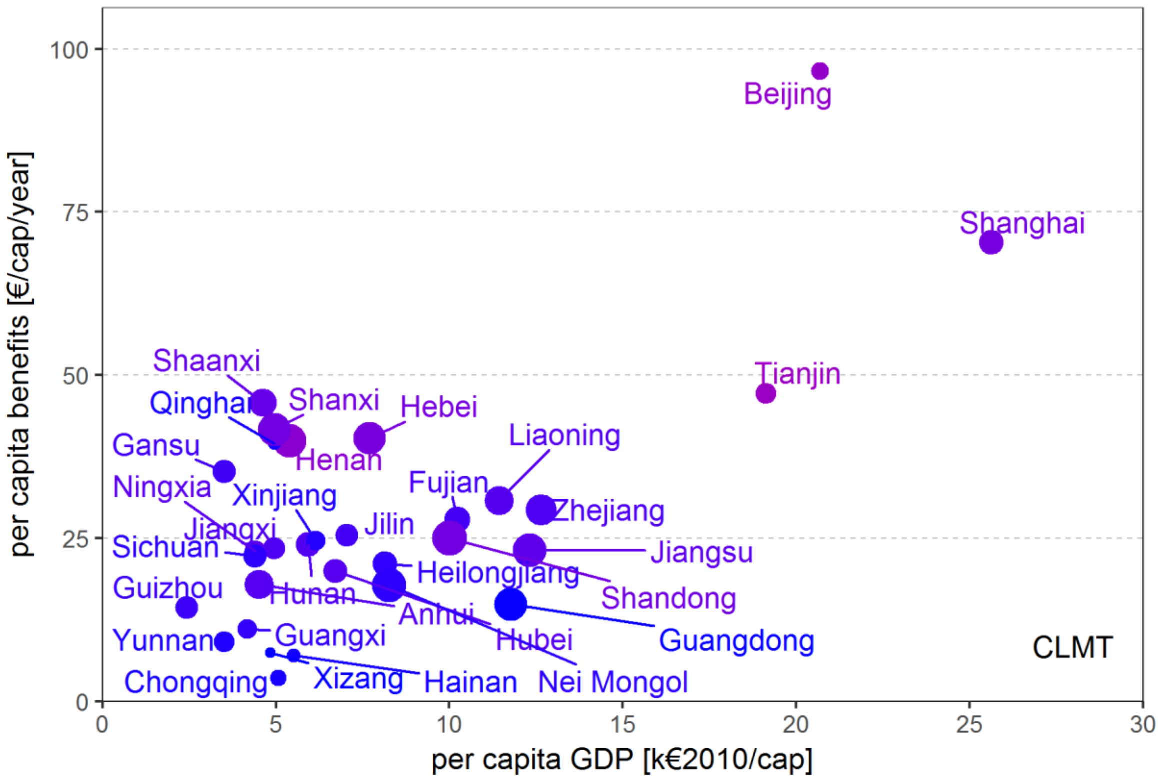

per capita benefits [€/cap/year]
per capita GDP [k€2010/cap]
CLMT
Beijing
Shanghai
Tianjin
Shaanxi
Qinghai
Shanxi
Hebei
Gansu
Henan
Liaoning
Fujian
Ningxia
Xinjiang
Zhejiang
Jiangxi
Jilin
Sichuan
Jiangsu
Heilongjiang
Guizhou
Hunan
Shandong
Anhui
Yunnan
Guangxi
Hubei
Guangdong
Chongqing
Xizang
Hainan
Nei Mongol

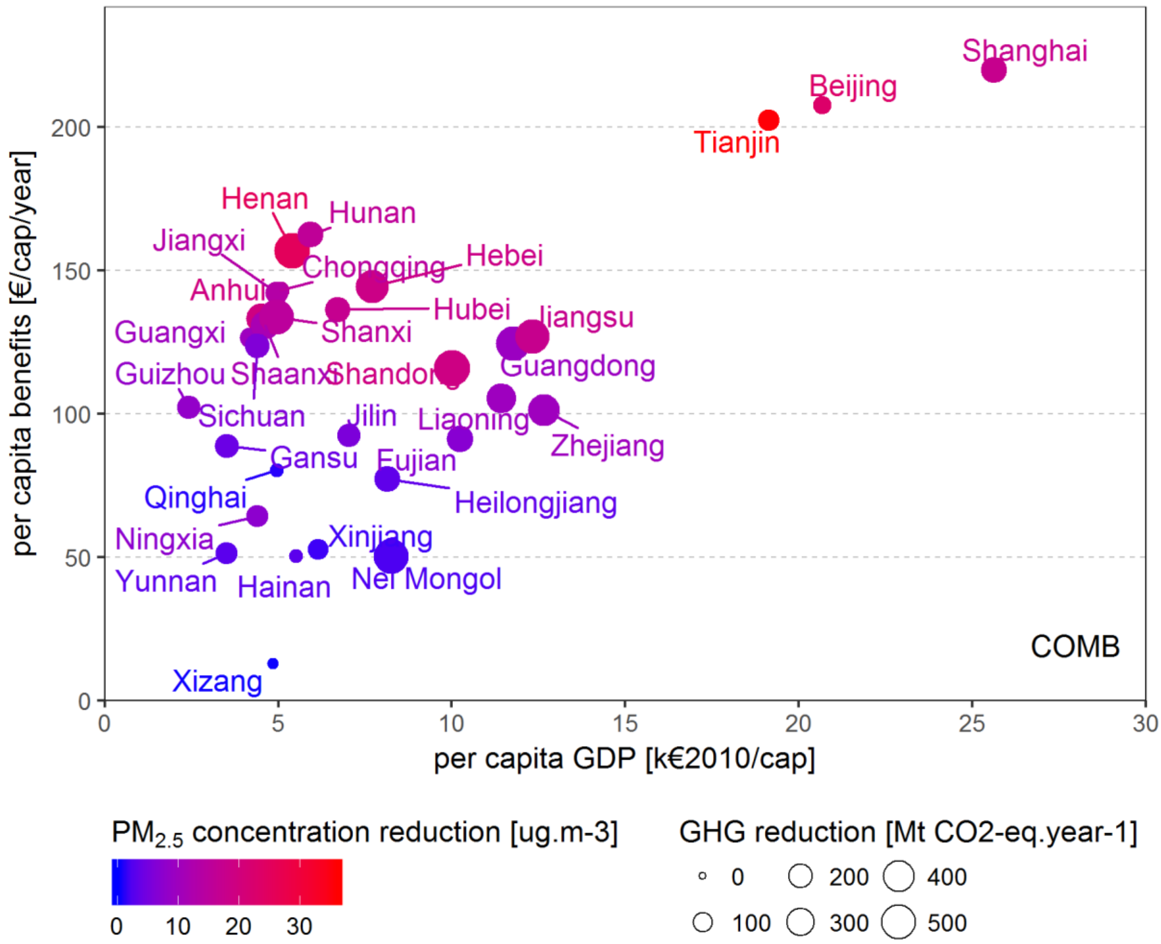

Figure S3. Per capita health benefits under the MTFR, CLMT, and COMB scenarios compared to the BAU scenario in Chinese provinces in 2030.

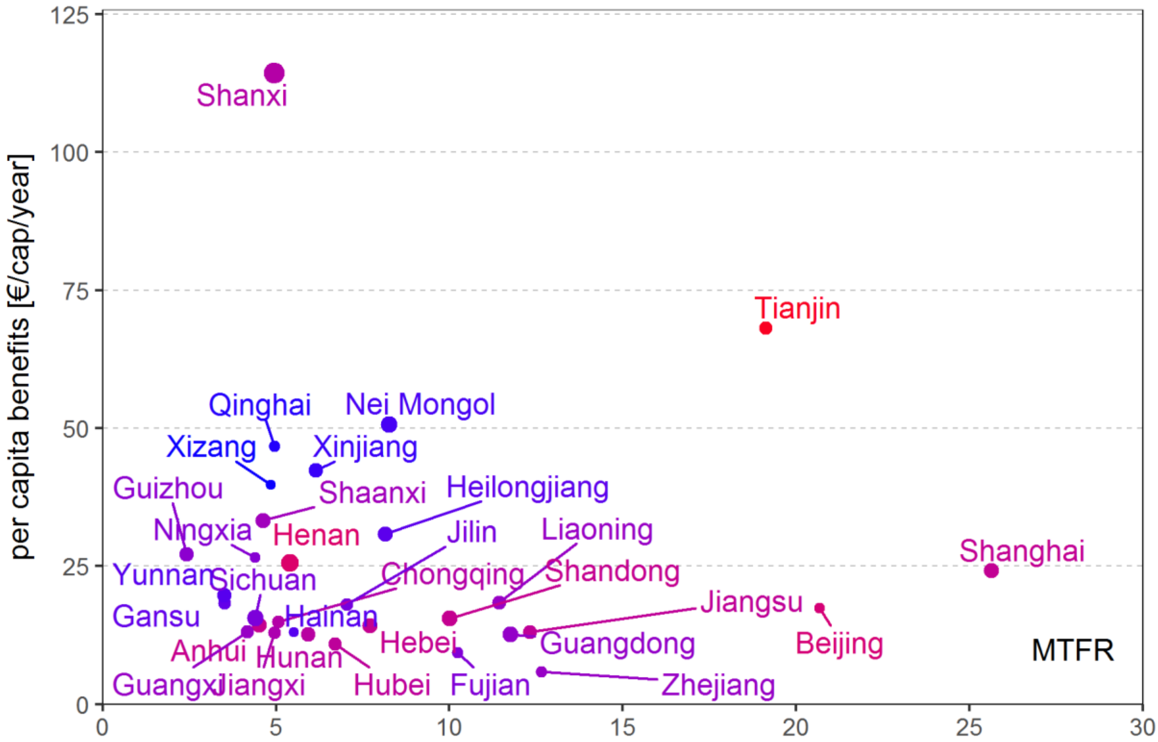
per capita benefits [€/cap/year]
125
100
75
50
25
0
0
5
10
15
20
25
30
Shanxi
Tianjin
Qinghai
Nei Mongol
Xizang
Xinjiang
Guizhou
Shaanxi
Heilongjiang
Ningxia
Henan
Jilin
Liaoning
Shanghai
Yunnan
Sichuan
Chongqing
Shandong
Jiangsu
Gansu
Hainan
Anhui
Hunan
Hebei
Guangdong
Beijing
Guangxi
Jiangxi
Hubei
Fujian
Zhejiang
MTFR

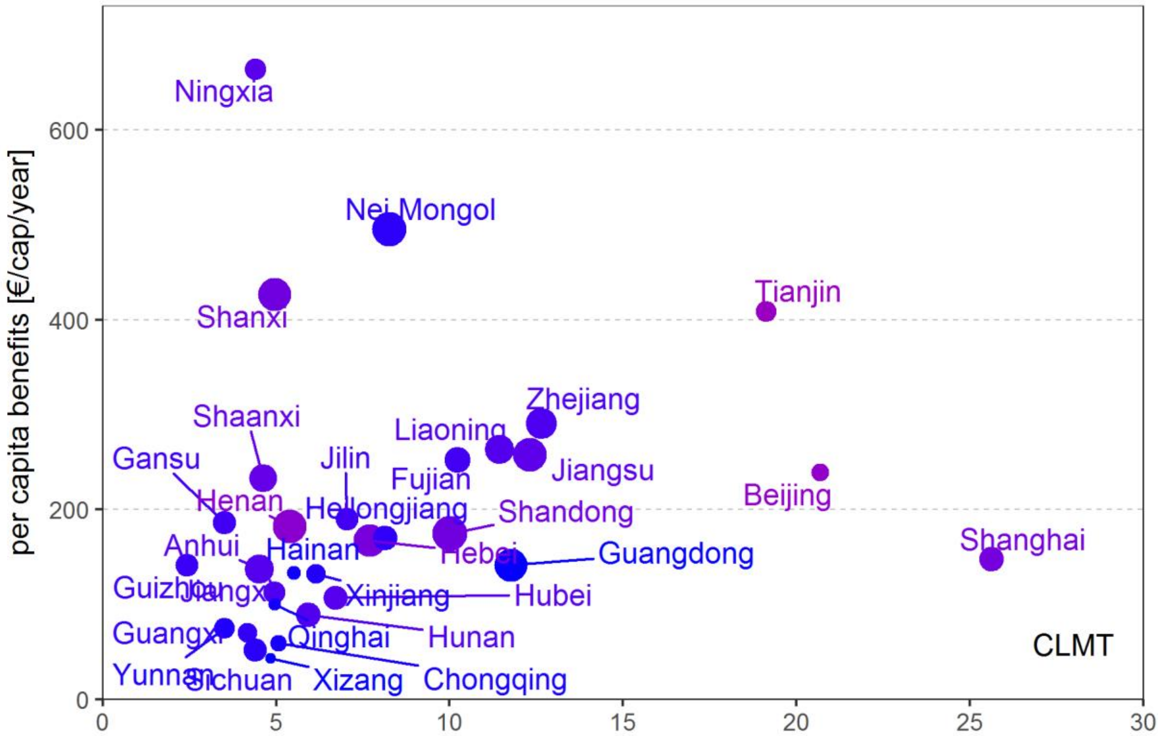
per capita benefits [€/cap/year]
600
400
200
0
0
5
10
15
20
25
30
Ningxia
Nei Mongol
Tianjin
Shanxi
Zhejiang
Shaanxi
Liaoning
Gansu
Jilin
Jiangsu
Fujian
Beijing
Henan
Heilongjiang
Shandong
Anhui
Hainan
Hebei
Guangdong
Shanghai
Guizhou
Jiangxi
Xinjiang
Hubei
Guangxi
Qinghai
Hunan
Yunnan
Sichuan
Xizang
Chongqing
CLMT

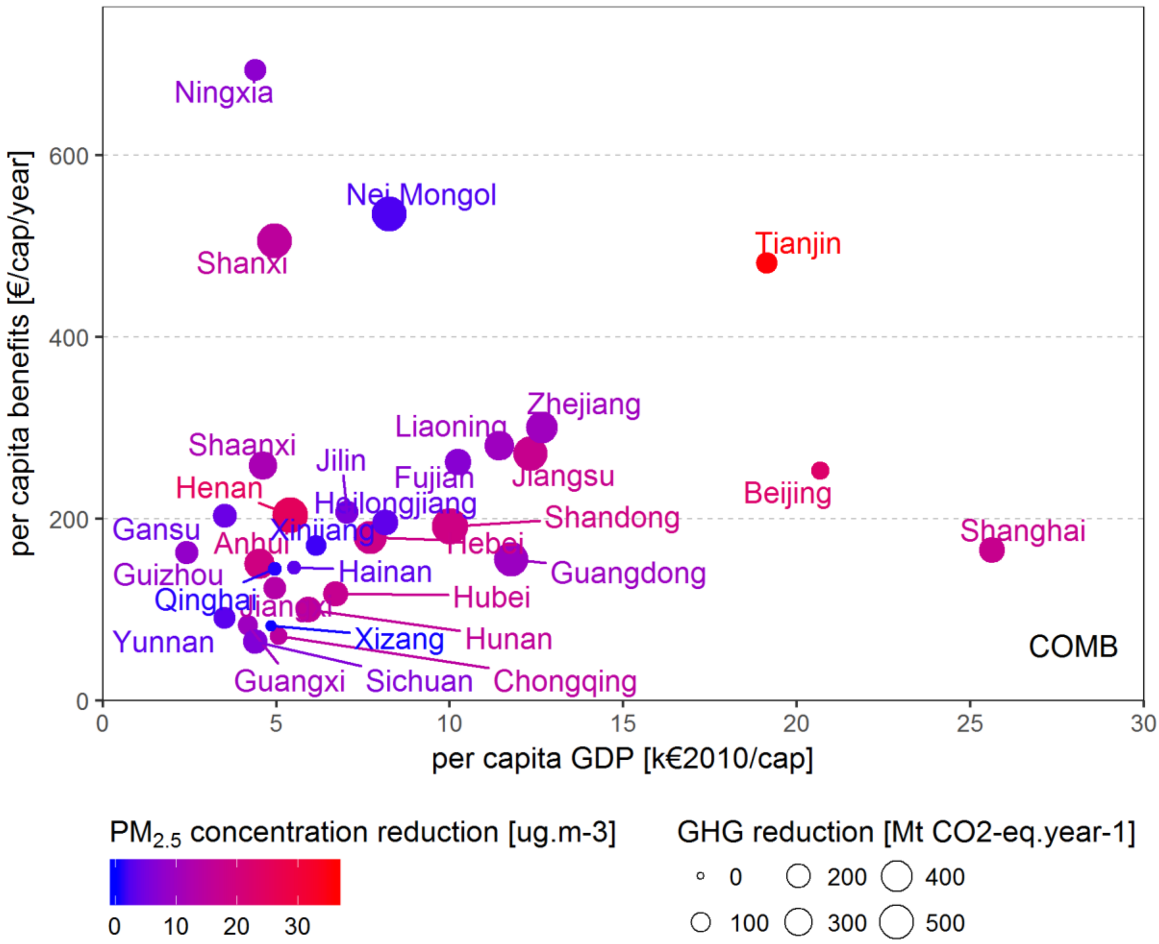

Figure S4. Per capita GHG reduction benefits under the MTFR, CLMT, and COMB scenarios compared to the BAU scenario in Chinese provinces in 2030.

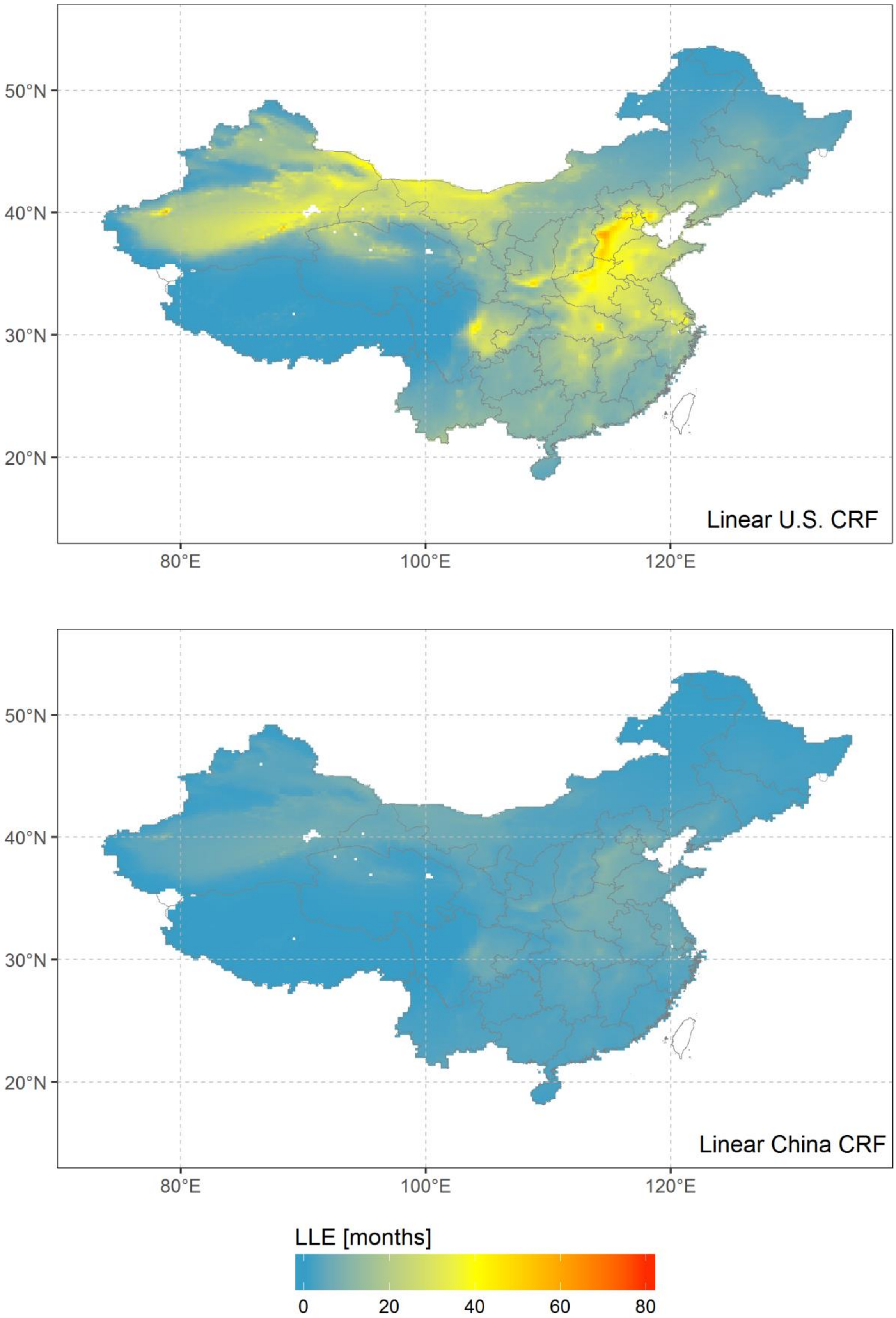

Figure S5. LLE attributable to $PM_{2.5}$ in BAU estimated using the linear CRFs.

Table S1. List of equations used for combining uncertain quantities of lognormal variables by addition.

Equation	Note
$\mu_{s1} = \sum_i \mu_{g,i} \exp(\frac{[\ln(\sigma_{g,i})]^2}{2})$ $\sigma_{s1} = \sqrt{\sum_i \mu_{g,i}^2 [\exp(2[\ln(\sigma_{g,i})]^2) - \exp([\ln(\sigma_{g,i})]^2)]}$	First estimate of the mean and standard deviation of the sum
$\mu = \mu_g \exp(\frac{[\ln(\sigma_g)]^2}{2})$ $\sigma = \mu\sqrt{(\mu/\mu_g)^2 - 1}$	Conversion of ordinary and geometric mean and standard deviation
$\mu_{eq,i} = 0.5[\mu_{g,i}\sigma_{g,i} + \mu_{g,i}/\sigma_{g,i}]$ $\sigma_{eq,i} = 0.5[\mu_{g,i}\sigma_{g,i} - \mu_{g,i}/\sigma_{g,i}]$ $\mu_{eq,sum} = \sum_i \mu_{eq,i}$ $\sigma_{eq,sum} = \sqrt{\sum_i \sigma_{eq,i}^2}$	Equivalent mean and standard deviation of each variable and the sum
$\mu_{g,s2} = \mu_{eq,sum}\sqrt{1 - (\frac{\sigma_{eq,sum}}{\mu_{eq,sum}})^2}$ $\sigma_{g,s2} = \sqrt{\frac{1 + \frac{\sigma_{eq,sum}}{\mu_{eq,sum}}}{1 - \frac{\sigma_{eq,sum}}{\mu_{eq,sum}}}}$	Second estimate of geometric mean and standard deviation of the sum
$\mu_{g,s} = (\mu_{g,s1} + \mu_{g,s2})/2$	Averaging the two estimates gives a

Equation	Note
$\sigma_{g,s} = (\sigma_{g,s1} + \sigma_{g,s2})/2$	good approximation

Note: for more details see Spadaro and Rabl (2008).